PROCESSING AND CHARACTERISATION OF PLASMA SPRAYED IRON ALUMINIDE COATINGS

A THESIS SUBMITTED IN PARTIAL FULFILMENT
OF THE REQUIREMENTS FOR THE DEGREE OF

Master of Technology

in

Metallurgical and Materials Engineering

By

ROJALEENA DAS

Department of Metallurgical and Materials Engineering
National Institute of Technology
Rourkela

2007

PROCESSING AND CHARACTERISATION OF PLASMA SPRAYED IRON ALUMINIDE COATINGS

A THESIS SUBMITTED IN PARTIAL FULFILMENT
OF THE REQUIREMENTS FOR THE DEGREE OF

Master of Technology

in

Metallurgical and Materials Engineering

By

ROJALEENA DAS

Under the Guidance of

Prof. S. C. MISHRA

Department of Metallurgical and Materials Engineering
National Institute of Technology
Rourkela

2007

National Institute of Technology
Rourkela

CERTIFICATE

This is to certify that thesis entitled, "PROCESSING AND CHARACTERISATION OF PLASMA SPRAYED IRON ALUMINIDE COATINGS**"** submitted by Ms. ROJALEENA DAS in partial fulfillment of the requirements for the award of Master of Technology Degree in Metallurgical and Materials Engineering at National Institute of Technology, Rourkela (Deemed University) is an authentic work carried out by her under my supervision and guidance.

To the best of my knowledge, the matter embodied in this thesis has not been submitted to any other university/ institute for award of any Degree or Diploma.

Date:

Prof. S.C.Mishra
Dept. of Metallurgical and Materials Engineering
National Institute of Technology
Rourkela-769008

ACKNOWLEDGEMENT

It is with a feeling of great pleasure that I would like to express my most sincere heartfelt gratitude to my guide **Prof. S. C. Mishra**, **Dept. of Metallurgical and Materials Engineering, NIT, Rourkela** for his invaluable guidance, motivation, untiring efforts and meticulous attention at all stages during my course of work.

I express my sincere thanks to **Prof. G. S. Agarwal**, **Head of the Department of Metallurgical and Materials Engineering, NIT, Rourkela** for providing me the necessary facilities in the department. I am also grateful to **Prof. K. N. Singh**, **M. Tech. co-ordinator**, for his constant concern and encouragement for execution of this work.

I also express my sincere gratitude to **Prof. Alok Satapathy, Dept. of Mechanical Engineering** for his timely help during the course of work.

I thankful to **Sri Rajesh Pattnaik, Sri Samir Pradhan & Sri Udayanath Sahu,** Metallurgical & Materials Engineering, Technical assistants, for their co-operation in experimental work.

Special thanks to **Ms. Anupama Sahu**, department of Metallurgical and Materials Engineering for being so supportive and helpful in every possible way.

Date: **Rojaleena Das**

Roll No. : 20504007

CONTENTS

ABSTRACT

Surface modification is a generic term now applied to a large field of diverse technologies that can be gainfully harnessed to achieve increased reliability and enhanced performance of industrial components. Intermetallic compounds find extensive use in high temperature structural applications. The Fe_3Al based intermetallic alloys offer unique benefits of excellent oxidation and sulfidation resistance at a potential cost lower than many stainless steels. These are mainly used in heating elements, regenerator disks, wrapping wire, hot gas filters, tooling, and shields. To obtain functional surface coating on machine components exhibiting selected in-service properties, proper combination of processing parameters has to be planned. These combinations differ by their influence on the coating properties and characteristics.

Plasma spraying is gaining acceptance as a development of quality coatings of various materials on a wide range of substrates. Coatings made with plasma route exhibit excellent wear, corossion resistance and high thermal shock resistance etc. Iron premixed with 30% aluminium is deposited on mild steel and copper substrates by atmospheric plasma spraying at various operating power level ranging from 11to 21kW .

After plasma spraying, the coated materials have been subjected to a series of tests. The particle sizes of the raw materials used for coating (iron with, 30 wt% aluminium powder) are characterized using Laser particle size analyzer of Malvern Instruments make. Thickness of the iron aluminide coatings are measured by using an optical microscope. X-ray diffraction technique is used to identify the different (crystalline) phases present in the coatings.

The coating adhesion strength is evaluated by coating pull out method, as per ASTM C-633 standard. Coated specimens are studied by JEOL JSM-6480 LV scanning electron microscope in order to know the surface and interface morphology. The porosity of the coatings is measured by putting polished cross sections of the coating sample under a microscope using image analyser. Microhardness measurement is done to know the hardness of the optically distinguishable phases by using Leitz Microhardness Tester Solid particle erosion is a wear process where particles strike against a surface and promote material loss. In this work, room

temperature solid particle (sand) erosion test is carried out by using ASTM G76 standards. Deposition efficiency is evaluated as the important factor that determines the techno-economics of the process.

Statistical analysis i.e. Artificial Neural Networks is gainfully employed to simulate property-parameter correlations in a space larger than the experimental domain. It is evident that with an appropriate choice of processing conditions a sound and adherent iron aluminide coating are achievable using iron aluminium powders.

LIST OF FIGURES

LIST OFTABLES

CHAPTER 1
INTRODUCTION

1.1 BACKGROUND

Surface damage can result in changes in surface condition and dimension of a mechanical component, and this may sometimes cause disastrous failure of an entire mechanical system.

Surface modification is a generic term now applied to a large field of diverse technologies that can be gainfully harnessed to achieve increased reliability and enhanced performance of industrial components. The incessant quest for higher efficiency and productivity across the entire spectrum of manufacturing and engineering industries has ensured that most modern-day components are subjected to increasingly harsh environments during routine operation. Critical industrial components are, therefore, prone to more rapid degradation as the parts fail to withstand the rigors of aggressive operating conditions and this has been taking a heavy toll of industry's economy. In an overwhelmingly large number of cases, the accelerated deterioration of parts and their eventual failure has been traced to material damage brought about by hostile environments and also by high relative motion between mating surfaces, corrosive media, extreme temperatures and cyclic stresses. Simultaneously, research efforts focused on the development of new materials for fabrication are beginning to yield diminishing returns and it appears unlikely that any significant advances in terms of component performance and durability can be made only through development of new alloys.

As a result of the above, the concept of incorporating engineered surfaces capable of combating the accompanying degradation phenomena like wear, corrosion and fatigue to improve component performance, reliability and durability has gained increasing acceptance in recent years. The recognition that a vast majority of engineering components fail catastrophically in service through surface related phenomena has further fuelled this approach and led to the development of the broad interdisciplinary area of surface modifications. A protective coating deposited act as a barrier between the surfaces of the component and the aggressive environment that it is exposed to during operation is now globally acknowledged to be an attractive means to

significantly reduce/suppress damage to the actual component by acting as the first line of defense.

Surface modification today is best defined as “the design of substrate and surface together as a system to give a cost effective performance enhancement, of which neither is capable on its own”. The development of a suitable high performance coating on a component fabricated using an appropriate high mechanical strength metal/alloy offers a promising method of meeting both the bulk and surface property requirements of virtually all imagined applications. The newer surfacing techniques, along with the traditional ones, are eminently suited to modify a wide range of engineering properties. The properties that can be modified by adopting the surface engineering approach include tribological, mechanical, thermo-mechanical, electrochemical, optical, electrical, electronic, magnetic/acoustic and biocompatible properties. It offer a wide range of driven by technological need and fuelled by exciting possibilities, novel methods for applying coatings, improvements in existing methods and new applications have proliferated in recent years. Surface modification technologies have grown rapidly, both in terms of finding better solutions and in the number of technology variants available, to quality and cost. The significant increase in the availability of coating process of wide ranging complexity that are capable of depositing a plethora of coatings and handling components of diverse geometry today, ensures that components of all imaginable shape and size can be coated economically.

One of cost-effective approaches against surface failure is coating. Various coating techniques have been successfully applied in industry to protect machinery and equipment from surface damage respectively caused by corrosion, oxidation and wear. However, when used in a harsh environment involving two or more damage modes, such as corrosion-wear or corrosion-erosion, many coatings perform poorly due to the synergistic action of wear and corrosion. Considerable efforts have been continuously made to develop high-performance coatings that can resist corrosive wear encountered in various industries such as mining, petroleum and chemical industries.

Existing surface treatment processes fall under three broad categories:

(a) Overlay Coatings:

This category incorporates a very wide variety of coating processes wherein a material different from the bulk is deposited on the substrate. The coating is distinct from the substrate in the as-coated condition and there exists a clear boundary at the substrate/coating interface. The adhesion of the coating to the substrate is a major issue.

(b) Diffusion Coatings:

Chemical interaction of the coating-forming element(s) with the substrate by diffusion is involved in this category. New elements are diffused into the substrate surface, usually at elevated temperatures so that the composition and properties of outer layers are changed as compared to those of the bulk.

(c) Thermal or Mechanical Modifications of Surfaces:

In this case, the existing metallurgy of the component surface is changed in the near-surface region either by thermal or mechanical means, usually to increase its hardness.

The type of coating to be provided depends on the application. There are many techniques available, e.g. electroplating, vapour depositions, thermal spraying etc. Of all these techniques, thermal spraying is popular for its wide range of applicability, adhesion of coating with the substrate and durability. It has gradually emerged as the most industrially useful method of developing a variety of coatings, to enhance the quality of new components as well as to reclaim worn/wrongly machined parts. The process can be applied to coat on variety of substrates of complicated shape and size using metallic, ceramic and /or polymeric consumables. The production rate of the process is very high and the coating adhesion is also adequate.

There has been a steady growth in the number of applications of thermally sprayed coatings. Availability of hardware and adaptability of the technique are the most important factors for this growth. The type of thermal spraying depends on the type of heat source employed and consequently flame spraying (FS), high velocity oxy-fuel spraying (HVOF), plasma spraying (PS) etc. come under the umbrella of thermal spraying. . Plasma spraying has been successfully applied to a wide range of industrial technologies. Automotive industry,

aerospace industry, nuclear industry, textile industry, paper industry and iron and steel industry are some of the sectors that have successfully exploited thermal plasma spray technology [**1, 2**]. Plasma spraying utilizes the exotic properties of the plasma medium to impart new functional properties to conventional and non-conventional materials and is considered as one highly versatile and technologically sophisticated thermal spraying technique. It is a very large industry with applications in corrosion, abrasion and temperature resistant coatings and the production of monolithic and near net shapes [**3**]. The process can be applied to coat on variety of substrates of complicated shape and size using metallic, ceramic and /or polymeric consumables. The production rate of the process is very high and the coating adhesion is also adequate. Since the process is almost material independent, it has a very wide range of applicability, e.g., as thermal barrier coating, wear resistant coating etc. Thermal barrier coatings are provided to protect the base material, e.g., internal combustion engines, gas turbines etc. at elevated temperatures. Zirconia (ZrO_2) is a conventional thermal barrier coating material. As the name suggests, wear resistant coatings are used to combat wear especially in cylinder liners, pistons, valves, spindles, textile mill rollers etc. alumina (Al_2O_3) ,titania (TiO_2) and zirconia (ZrO_2) are the some of the conventional wear resistant coating materials [**4**].

Aluminide coating is one of overlay coatings widely used in industry to resist oxidation and high-temperature corrosion [**5-7**]. An aluminide coating formed on steel substrate usually consists of an outward-grown FeAl layer, an intermediate layer with Fe_3Al and FeAl intermetallic compounds [**8**] and an inner layer of solid solution containing Fe and Al [**9**] .This type of coating has recently been applied to resist erosion at elevated temperatures, for instance, to protect sinter machine cooler grates from erosion caused by high-temperature burden, as well as the oxidation from excess air and corrosion from combustion product [**10**]. The aluminide coating has demonstrated its efficiency in preventing erosion or low-stress wear at elevated temperatures. In order to further improve the performance of aluminide coating and in particular, expand its application, research was conducted authors to modify aluminide coating.

Particulates ingested into the engine or formed as a result of incomplete combustion are known to cause erosion problems in gas turbines [**1l, 12**]. Previous high temperature erosion studies [**13 – 15**] using uncoated turbine blade materials have shown that the oxidation characteristics of the alloy are of importance in determining its erosion behaviour. Under a wide

range of conditions typical of those found in gas turbines the erosion of aluminide coatings is shown to be controlled by the formation and removal of surface scales. This implies that the use of aluminide coatings will increase the erosion resistance of typical turbine blade materials because of the superior oxidation and corrosion resistance of this coating.

One major limitation of the process is a relatively high price of the plasma sprayable consumables. The objective of this work is to evaluate the potential of iron aluminide, as plasma consumable30%Aluminium is premixed with iron. Coatings have been produced on two selected substrates (commercially available copper and mild steel) using all these non-conventional coating materials. The performance of the coating developed using the mixture have been compared.

The coatings have been characterized for their hardness, porosity, adhesion strength and microstructure. The significant phase changes associated with the plasma processing during the coating deposition have been studied. In addition, the coating deposition efficiencies at various operating conditions have also been evaluated.

One less studied area in case of metallic coatings is their resistance to solid particle erosion. This aspect is studied in the present work by subjecting the coatings to solid particle impingement at different impact angles. The capabilities of the coatings to sustain the erosive attack have been assessed.

A qualitative analysis of the experimental results with regard to coating deposition efficiency, erosion wear rate using statistical techniques is presented. The analysis is aimed at identifying the operating variables/factors significantly influencing the deposition, erosion wear rate of iron aluminide on metals. Factors are identified in accordance to their influence on the coating deposition, erosion wear rate. A prediction model based on artificial neural network is also presented considering the significant factors. Neural computation is used since plasma spraying is a complex process that has many variables and multilateral interactions. This technique involves construction of a database, training, validation and then provides a set of predicted results related to the coating deposition efficiency, erosion wear rate at various operating parameters.

1.2 OBJECTIVE

The objective of the present investigation can be stated as following:

a. To explore the coating potential of Iron aluminide on different metal substrates by plasma spraying.

b. To develop a series of plasma sprayed coatings from iron aluminide on metal substrates and to find coating deposition efficiency, porosity and thickness.

c. Micro-structural characterization to evaluate the soundness of the coatings.

d. X-ray diffractogram for phase analysis.

e. Mechanical characterization to evaluate the micro-hardness and interface bond strength of the coatings.

f. To asses the capabilities of the coatings to combat wear with a special reference solid particle erosion wear.

g. Complementing the experimental results, in regard to coating deposition efficiency and erosion rate by predicted results obtained from an artificial neural network analysis.

CHAPTER 2
LITERATURE SURVEY

2.1 PREAMBLE

This chapter deals with the literature survey of the broad topic of interest namely the development of surface modification technology for tribological applications. This treatise embraces various coating techniques with a special reference to plasma spraying, the coating materials and their characteristics. The performances of wear resistant coatings under various conditions have been reviewed critically along with the corresponding failure mechanisms. At the end of the chapter a summary of the literature survey and the knowledge gap in the earlier investigations are presented.

2.2 SURFACE ENGINEERING

Surface engineering is a discipline of science, encompassing

1. Manufacturing process of surface layers, thus in accordance with the accepted terminology-superficial layers and coatings, produced for both technological and end use purposes.
2. Connected phenomena.
3. Performance effects obtained by them.

Surface engineering encompasses all scientific and technical problems connected with the development/growth of surface layers prior to end use or service(viz. technological layers), or during service (i.e. service generated layers), on or under the surface(superficial layers), or on a substrate (coatings) with properties differing from that of the core (structural) material, as shown in fig 2.1. It also includes research of connected phenomena's and with potential usable properties of surface layers, as well as problems connected with layer design [**16**].

Thus surface engineering encompasses the total field of research and technical activity aimed at the design, manufacture, investigation and utilization of surface layers, both technological and for end use, with properties better than those of the core, such as mainly anti-corrosion, anti fatigue, anti wear and decorative. Other application includes such as optical, thermo-physical, electrical, magnetic, adhesive, ablation, passivation, inhibition, catalytic, biocompatibility, diffusion etc.

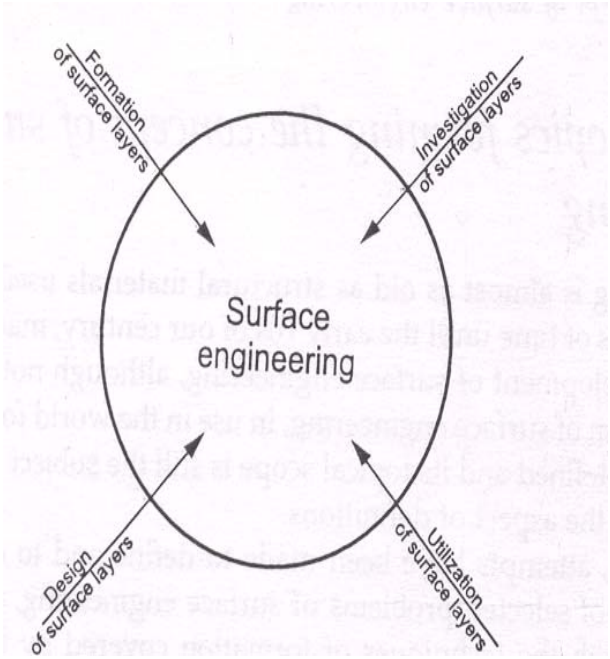

Fig. 2.1 Schematic representation of the area of activity of surface engineering

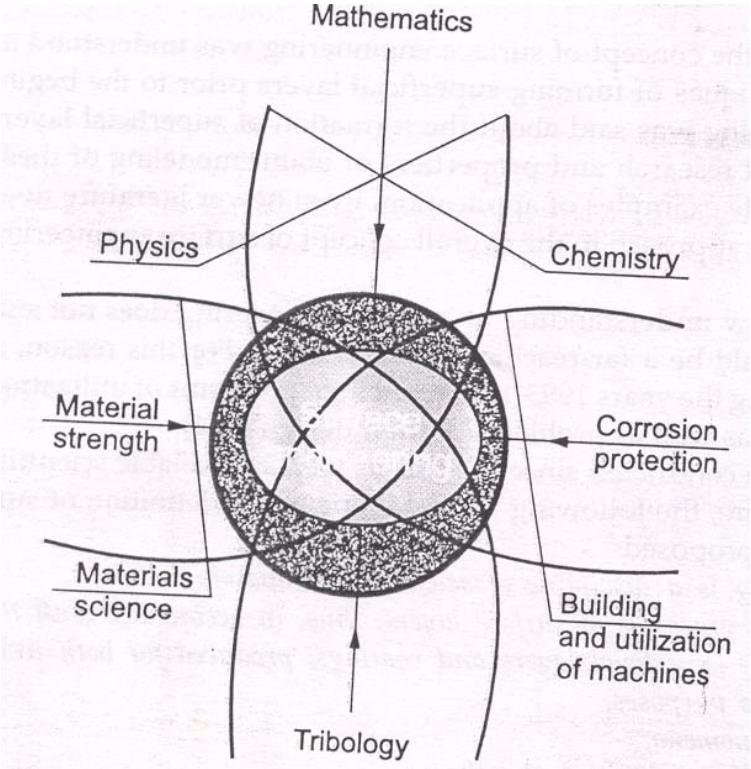

Fig.2.2 Scientific and technical activity adding up to create surface engineering.

Surface engineering has a lot in common with fundamental and applied (technical) science. Surface engineering draws inspiration from fig.2.2.

1) Fundamental sciences: physics, chemistry, partially mathematics and constitutes their application to material science;

2) Applied (technical) science; sciences dealing with materials science and material engineering, with special emphasis on heat treatment, construction and use of machines, with special emphasis on material strength, primarily fatigue, tribology and corrosion protection, electrical engineering, electronics, optics, thermo kinetics, the science of magnetism etc. [**17**].

The object of material science and material engineering-the material constitutes the fundamental substance, the surface properties of which are improved, enhanced and controlled by surface engineering. The knowledge of material substrate or core structures is the basic condition of producing layers on it. Methods of formation (producing) surface layers are included in the area of machine building, as manufacturing methods. [**18**].

The properties of surface layers produced are evaluated by methods used in surface engineering, as well as in investigation and use of machines. These methods are used predominantly in areas such as tribology, corrosion protection, material strength etc.

Some methods of designing of surface layer properties, used in surface engineering, are also derived from –besides mathematics material engineering and machine building. This pertains to material strength and tribology.

The utilization of surface layers or their production during the coarse of service belongs to the area of machine service and takes into account, first and foremost, problems of tribology and corrosion protection.

The role of surface engineering in the process of manufacture of the material product is as follows

Raw material + Thermal energy = Product

Product + Surface engineering = Quality product

2.3 SURFACE MODIFICATION(The key to obtain optimum performance)

The past decade has seen a rapid development in the range of techniques which are available to modify the surfaces of engineering components. In the last two decades this in turn has led to the emergence to the new field of surface modification. It describes the interdisciplinary activities aimed at tailoring the surface properties of engineering materials. Surface Engineering is the name of the discipline and surface modification is the philosophy behind it. The object of surface engineering is to up grade their functional capabilities keeping the economic factors in mind [**19**].It is usually necessary to apply a surface treatment or coating on a base component (substrate) in order to design a composite system, which has a performance, which cannot be achieved by either of the base component or the surface layer alone [**20**]. Thus, through a surface modification process, we assemble two (or more) materials by the appropriate method and exploit the qualities of both [**21, 22**]. The concept can be elucidated with few examples [**23**].

Aero-engines: In the parts of modern aero engines-turbine blades/vanes, stator blades, combustion cans/vanes etc., the base alloys have been designed primarily for high temperature strength and these advanced materials may not provide optimal corrosion or oxidation resistance, especially to satisfy the requirements for a service life. In such cases the only option is to rely on effective surface coating to prevent or minimize the degradation processes. Oxidation and corrosion resistance coatings are typically M-Cr-Al-X alloys (VPS) (M=Ni, Co, Co-Ni and X=Y, Si, Ta etc.).This concept is also now applied to adiabatic diesel engines. A thermal barrier coating that includes ZrO_2+Y_2O_3 with a bond coating CoCrAlY is applied onto its critical components-piston crown and cylinder head. The engine efficiency is increased up to 50%.

Cutting tools: Cutting tools are subjected to a high degree of abrasion.WC-Co composite is a very popular cutting tool material, and is well known for his high hardness and wear resistance. If a thin coating of TiN (CVD) is applied on to the WC-Co insert, its capability increases considerably [**24**]. TiN is more capable of combating abrasion. On the other hand, TiN is extremely brittle, but the relatively tough core of WC-Co composite protects it from fracture.

Surface modification is a versatile tool for technological development provided it is applied judiciously keeping in mind the following issues.

- The coating-surface treatment should not impair the properties of the bulk material.
- The choice of technique must be capable of coating the component, in terms of both size and shape.
- The technological value addition should justify the cost.

2.4 TECHNIQUES OF SURFACE MODIFICATION

Today a large number of commercially available technologies are present in the industrial scenario and figure 2.3 exhibits some of them [**25**]. An overview of such technologies is presented below.

2.4.1 Plating

Amongst plating processes, electroplating is quite popular. The substrate (necessarily conducting) forms an electrode (cathode) and is submerged in an appropriate electrolyte [**26**]. As current passes through the electrolytic cell, ions of plating material emerge from the electrolyte and deposit on to the cathode (the substrate). In electro less plating, deposition occurs by catalytic reduction of the solute present in the plating bath. Electrochemical conversion coating appears on the surface of the substrate (which acts as an electrode) as a result of a chemical reaction between the electrolyte and the surface. For example in presence of H_2SO_4 (electrolyte) the top layer of aluminum (electrode) is oxidized to form aluminum oxide [**27**]. Electroforming is the process of electro- depositing a material on a removable mandrel to make a part. Plating can be used for modification of physical, mechanical or corrosion properties [**28**].

Plating techniques cater to a large number of materials. Composite coatings with non-conducting materials like diamond, PTFE is also possible by plating. It caters to wear, corrosion, rebuilding and electrical applications. Some of the processes are capable of providing uniform coating throughout the surface even in deep holes and re-entrant corners (electroless plating). Selective areas of a surface can be plated too [**27, 29, and 30**].

But electroplating is prone to metallurgical embrittlement and provides only moderate adhesion where as electroless plating is quite slow [**26, 31**].

2.4.2 Diffusion Processes

As the name suggests, the process involves the diffusion of an element into the substrate matrix [**32**]. The process is normally conducted at an elevated temperature to promote diffusion. The diffusing species create a layer on the substrate and the properties of that layer are modified. The elements used as diffusing species are carbon, nitrogen, aluminum, chromium, silicon, boron, etc. The choice of the diffusing species depends on applications, but carbon and nitrogen are the two most widely used elements and the processes are known as carburizing and nitriding respectively [**33**]. Both processes are normally carried out on steel substrates. The substrate is kept in an environment rich in carbon or nitrogen. At a high temperature, the elements slowly diffuse into the substrates owing to the concentration gradient. Carburizing enriches the carbon content of the substrate case and upon quenching the case layer hardens owing to the martensitic transformation. Nitriding also creates a very hard layer on the substrate surface. Here hardening occurs owing to a solid solution strengthening. These two processes are mainly used for wear applications and so are boronising and carbonitriding. Chromising, siliconising, and aluminizing on the other hand are for corrosion /oxidation resistance applications [**34, 35**].

But diffusion processes have certain limitations as well. They cannot cater to applications like rebuilding. Some processes often create distortion (case carburizing). Some of the processes are very slow and the case depth obtained is limited (gas carburizing). Some of the processes are carried out in aggressive environment (salt nitriding) with potential environmental hazard. Applications are limited to metals only.

2.4.3 Surface Hardening

The process involves heating a component surface (or part of it) beyond a critical temperature and quickly cooling it by quenching to induce martensitic transformation. The process is restricted to cast iron and steels. Here a heat source for raising the temperature of the work piece is needed. The process is named after the heat source used and typical examples are flame hardening (oxy-acetylene flame), induction hardening (induction heating), laser hardening (laser beam), electron beam hardening (electron beam) etc. [**36**] . The carbon content of the work piece must be at least 0.6%, otherwise martensitic transformation may not occur. Except for the ion implantation process, these processes do not involve any material addition. In the ion

implantation process, suitable materials are taken in ion form and they are directed at the surface to be implanted on. These processes are utilized to develop a hard case of low thickness, while retaining the softness of the core [**37**].

A small part of a big component can be hardened (flame hardening) and no material addition is required. Adhesion does not impose any restriction, since the hardened layer is an integral part of the original component. But the process is restricted to ferrous materials. Sometime the process is prone to distortion. Some of the processes require highly skilled manpower (e.g., flame hardening). Except for flame hardening, the set-up cost is high for all other processes.

2.4.4 Thin Film Coating

In this process a thin layer of few microns thick, of a pure element or a compound can be deposited on substrate [2**5**]. This technique can be broadly classified into two categories:

(a) Physical vapour deposition

(b) Chemical vapour deposition

2.4.4 (a) Physical Vapour Deposition (PVD)

This process is carried out in an evacuated chamber. The target (substrate) and the coating material are kept facing each other. The coating material is heated using a heat source like electrical heater or electron beam, in low pressure. The coating material evaporates directly from solid state and deposits on the target. This is known as thermal evaporation [**38**]. In another process, known as sputter coating [**39**], the target and coating materials are connected to two electrodes (anode and cathode, respectively) of a suitable power supply and an inert gas is released in the space between them. The gas undergoes ionization in the electric field. The positive ions rush towards the cathode (i.e., the coating material) and dislodge ions from it. These ions move toward the anode and deposit on the target. Ion plating is a combination of these two processes where the coating material is heated and at the same time gas plasma is created to expedite the process [**40**].

Using this process pure elements as well as compounds can be deposited. It is quite simple, involves low cost equipment and addresses many fields of applications, e.g., electronic, electrical, wear, etc. This is a line of sight process, and therefore parts having complicated shape may not be coated. Since it is conducted in vacuum, large parts cannot be coated [**25]**.

2.4.4 (b) Chemical Vapour Deposition (CVD)

The material to be coated is kept in an evacuated chamber equipped with the facility of electrical heating. After the substrate is heated to the required temperature, the appropriate gases are introduced into the reactor for chemical reaction in contact with the hot substrate. One of the reaction products is a solid, which deposits on the substrate surface. The residual gases are taken out of the chamber [**41**].

Intricate shapes can be coated by this technique. Rate of deposition is higher than PVD. Certain items can be deposited using CVD only. But since it is carried out at a high temperature (700°C or above), thermal damages may come into play. Set up is more complicated than PVD [**42**].

2.4.5 Hard facing by Welding

Welding conventionally is a process of joining two metallic parts. Shield Metal Arc Welding (SMAW) is the most common welding process. Here the base metals are kept close to each other and an electric arc is created between the base metal (near the junction) and the consumable electrode. As a result both the consumable electrode (filler material) and the edge of the base metal melt. The filler material of the electrode transfers to the molten weld pool and upon freezing of such pool a solid weld bead is formed. The strength of the weldment is supposed to be greater than that of the base material [**43**]. In the case of the hard facing, the filler material is deposited onto the base material to form a metallurgically bonded second layer. Now the first layer of the deposit is diluted by the diffusion of the base material constituents into it. Normally a second layer is also deposited at the top of the first one. In welding either similar or otherwise compatible filler material are normally used for the joining purpose. Alloyed electrodes, with a tailored composition to suit particular situations of surfacing, are also used

[**44**]. There are many techniques of welding and are shown in Figure 2.3. Each has its own application domain.

Strongest possible bonding is obtained in this process. All weldable metals and alloys can be used. It can be carried out with low cost equipment. A thick layer can be built up rapidly. The process can be entirely automated. But this technique is restricted to metallic materials. Products are vulnerable to residual stress related distortion. The hard faced layer may undergo dilution by the diffusion of base material constituents. Products may require a post-weld finishing operation in many applications [**43, 45**].

2.4.6 Thermal Spraying

It is the generic category of material processing technique that apply consumables in the form of a finely divided molten or semi molten droplets to produce a coating onto the substrate kept in front of the impinging jet. The melting of the consumables may be accomplished in a number of ways, and the consumable can be introduced into the heat source in wire or powder form. Thermal spray consumables can be metallic, ceramic or polymeric substances. Any material can be sprayed as long as it can be melted by the heat source employed and does not undergo degradation during heating [**43, 46]**.

The nature of bonding at the coating-substrate interface is not completely understood. It is normally assumed that bonding occurs by the mechanical interlocking. Under this circumstance it is generally possible to ignore the metallurgical compatibility [**25**]. This is an extremely significant feature of thermal spraying. Another interesting aspect of thermal spraying is that the surface temperature seldom exceeds 200^0 C. Hard metal or ceramic coating can be applied to thermosetting plastics. Stress related distortion problems are also not so significant. The spraying action is achieved by the rapid expansion of combustion gases (which transfer the momentum to the molten droplets) or by a separate supply of compressed air.

There are two basic ways of generating heat required for melting the consumables **[46, 47**].

(i) Combustion of a fuel gas

(ii) High energy electric arc

Thermal spraying processes divided into different categories.

2.4.6(i) Gas Combustion Processes

(a) Oxy-fuel/ wire

(b) Oxy-fuel / powder

(c) Detonation gun

(d) HVOF

2.4.6(ii) Arc Processes

(e) Electric arc

(f) Plasma arc

The processes mentioned above are discussed briefly in the following articles but plasma spraying has been discussed separately.

2.4.6 (i) (a) Flame Spraying with Wire

The arrangement is shown in figure 2.4, and the set-up consists of a spraying gun, a wire feeding arrangement, oxygen and acetylene gas cylinders and an air compressor [**25**]. A proportionate mixture of oxygen and acetylene is taken inside a chamber located in the gun itself, and the mixture is set ablaze. The flame comes out though the muzzle of the gun. The tip of the wire is fed to the flame which melts quickly and forms a droplet. A compressed air jet dislodges the molten droplet and carries it, in atomized form, to the target surface kept in front of the gun. Meanwhile the roller of the wire feeding arrangement rotates continuously at a fixed, preset speed to advance the wire to flame [**43, 46, 48, 49**]. The set up cost for flame spraying is quite low. Thick metallic layer can be deposited easily and hence it is quite useful for rebuilding purpose. But it is applicable to metallic materials only [**25**].

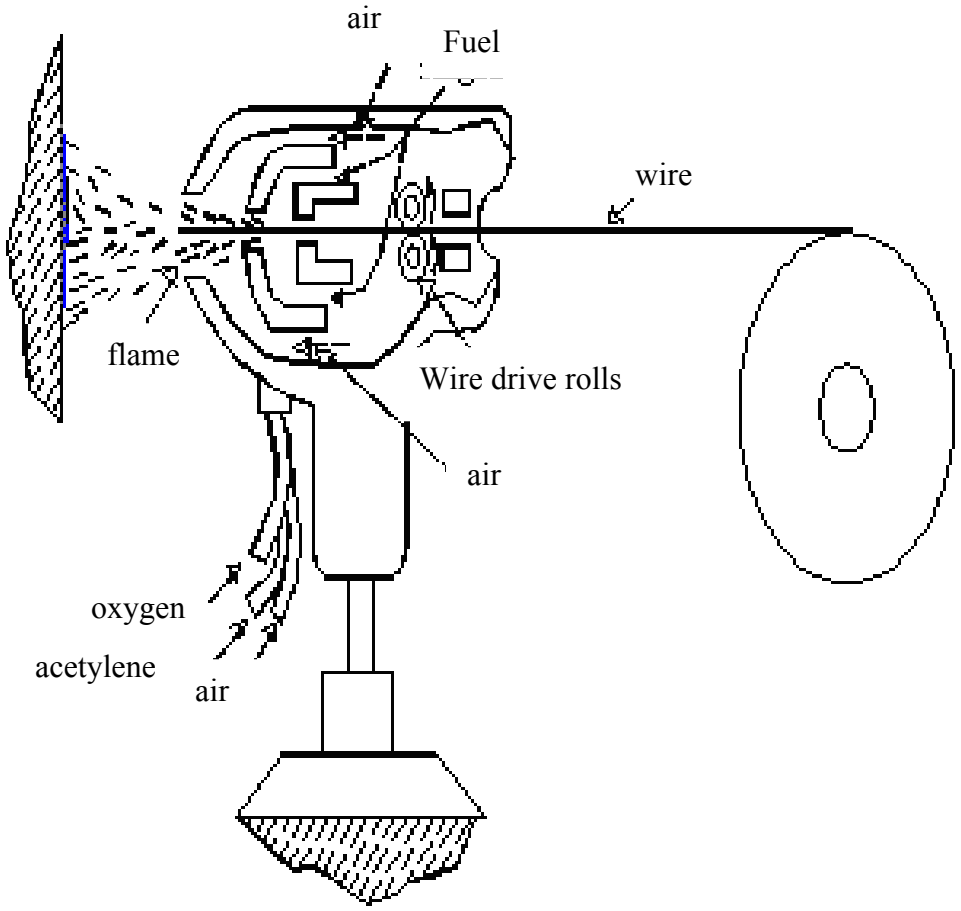

Fig. 2.4 Arrangement for the wire flame spraying.

2.4.6 (i) (b) Flame Spraying with Powder

The arrangement is shown in Figure 2.5. The process is carried out with a gun in which facility for fuel gas (oxy-acetylene) injection and powder storage are integrated. The flame is kept at a convenient distance from the substrate. The consumable-powders are kept inside the hopper integrated with the gun and can be released to the flame by the action of a trigger. The powder is gravity fed to the flame; it melts and deposits on to the substrate to form a coating. In some cases the flame is taken close to the coating immediately after deposition for further melting. In this case the bond strength achieved is higher, but the temperature of the substrate increases nsiderably **[25, 46,47].**

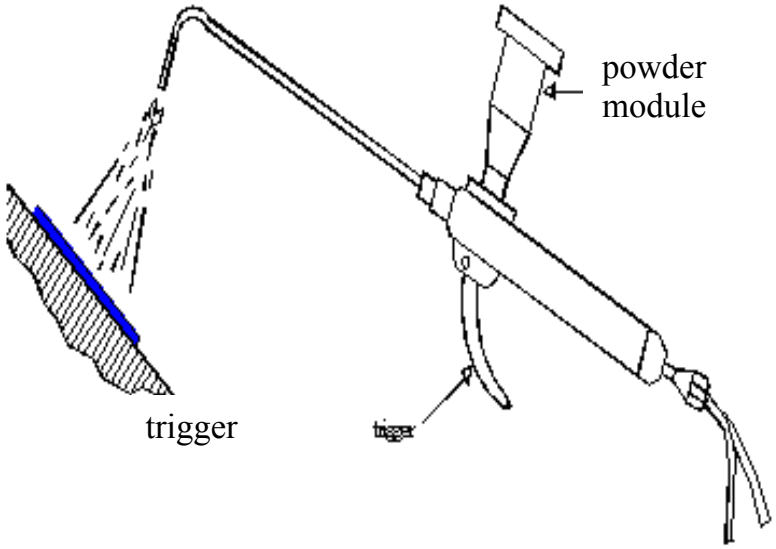

Fig. 2.5 Arrangement for the flame spraying with powders.

The equipment cost is low. A large number of alloys (even cermets) are available in powder form. But ceramic materials cannot be deposited by this method. The deposition rate is very slow.

2.4.6 (i) (c) Detonation Gun Coating

This is a proprietary coating process. The basic set up is shown in Figure 2.6. Consumable powder is fed into the gun under a small gas pressure. Valves are opened to allow oxygen and acetylene to enter the combustion chamber of the gun. The mixture is then detonated by the sparks from spark plugs and an explosion occurs immediately. The temperature of the detonation fuel is about 3800^0 C, and it is a sufficiently high temperature to melt most of the materials. Immediately after the detonation, hot particles (undergoing melting) rush toward the target at a very high velocity. This factor is very important for having a well-bonded, dense coating. Detonation cycles are repeated four to eight times per second and nitrogen gas is used to flush out the combustion products after each cycle.

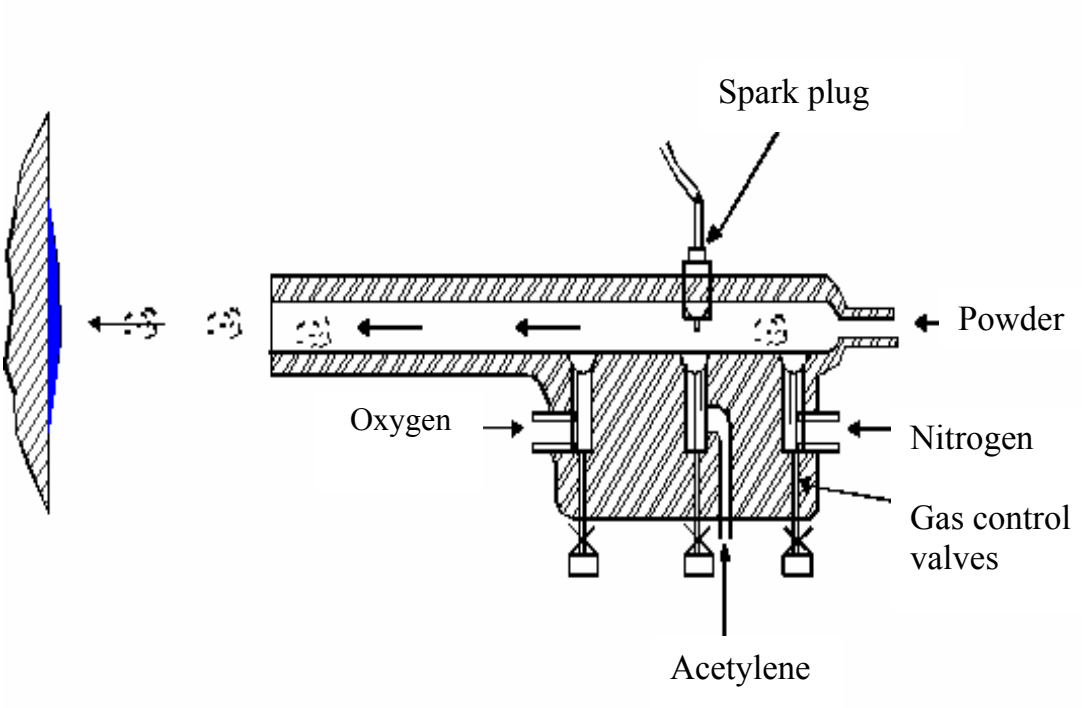

Fig. 2.6 Arrangement for the D-gun coating

This process produces very loud noise, and therefore the spraying is conducted inside a sound proof room. It also requires an elaborate arrangement for fuel and purge gas control, powder feeding, gun cooling and spark plug operation [**25, 46, and 47**]. Using this technique metals, alloys and ceramics can be melted .Well bonded and dense coating can be produced. But the process is expensive and involves very elaborate arrangement. The process also produces loud noise.

2.4.6(i) (d) High Velocity Oxy-Fuel Spraying (HVOF)

The arrangement is shown in Figure 2.7. Oxygen and fuel gas (propylene or hydrogen) mixture is introduced in the combustion chamber of the gun. It lights into a flame when ignited and the burnt gas acquires a very high temperature and escapes from the confinement of the small chamber at a high velocity in the process of expansion. The flame is at right angle to the muzzle of the gun. From one end of the gun, powder is fed in the center of the flame by a carrier gas.

The particles melt and are immediately carried to the target by the gas, escaping at a very high velocity through the nozzle of the gun [**50, 51, 52**]

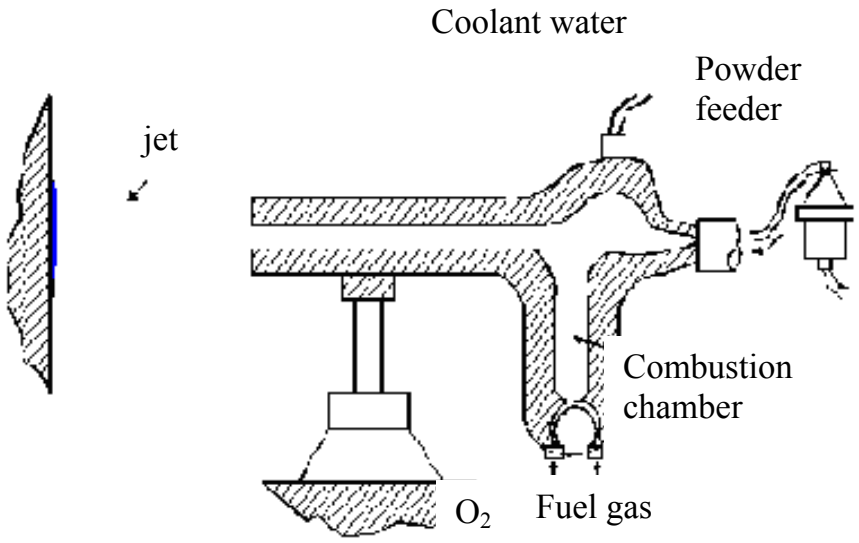

Fig. 2.7 Arrangement for the HVOF spraying

Advantages of this spraying technique include good substrate-coating adhesion, high coating density. It is applicable to both metals and ceramics. It involves less set up cost as compared to plasma or detonation gun.

2.4.6 (ii) (a) Electric Arc Spraying

The arrangement is shown in Figure 2.8. An electric arc is created between the tips of two conducting wires. The heat produced melts the tips and these molten tips are dislodged and directed to a target by a compressed air jet. The wires are fed by the independent wire feed mechanisms. Electric power is supplied by a rugged welding power supply. The process is capable of spraying at a very high deposition rate [**25, 53**].

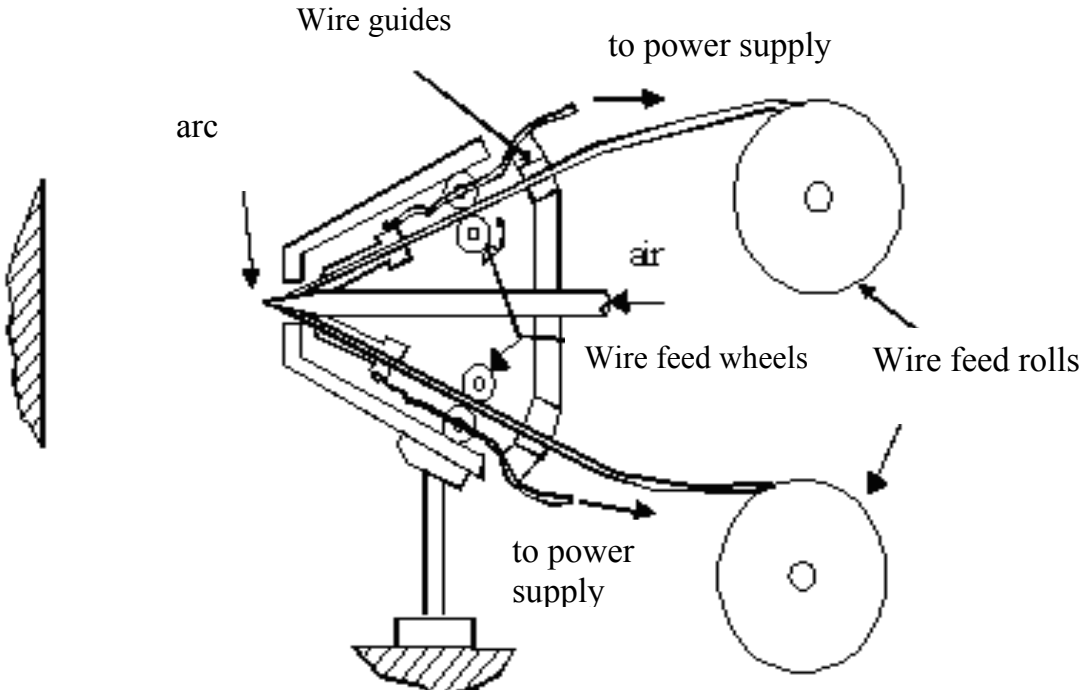

Fig. 2.8 Arrangement for the electric arc spraying

The set up for electric arc spraying is simple and cheap. But only conducting materials can be sprayed. The substrate-coating adhesion and density is not comparable to plasma spraying or detonation gun.

2.4.6(ii) (b) Plasma Spraying

Plasma spraying is the most versatile thermal spraying process and the general arrangement is shown in Figure 2.9. An arc is created between tungsten tipped copper cathode and an annular copper anode (both water cooled). Plasma generating gas is forced to pass through the annular space between the electrodes. While passing through the arc, the gas undergoes ionization in the high temperature environment resulting plasma. The ionization is achieved by collisions of electrons of the arc with the neutral molecules of the gas. The plasma protrudes out of the electrode encasement in the form of a flame. The consumable material, in the powdered form, is poured into the flame in metered quantity. The powders melt immediately

and absorb the momentum of the expanding gas and rush towards the target to form a thin deposited layer. The next layer deposits onto the first immediately after, and thus the coating builds up layer by layer [**3, 25, 43, 49**],

The coating-substrate interface bond mechanism is purely mechanical. Plasma spray deposits typically have lamellar structure with fine-grained microstructure within the lamellae.

The temperature in the plasma arc can be as high as $10{,}000^0$C and it is capable of melting anything. Elaborate cooling arrangement is required to protect the plasma gas from excessive heating. The equipment consists of the following modules [**54**].

The plasma gas:

It is the device which houses the electrodes and in which the plasma reaction takes place. It has the shape of a gun and it is connected to the water cooled power supply cables, powder supply hose and gas supply hose.

The power supply unit:

Normally plasma arc works in a low voltage (40-70 volts) and high current (300-1000 Amperes), DC ambient. The available power (AC, 3 phase, 440 V) must be transformed and rectified to suit the reactor. This is taken care of by the power supply unit.

The powder feeder:

The powder is kept inside a hopper. A separate gas line directs the career gas which fluidizes the powder and carries it to the plasma arc. The flow rate of the powder can be controlled precisely.

The coolant water supply unit: It circulates water into the plasma gas, the power supply unit, and the power cables. Units capable of supplying refrigerated water are also available.

The control unit:

Important functions (current control, gas flow rate control etc.) are performed by the control unit. It also consists of the relays and solenoid valves and other interlocking arrangements essential for safe running of the equipment. For example the arc can only be started if the coolant supply is on and water pressure and flow rate is adequate.

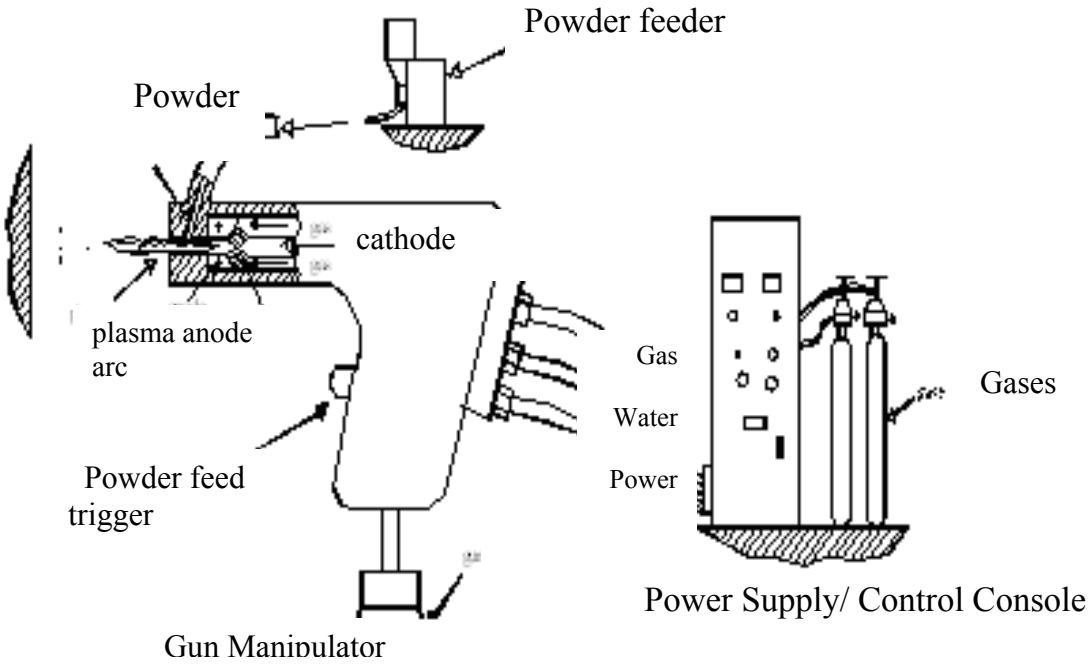

Fig. 2.9 Arrangement for the plasma spraying

The Requirements for Plasma Spraying

Roughness of the substrate surface:

A rough surface provides a good coating adhesion. A rough surface provides enough room for anchorage of the splats facilitating bonding through mechanical interlocking. A rough surface is generally created by shot blasting technique. The shots are kept inside a hopper, and compressed air is supplied at the bottom of the hopper. The shots are taken afloat by the compressed air stream into a hose and ultimately directed to an object kept in front of the exit nozzle of the hose. The shots used for this purpose are irregular in shape, highly angular in nature, and made up of hard material like alumina, silicon carbide, etc. Upon impact they create small craters on the surface by localized plastic deformation, and finally yield a very rough and

highly worked surface. The roughness obtained is determined by shot blasting parameters, i.e., shot size, shape and material, air pressure, standoff distance between nozzle and the job, angle of impact, substrate material etc. [**55**] . The effect of shot blasting parameters on the adhesion of plasma sprayed alumina has been studied [**52, 56**]. Mild steel serves as the substrate material. The adhesion increases proportionally with surface roughness and the parameters listed above are of importance. A significant time lapse between shot blasting and plasma spraying causes a marked decrease in bond strength [**57**].

Cleanliness of the substrates:

The substrate to be sprayed on must be free from any dirt or grease or any other material that might prevent intimate contact of the splat and the substrate. For this purpose the substrate must be thoroughly cleaned (ultrasonically, if possible) with a solvent before spraying. Spraying must be conducted immediately after shot blasting and cleaning. Otherwise on the nascent surfaces, oxide layers tend to grow quickly and moisture may also affect the surface. These factors deteriorate the coating quality drastically [**57**].

Bond coat:

Materials like ceramic cannot be sprayed directly onto metals, owing to a large difference between their thermal expansion coefficients. Ceramics have a much lower value of α and hence undergo much less shrinkage as compared to the metallic base to form a surface in compression. If the compressive stress exceeds a certain limit, the coating gets peeled off. To alleviate this problem a suitable material, usually metallic of intermediate a value is plasma sprayed on to the substrate followed by the plasma spraying of ceramics. Bond coat may render itself useful for metallic top coats as well. Molybdenum is a classic example of bond coat for metallic top coats. Molybdenum adheres very well to the steel substrate and develops a somewhat rough top surface ideal for the top coat spraying. The choice of bond coats depends upon the application. For example, in wear application, an alumina and Ni-AI top and bond coats combination can be used [**58**]. In thermal barrier application, CoCrAlY or Ni-AI bond coat [**59**] and zirconia top coat are popular. Ceramic coatings when subjected to hertzian loading deform elastically and the metallic substrate deforms plastically. During unloading, elastic recovery of the coating takes place, whereas for the metallic substrate a permanent set has already taken place. Owing to this

elastoplastic mismatch the coating tends to spall off at the interface. A bond coat can reduce this mismatch as well [**60**].

Cooling water:

For cooling purpose distilled water should be used, whenever possible. Normally a small volume of distilled water is recirculated into the gun and. it is cooled by an external water supply from a large tank. Sometime water from a large external tank is pumped directly into the gun [**54**].

Process parameters in plasma spraying

In plasma spraying one has to deal with a lot of process parameters, which determine the degree of particle melting, adhesion strength and deposition efficiency of the powder [**61**]. Deposition efficiency is the ratio of amount of powder deposited to the amount fed to the gun. An elaborate listing of these parameters and their effects are reported in the literature [**62-65**].

Some important parameters and their roles of plasma spraying are listed below:

Arc power:

It is the electrical power drawn by the arc. The power is injected in to the plasma gas, which in turn heats the plasma stream. Part of the power is dissipated as radiation and also by the gun cooling water. Arc power determines the mass flow rate of a given powder that can be effectively melted by the arc. Deposition efficiency improves to a certain extent with an increase in arc power, since it is associated with an enhanced particle melting [**57, 62, 66**]. However, increasing power beyond a certain limit may not cause a significant improvement. On the contrary, once a complete particle melting is achieved, a higher gas temperature may prove to be harmful. In the case of steel, at some point vaporization may take place lowering the deposition efficiency.

Plasma gas:

Normally nitrogen or argon doped with about 10% hydrogen or helium is used as a plasma gas. The major constituent of the gas mixture is known as primary gas and the minor is

known as the secondary gas. The neutral molecules are subjected to the electron bombardment resulting in their ionization. Both temperature and enthalpy of the gas increase as it absorbs energy. Since nitrogen and hydrogen are diatomic gases, they first undergo dissociation followed by ionization. Thus they need higher energy input to enter the plasma state. This extra energy increases the enthalpy of the plasma. On the other hand, the mono-atomic plasma gases, i.e. argon or helium, approach a much higher temperature in the normal enthalpy range. Good heating ability is expected from them for such high temperature [**67**]. In addition, hydrogen followed by helium has a very high specific heat, and therefore is capable of acquiring very high enthalpy. When argon is doped with helium the spray cone becomes quite narrow which is especially useful for spraying on small targets.

Carrier gas:

Normally the primary gas itself is used as a carrier gas. The flow rate of the career gas is an important factor. A very low flow rate cannot convey the powder effectively to the plasma jet, and if the flow rate is very high then the powders might escape the hottest region of the jet. There is an optimum flow rate for each powder at which the fraction of unmelted powder is minimum and hence the deposition efficiency is maximum [**62**].

Mass flow rate of powder:

Ideal mass flow rate for each powder has to be determined. Spraying with a lower mass flow rate keeping all other conditions constant results in under utilization and slow coating buildup. On the other hand, a very high mass flow rate may give rise to an incomplete melting resulting in a high amount of porosity in the coating. The unmelted powders may bounce off from the substrate surface as well keeping the deposition efficiency low [**61, 62].**

Torch to base distance:

It is the distance between the tip of the gun and the substrate surface. A long distance may result in freezing of the melted particles before they reach the target, whereas a short standoff distance may not provide sufficient time for the particles in flight to melt [**57, 62**]. The relationship between the coating properties and spray parameters in spraying alpha alumina has been studied in details [**68**]. It is found that the porosity increases and the thickness of the coating

(hence deposition efficiency) decreases with an increase in standoff distance. The usual alpha-phase to gamma-phase transformation during plasma spraying of alumina has also been restricted by increasing this distance. A larger fraction of the unmelted particles go in the coating owing to an increase in torch to base distance.

Spraying angle :

This parameter is varied to accommodate the shape of the substrate. In coating alumina on mild steel substrate, the coating porosity is found to increase as the spraying angle is increased from 30° to 60°. Beyond 60° the porosity level remains unaffected by a further increase in spraying angle [**69]**. The spraying angle also affects the adhesive strength of the coating [**70, 71**]. The influence of spraying angle on the cohesive strength of chromia, zirconia 8-wt% yttria and molybdenum has been investigated, and it has been found that the spraying angle does not have much influence on the cohesive strength of the coatings [**72**].

Substrate cooling:

During a continuous spraying, the substrate might get heated up and may develop thermal-stress related distortion accompanied by a coating peel-off. This is especially true in situations where thick deposits are to be applied. To harness the substrate temperature, it is kept cool by an auxiliary air supply system. In addition, the cooling air jet removes the unmelted particles from the coated surface and helps to reduce the porosity [**57**].

Powder related variables:

These variables are powder shape, size and size distribution, processing history, phase composition etc. They constitute a set of extremely important parameters. For example, in a given situation if the powder size is too small it might get vaporized. On the other hand a very large particle may not melt substantially and therefore will not deposit. The shape of the powder is also quite important. A spherical powder will not have the same characteristics as the angular ones, and hence both could not be sprayed' using the same set of parameters [**49, 73, 74**].

Preheating of the substrate:

The nascent shot blasted surface of the substrate absorbs water and oxygen immediately after shot blasting. Before spraying, the substrate should be preheated to remove moisture from the surface and also for a sputter cleaning effect of the surface by the ions of the plasma [**57**].

Angle of powder injection:

Powders can be injected into the plasma jet perpendicularly, coaxially, or obliquely. The residence time of the powders in the plasma jet will vary with the angle of injection for a given carrier gas flow rate. The residence time in turn will influence the degree of melting of a given powder. For example, to melt high melting point materials a long residence time and hence oblique injection may prove to be useful. The angle of injection is found to influence the cohesive and adhesive strength of the coatings as well [**54**].

2.5 PLASMA SPRAYING AND ITS INDUSTRIAL APPLICATIONS

Plasma spraying has certain unique advantages over other competing surface engineering techniques. By virtue of the high temperature (10,000-15,000K) and high enthalpy available in the thermal plasma jet, any powder, which melts without decomposition or sublimation, can be coated keeping the substrate temperature as low as 50^0C. The coating process is fast and the thickness can go from a few tens of microns to a few mm. Plasma spraying is extensively used in hi-tech industries like aerospace, nuclear energy as well as conventional industries like textiles, chemicals, plastics and paper mainly as wear resistant coatings in crucial components.

There has been a steady growth in the number of applications of thermally sprayed coatings. Availability of hardware and adaptability of the technique are the most important factors for this growth. Plasma spraying has been successfully applied to a wide range of industrial technologies. Automotive industry, aerospace industry, nuclear industry, textile industry, paper industry and iron and steel industry are some of the sectors that have successfully exploited thermal plasma spray technology [**75, 76**].

The main uses of plasma spray coating are shown in the tables given below:

- Automotive Industry and the production of Combustion engines
- Glass Industry
- Hydraulic equipment
- Chemical Industry
- Air craft jet engine

Automotive Industry and the production of Combustion engines:

Plasma sprayed coatings used, in automotive industries of many industrially advanced countries, endure higher working pressure and temperature to improve wear resistance, good friction properties, resistance against burn-off and corrosion due to hot combustion products and resistance against thermal loading.

Some of the several applications developed for the automotive industry at the Slovak Academy of Sciences (SAV) in Bratislava are spraying torsion bars with aluminium coatings against corrosion. The plasma spraying technology is introduced in the production of gear-shift forks for gear boxes in fiat car factory and on the critical parts of big Diesel engines. The coating materials and their advantages are given below, Table 2.1.

Glass Industry:

Molten glass quickly wears the surface of metal which comes in contact with it. In order to protect the metal tools, plasma sprayed coatings are made onto it. The machine parts, typical coatings used and their advantages are tabulated below, Table 2.2.

Critical machinery parts	Typical coatings applied	Advantages
Steel piston rings	Friction surface sprayed with Mo or other alloys type Mo+NiCrBSi, Mo+Chromium Carbide+NiCr, Al_2O_3+TiO_2	Engine speed increases. The variation of speed of the engine depends upon the type pf coating material to be sprayed. Shelf life of piston ring increases. Coating (especially Mo) provides good plasticity, resistance against seizing & is easily hardened by hammering at engine run. The porosity of Mo layer ensures excellent sliding property and self-lubrication.
Gear-shift forks for gear boxes	Bronze forks replaced with steel, coated with a layer of bronze 0.4mm over a bond coat Fe Al.	Wear resistance increases
Synchron rings in gear boxes & on crank-shaft pins	Mo alloy coating is applied on the frictional surfaces	Improves friction wear resistance
Ship engine valves	Al_2O_3+TiO_2+Y_2O_3 on valve shanks	Improve wear resistance & thermal insulation
	NiCrAl on valve heads	Improve resistance against high temperature corrosion
	ZrO_2+Y_2O_3 on valve discs	Improve thermal insulation & resistance against high temperature corrosion

Table 2.1 Application of plasma spray coating in Automotive Industry.

Machine tools	Typical coatings applied	Advantages
Cast iron pressing mandrels used for production of goblets, bowls and other utility glass products	Ni-Al coating sprayed 0.15 to 0.3 mm thick	Protect the base metal from the thermal, abrasive and corrosive effects of molten glass, hence increasing the shelf life of machine tools.
	Thermally insulating and wear resistant ceramic coatings, e.g. $ZrSiO_4$, ZrO_2, Al_2O_3	Prevent sticking of molten glass
Plungers of glass melting, dip rings & pans and on the lining of platinum furnaces for glass fiber production.	Heat resistance coatings, $ZrSiO_4$, ZrO_2+SiO_2+Y_2O_3	Protect the parts of equipments and Reduces the loss due to diffusion of $PtRh_7$ alloy into the lining material in glass fiber production.
Glassmaking water cooled mandrels for production of packing glass	Wear resistance coatings, WC-Co, Al_2O_3+TiO_2, NiCrBSi alloys	Prolonged the life of parts

Table -2.2 Application of plasma spray coating in Glass industry.

Hydraulic machines and mechanisms:

The range of possible applications in this field is very extensive, mainly in water power plants, in production and work of pumps, where many parts are subjected to combined effects of wear, corrosion, erosion and cavitations. Specific applications in this field are mentioned below, Table 2.5.

Critical parts	Typical coatings	Advantages
Turbine blades	WC, Al_2O_3	Resistance against cavitations.
Pump parts	Seal bushings of stainless steel sprayed with $ZrSiO_4$. This working layer is sprayed on a NiAl interlayer.	Wear resistance with extraordinary corrosion resistance in pumping H_2SO_4 in chemical plants.
Piston rod of Hydraulic cylinders	Coating of Cr_2O_3 or NiCrBSi is made. Steel rods coated with bronze layer replace all bronze.	Reduces frictional wear and also contribute in saving of non-ferrous metals.

Table 2.3 Application of plasma spray coating in Hydraulic Equipment.

Chemical Plants:

The base metal of machine parts is subjected to different kind of wear in chemical plants. In such cases plasma sprayed coatings are applied to protect the base metal. They can be used for various blades, shafts, bearing surfaces, tubes, burners, parts of cooling equipments etc.Few specific applications are tabulated below, Table 2.4.

Aircraft Jet engines:

The working parts of Aircraft jet engines are subjected to serve mechanical, chemical and thermal stresses. A jet engine has a number of construction nodes where plasma coating is employed with much success in order to protect them. There are for example, face of the blower box, compressor box and disc, guide bearing, fuel nozzles, blades, combustition chambers. Few specific applications are tabulated below, Table 2.5.

Critical parts	Typical coatings	Advantages
Blades of a chemical mixer	NiCrBSi	Increases wear resistance of surfaces.
Roll for the production of plastic foils	Al_2O_3	Increases wear resistance of surfaces and keep the foil from adhering to the surface.
Fan blades		Increases resistance against abrasion and aggressive vapors
Polymer Cutter Nozzle worn by rotary friction movement during the production of granulated polymer	Cutter nozzle sprayed with WC+ 12% Co deposited on the annulus	WC having the property of hard, tough and wear resistance prolongs the life of equipment.
Induction Flow meter	$ZrSiO_4$ on the internal surfaces	Provide resistance to wear, hot and corrosion of aggressive fluids like NH_4NO_3,NH_4OH and the meter functions properly forming a dielectric layer

Table 2.4 Application of Plasma Spray Coating in Chemical Industries

Critical parts	Typical coatings	Advantages
Different running and stationary blades of jet engines	MCrAlY, NiCrAlY, FeCrAlY, CoNiCrAlY	To protect from the adverse environment of high pressure and high temperature.
Combustition chambers and guide blades	ZrO_2+MgO,ZrO_2+Y_2O_3 as working layer and NiCr as self bonding layer	Heat resistance

Table 2.5 Application of plasma spray coating in Air craft jet Engine.

2.6 METALLIC COATINGS

Metallic coatings can be easily applied by flame spraying or welding techniques making the process very economical. Moreover plasma sprayable metallic consumables are also available in abundant quantity. Metallic wear resistant materials are classified into three categories:

(i) Cobalt based alloys

(ii) Nickel based alloys

(iii) Iron based alloys

The common alloying elements in a cobalt-based alloy are Cr, Mo, W and Si. The microstructure is constituted by dispersed carbides of M_7C_3 type in a cobalt rich FCC matrix. The carbides provide the necessary abrasion resistance and corrosion resistance. Hardness at

elevated temperatures is retained by the matrix [**77, 78**]. Sometimes a closed packed intermetallic compound is formed in the matrix, which is known as the Laves phase. This phase is relatively soft but offers significant wear resistance [**79**]. The principal alloying elements in Ni-based alloys are Si, B, C and Cr. The abrasion resistance can be attributed to the formation of extremely hard chromium borides. Besides carbides, Laves phase is also present in the matrix [**77**].

Iron based alloys are classified into pearlitic steels, austenitic steels, martensitic steels and high alloy irons. The principal alloying elements used are Mo, Ni, Cr and C. The softer materials, e.g., ferritic, are for rebuilding purpose. The harder materials, e.g., martensitic, on the other hand provide wear resistance. Such alloys do not posses much corrosion, oxidation or creep resistance [**77, 80, 81]**. Nickel aluminide is another example of coating material for wear purpose. The pre alloyed Ni-Al powders, when sprayed, react exothermically to form nickel aluminide. This reaction improves the coating substrate adhesion. In addition to wear application, it is also used as bond coat for ceramic materials [**59**].

NiCoCrAlY is an example of plasma sprayable super alloy. It shows an excellent high temperature corrosion resistance and hence finds application in gas turbine blades. The compositional flexibility of such coatings permits tailoring of such coating composition for both property improvement and coating substrate compatibility. In addition, it serves as a bond coat for zirconia based thermal barrier coatings [**82**].

2.7 IRON ALUMINIDE

The Fe-Al based alloys offer unique benefits of excellent oxidation and sulfidation resistance at a potential cost lower than many stainless steels. Such benefits of Fe-Al based alloys have been observed since the 1930's [**123**] However, development of these materials has been limited by, at least two major issues:

- Poor room-temperature (RT) ductility and
- Low high- temperature strength.

Recent understanding of environmental effects on RT ductility of these alloys has led to progress toward taking commercial advantage of good properties of Fe_3Al-based materials. The cause of low ductility appears to be related to hydrogen formed from the reaction of aluminum in the alloy with moisture in the air.

$$2Al + 3H_2O \rightarrow Al_2O_3 + 6H$$

The environmental effect has been reduced in these intermetallic alloys by two methods. The first deals with producing a more hydrogen-resistant microstructure through thermo-mechanical processing and the second has dealt with compositional modification.

The alloys shows reduced environmental effect have been melted and processed by many different methods. These materials have been tested for their aqueous corrosion response in various media and their resistance to stress corrosion cracking. Oxidation and sulfidation data have been generated over a range of compositions. Several commercial applications have been identified for the newly developed iron aluminides. The potential applications are tabulated below. [**83**]

Applications	Component systems
Heating elements	Toasters, stoves, Ovens, Cigarette lighters & dryers
Regenerator Disks	Automotive gas-turbine engines
Wrapping wire	Insulation wrapping for investment casting molds
Hot-gas filters	Coal gasification systems
Tooling	Dies for super plastic forming of titanium based alloys
Shields	Coal-fired power plants to protect the super heater and reheated tubes.
Molten metals	Sensor sheathing material for molten aluminum, zirconium and cadmium
Others	Components needing high temperature sulfidation and oxidation resistance.

Table 2.6 Commercial applications newly developed iron aluminides.

Fe-Al is currently of commercial interest because of its excellent oxidation resistance, retention of good strength to intermediate temperatures and its low density. The mechanical behaviour of Fe-Al depends strongly on both temperature and Fe: Al ratio.

2.8 WEAR

Loss of material occurs as a natural consequence when two surfaces with a relative motion interact with each other. Wear may be defined as the progressive loss of material from contacting surfaces in relative motion. Scientists have developed various mechanisms/ theories for describing wear process in which the Physico-Mechanical characteristics of the materials and the physical conditions (e.g. the resistance of the rubbing body and the stress state at the contact area etc.) are taken in to consideration. In 1940 Holm [**84]** starting from the atomic mechanism of wear, calculated the volume of substance worn over unit sliding path.

Wear of metals is probably the most important yet at least understood aspects of tribology. It is certainly the youngest of the tri of topics, friction, lubrication and wear, to attract scientific attention, although its practical significance has been recognizes throughout the ages.

Wear is not an intrinsic material property but characteristics of the engineering system which depend on load, speed, temperature, hardness, presence of foreign material and the environmental condition [**85**]. Widely varied wearing conditions causes wear of materials. It may be due to surface damage or removal of material from one or both of two solid surfaces in a sliding, rolling or impact motion relative to one another. In most cases wear occurs through surface interactions at asperities. During relative motion, material on contacting surface may be removed from a surface, may result in the transfer to the mating surface, or may break loose as a wear particle. The wear resistance of materials is related to its microstructure may take place during the wear process and hence, it seems that in wear research emphasis is placed on microstructure [**86**]. Wear of metals depends on many variables, so wear research programs must be planned systematically. Therefore researchers have normalized some of the data to make them more useful. The wear map proposed by Lim and Ashby [**85**] is very much useful in this regard to understand the wear mechanism in sliding wear, with or without lubrication.

2.8.1 TYPES OF WEAR

In most basic wear studies where the problems of wear have been a primary concern, the so-called dry friction has been investigated to avoid the influences of fluid lubricants.

Dry friction' is defined as friction under not intentionally lubricated conditions but it is well known that it is friction under lubrication by atmospheric gases, especially by oxygen [**87**].

A fundamental scheme to classify wear was first outlined by Burwell and Strang [**88**]. Later Burwell [**89**] modified the classification to include five distinct types of wear, namely (1) Abrasive (2) Adhesive (3) Erosive (4) Surface fatigue (5) Corrosive.

2.8.1 (a) Abrasive wear

Abrasive wear can be defined as wear that occurs when a hard surface slides against and cuts groove from a softer surface. It can be account for most failures in practice. Hard particles or asperities that cut or groove one of the rubbing surfaces produce abrasive wear. This hard material may be originated from one of the two rubbing surfaces. In sliding mechanisms, abrasion can arise from the existing asperities on one surface (if it is harder than the other), from the generation of wear fragments which are repeatedly deformed and hence get work hardened for oxidized until they became harder than either or both of the sliding surfaces, or from the adventitious entry of hard particles, such as dirt from outside the system.As shown in fig.2.10.

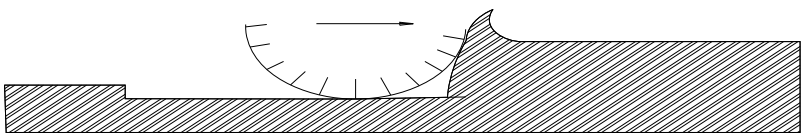

Fig. 2.10 Schematic representations of the abrasion wear mechanism

Two body abrasive wear occurs when one surface (usually harder than the second) cuts material away from the second, although this mechanism very often changes to three body abrasion as the wear debris then acts as an abrasive between the two surfaces. Abrasives can act as in grinding where the abrasive is fixed relative to one surface or as in lapping where the abrasive tumbles producing a series of indentations as opposed to a scratch. According to the recent tribological survey, abrasive wear is responsible for the largest amount of material loss in industrial practice [**90**].

(b) Adhesive wear

Adhesive wear can be defined as wear due to localized bonding between contacting solid surfaces leading to material transfer between the two surfaces or the loss from either surface. For adhesive wear to occur it is necessary for the surfaces to be in intimate contact with each other. Surfaces, which are held apart by lubricating films, oxide films etc. reduce the tendency for adhesion to occur.As shown in fig .2.11.

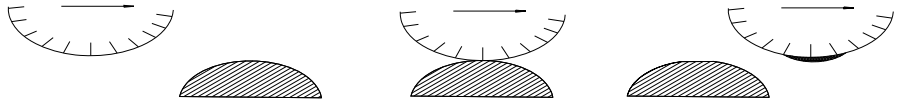

Fig .2.11 Schematic representations of the adhesive wear mechanism

(c) Erosive wear

Erosive wear can be defined as the process of metal removal due to impingement of solid particles on a surface. Erosion is caused by a gas or a liquid, which may or may not carry, entrained solid particles, impinging on a surface. When the angle of impingement is small, the wear produced is closely analogous to abrasion. When the angle of impingement is normal to the surface, material is displaced by plastic flow or is dislodged by brittle failure.As shown in fig.2.12.

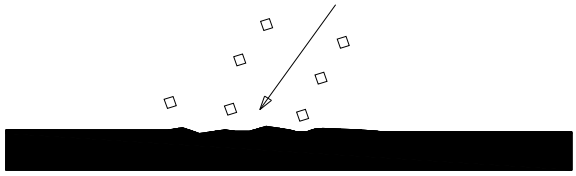

Fig. 2.12 Schematic representations of the erosive wear mechanism

(d) Surface fatigue wear

Wear of a solid surface caused by fracture arising from material fatigue. The term 'fatigue' is broadly applied to the failure phenomenon where a solid is subjected to cyclic loading involving tension and compression above a certain critical stress. Repeated loading causes the generation of micro cracks, usually below the surface, at the site of a pre-existing point of weakness. On subsequent loading and unloading, the micro crack propagates. Once the crack reaches the critical size, it changes its direction to emerge at the surface, and thus flat sheet like particles is detached during wearing. The number of stress cycles required to cause such failure decreases as the corresponding magnitude of stress increases. Vibration is a common cause of fatigue wear.As shown in fig.2.13.

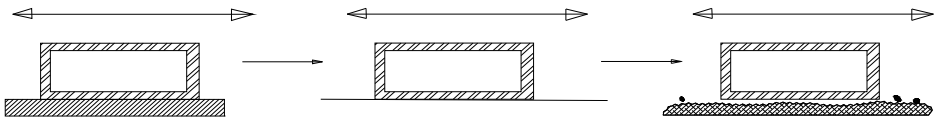

Fig. 2.13 Schematic representations of the surface fatigue wear mechanism

(e) Corrosive wear

Most metals are thermodynamically unstable in air and react with oxygen to form an oxide, which usually develop layer or scales on the surface of metal or alloys when their interfacial bonds are poor. Corrosion wear is the gradual eating away or deterioration of unprotected metal surfaces by the effects of the atmosphere, acids, gases, alkalis, etc. This type of wear creates pits and perforations and may eventually dissolve metal parts.

2.9 EROSION WEAR OF METALLIC COATINGS

The loss of material caused by the impingement of material on substrate surface is called erosive wear [**91**]. Erosion is a serious problem in many engineering systems, including steam and jet turbines, pipelines and valves used in slurry transportation of matter, and fluidized bed combustion systems [**92**]. Gas and steam turbines operate in environments where the ingestion of solid particles is inevitable. In industrial applications and power generation, such as coal-burning boilers, fluidized beds, and gas turbines, solid particles are produced during the combustion of heavy oils, synthetic fuels, and pulverized coal and causes erosion of materials. In such environments, protective coatings on the surface of super alloys are frequently used [**92, 94**]. These may include the enhancement of mechanical properties, visual appearance or corrosion resistance or may provide special magnetic and optical properties; the mechanisms of coating damage in this type of test depend on the coating material and its thickness, the properties of the interface, the substrate material and the test conditions [**95**].

Solid Particle Erosion (SPE) is a wear process where particles strike against surfaces and promote material loss. During flight a particle carries momentum and kinetic energy, which can be dissipated during impact, due to its interaction with a target surface. Different models have been proposed that allow estimations of the stresses that a moving particle will impose on a target [**96]**. It has been experimentally observed by many investigators that during the impact the target can be locally scratched, extruded, melted and/or cracked in different ways [**97, 98 and 99**]. The imposed surface damage will vary with the target material, erodent particle, impact angle, erosion time, particle velocity, temperature and atmosphere [**99, 100**].

Plasma sprayed coatings are used today as erosion or abrasion resistant coatings in a wide variety of applications [**101**]. Extensive research shows that the deposition parameters like energy input in the plasma and powder properties affect the porosity, splat size, phase composition, hardness etc. of plasma sprayed coatings [**102-106**]. These in turn, have an influence on the erosion wear resistance of the coatings. Quantitative studies of the combined erosive effect of repeated impacts are very useful in predicting component lifetimes, in comparing the performance of materials and also in understanding the underlying damage mechanisms involved.

Resistance of engineering components encountering the attack of erosive environments during operation can be improved by applying metallic coatings on their surfaces. Fe based coatings are used in applications when wear resistance combined with oxidation or hot corrosion resistance is required. Fe based alloys represent a significant part of overall thermal spray business. These materials are widely used as bond coats and top coats in number of applications requiring combination of properties, such as good wear resistance and corrosion resistance at the same time.

2.10 RECENT STUDIES ON IRON ALUMINIDE

A recent experimental study has done by Thierry Grosdidier et al. [**107**] On Synthesis of bulk FeAl nanostructured materials by HVOF spray forming and Spark Plasma Sintering where two consolidation processing techniques: has taken i.high Velocity Oxy-Fuel (HVOF) spray forming and ii Spark Plasma Sintering (SPS) to obtain bulk nanostructured materials from an Y_2O_3 reinforced Fe-40Al (at.%) milled powder. By studying their microstructure formation mechanisms they concluded that HVOF spray forming is more effective to retain fine nanograins, in particular within retained unmelted powder particles. Comparatively, SPS has a much higher potential to create submicrometer microstructures within which the oxides are more homogeneously distributed.

Binshi Xua, , Zixin Zhua etal [**108**] studied on Sliding wear behavior of Fe–Al and Fe–Al/WC coatings prepared by high velocity arc spraying the microstructure and tribological

behavior of Fe–Al and Fe–Al/WC iron aluminide based coatings against Si_3N_4 under dry sliding at room temperature using a pin-on-disc tribotester. The coatings were prepared by high velocity arc spraying (HVAS) and cored wires. The effect of normal load on friction coefficient and wear rate of the coatings was studied. They showed that, the main phases in both coatings were mainly iron aluminide (Fe_3Al and FeAl) and α. WC/W_2C particles were embedded in the matrix of the composite coating. With adding WC hard particles, the Fe–Al/WC composite coating exhibited higher wear-resistance than Fe–Al coating.

A Study by J.M. Guilemany a, et al [**109]** suggested that when Fe–40Al coatings are obtained by high velocity oxy-fuel, Interesting properties that intermetallics possess have made them to be promising materials to be used either as bulk materials or as coatings, both at medium or elevated temperature environments. This group of materials possesses a long-range order, which can be kept by some intermetallics until their melting point, which is the main reason why they possess a good stability at high temperatures. Some other properties can be summarized as follows: high thermal conductivity; low density; great strength, particularly at high temperatures; good oxidation resistance at high temperatures (because of the formation of oxide films); low ductility, brittle fracture at room temperature.

T. Grosdidiera,c,et al [**110**] produced a thick nanostructured and microstructured FeAl deposits by Spray forming and they obtained a thick freestanding nanostructured deposit (5 mm) and Compare it with the microstructure obtained in a thin (300 mm) both by HVOF and discuss the effect of the processing conditions on microstructure formation and associated hardness.

C. Houngninou, et al [**111**], Synthesized and characterized a pack cemented aluminide coatings on metals and studied the exposition of metallic materials to high temperature environments leads to their corrosion because of oxidation or sulphidation. One way to protect such materials is to produce an Al_2O_3 layer which needs to be continuous enough to limit diffusion of oxygen or metallic elements, and withstand this corrosion. Since a few years, it has been proved that aluminide compounds are one of the most effective materials to achieve this goal. Indeed, they possess sufficient Al and many beneficial mechanical properties when exposed to high temperature conditions to make possible the formation of a protective Al_2O_3

scale. This study is aimed at the elaboration of iron, nickel and molybdenum aluminides by modification of the surface of the base materials by a pack cementation process.

M. Martinez etal [**112**] Related between composition, microstructure and oxidation in iron aluminides studied the relation between chemical composition, microstructure and oxidation properties has been investigated on various FeAl based alloys, the aim being to induce changes in the microstructure of the compound by selective oxidation of aluminium. Oxidation kinetics that was evaluated on bulk specimens showed that, due to fast diffusion in the alloys, no composition gradient is formed during the aluminium selective oxidation. Accordingly, significant aluminium depletion in the compound could be observed in the thinnest part of oxidized wedge-shape specimens. Another way to obtain samples of variable aluminium content was to prepare diffusion couples with one aluminide and pure iron as end members.

Against with this few backgrounds, the present research work has been undertaken, with an objective to explore the coating potential of iron aluminide. Attempts have been made in this work to deposit iron aluminide coatings on metal substrates at various operating conditions of plasma and to establish their suitability for some typical tribological applications.

The future possesses challenges to the scientists, technologists and engineers towards sound management of iron aluminide coating. It will continue to be an important area of concern in coming years. The present investigation is a step in this direction.

CHAPTER 3
MATERIALS AND METHODS

3.1 INTRODUCTION

This chapter deals with the details of the experimental procedures followed in this study. The coating procedure itself requires some basic preparation, i.e., shot blasting and cleaning. After plasma spraying, the coated materials have been subjected to a series of tests,e.g.,microstuctural characterization of the surfaces and cross sections, microhardness measurement,X-ray diffraction studies, adhesion test, erosion wear test etc. The details of each process are described here.

3.2 PROCESSING OF THE COATINGS

3.2.1 Substrate preparation

Commercially available copper and mild steel have been chosen as different substrate materials. The specimens are rectangular having a dimension 50 mm x 25 mm x 3 mm. The specimens are grit blasted at a pressure of 3 kg/cm^2 using alumina grits having a grit size of 60. The standoff distance in shot blasting is kept between 120-150 mm. The average roughness of the substrates is 6.8 μm. The grit blasted specimens are cleaned with acetone in an ultrasonic cleaning unit. Spraying is carried out immediately after cleaning.

3.2.2 Powder preparation

Fe-Al powders are milled in a planetary ball mill for 3 hours to get a homogenous mixture. In this study Fe-Al Powders in the size range 40 to 100 micrometer mostly about 75 micrometer are used as raw powder for coating deposition at various substrate.

3.3 DEVLOPMENT OF COATING

Plasma spraying is a process that combines particle melting, quenching and consolidation in a single operation. The process involves injection of powder particles (metallic, ceramic or cermet powders) into the plasma jet created by heating an inert gas in an electric arc confined within a Water-cooled nozzle. The temperature at the core of the plasma jet is 10,000-15,000 ^{0}K. The particles injected into the plasma jet undergo rapid melting and at the same time

are accelerated. These molten droplets moving at high velocities (exceeding 100 mt/sec) impact on the surface of the substrate forming adherent coating. Fig 3.1 shows the Schematic diagram of the plasma spraying process.

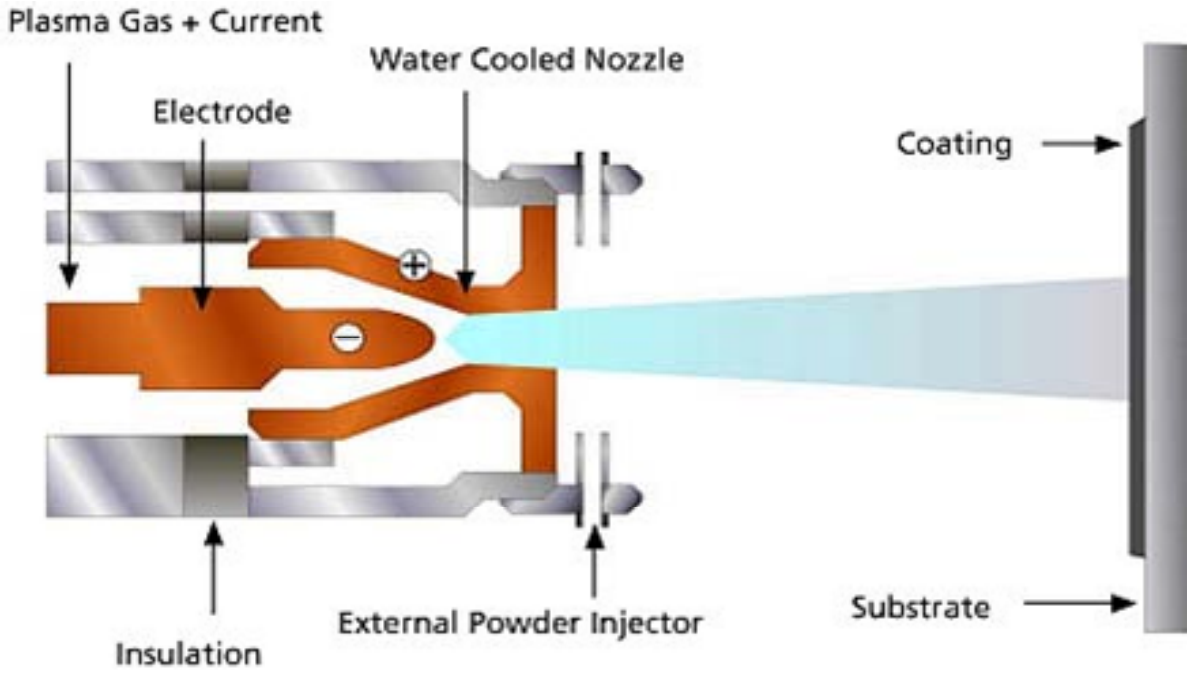

Fig. 3.1 Schematic diagram of the plasma spraying process

The coating is incrementally built up by impact of successive particles by the process of flattening, cooling and solidification. By virtue of the high cooling rates, typically 10^5 to 10^6 K/sec., the resulting microstructures are fine-grained and homogeneous. This results in a typical lamellar structure as shown in Fig.3.2. The coating-substrate interface bond mechanism is purely mechanical. Plasma spray deposits typically have lamellar structure with fine-grained microstructure within the lamellae.

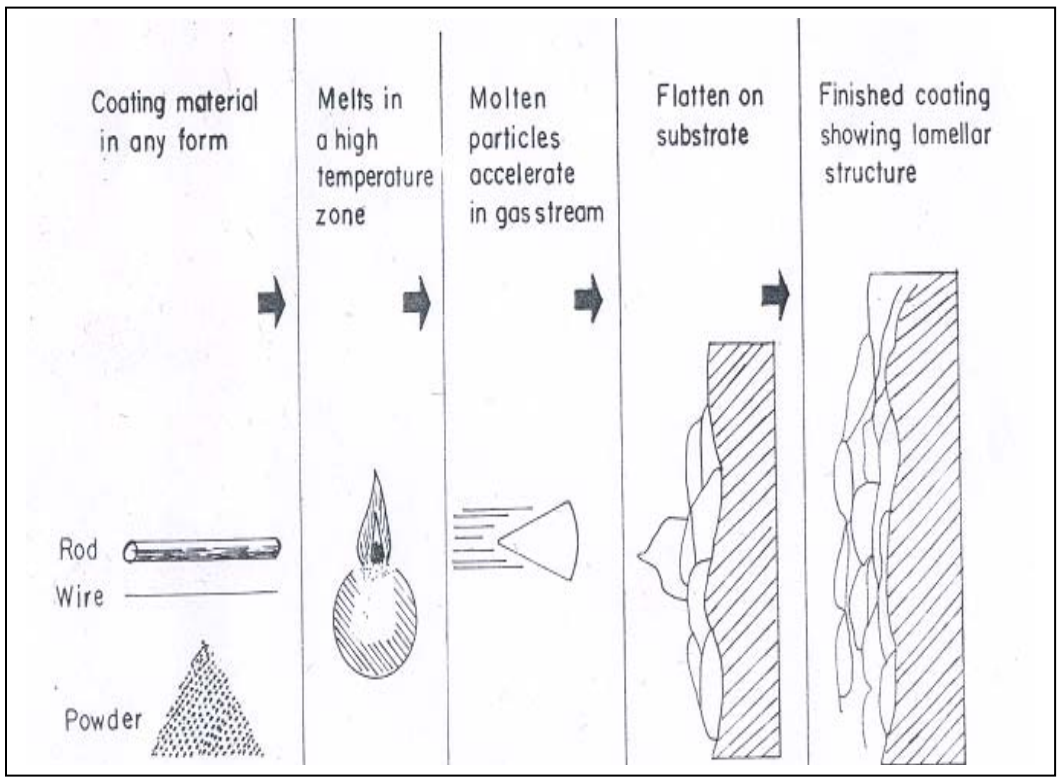

Fig. 3.2 Schematic Diagram Showing Steps for Coating Process

The complete experimental setup together with brief specifications of equipments and methodology are done in the plasma spray system developed at the Laser & Plasma Technology Division, Bhabha Atomic Research Centre, Mumbai, has been used for plasma spray experiments. The experimental set up is shown in Figure 3.3.

The spray system consists of

(1) DC plasma spray torch.

(2) Power supply.

(3) Control console.

(4) Gas feeding system.

(5) Water cooling arrangement.

(6) Powder feeder.

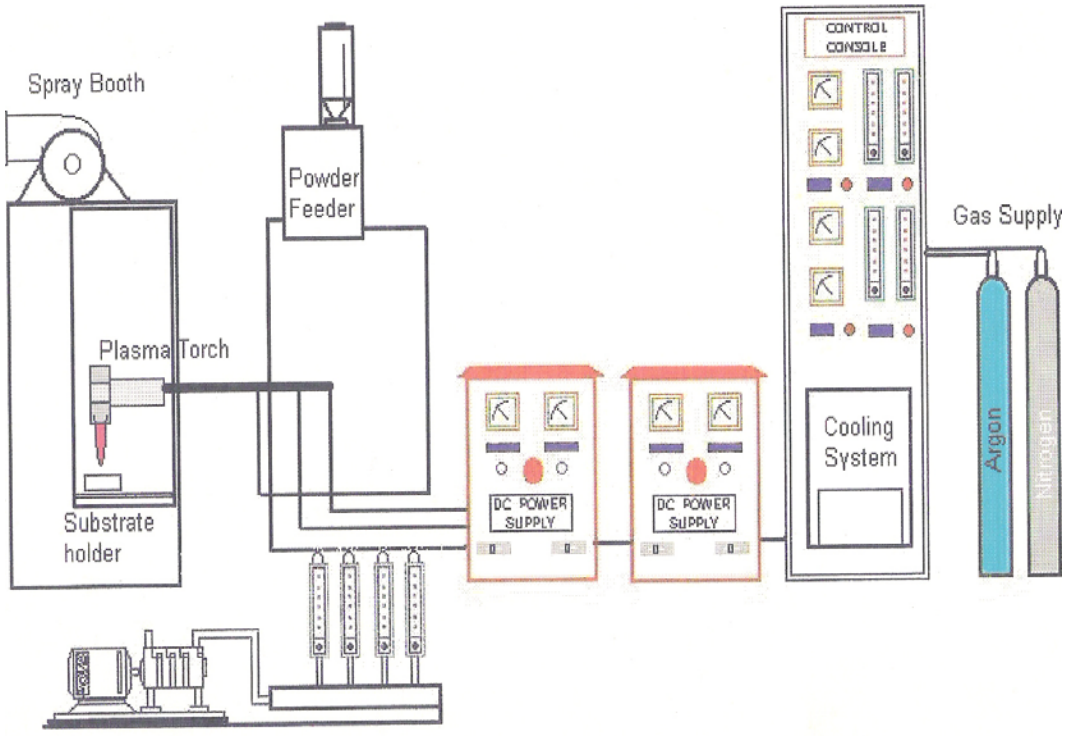

Fig. 3.3 General arrangement of the plasma spraying equipment

Argon is used as the primary plasmagen gas and nitrogen as the secondary gas. The powders are deposited at spraying angle of 90°. The powder feeding is external to the gun. The properties of the coatings are dependent on the spray process parameters.

The operating parameters during coating deposition process are listed in table 3.1.

Operating Parameters	**Values**
Plasma Arc Current (amp)	200, 250, 300, 400
Arc Voltage (volt)	30, 36, 40
Torch Input Power (kW)	11,15,18,21
Plasma Gas (Argon) Flow Rate (lpm)	20
Secondary Gas (N_2) Flow Rate (lpm)	2
Carrier Gas (Argon) Flow Rate (lpm)	7
Powder Feed Rate (gm/min)	10
Torch to Base Distance TBD (mm)	100

Table 3.1 Operating parameters during coating deposition

3.4 CHARACTERIZATION OF COATINGS

3.4.1 Particle Size Analysis

The particle sizes of the raw materials used for coating (iron with, 30 wt% aluminium powder) are characterized using Laser particle size analyzer of Malvern Instruments make.

3.4.2 Coating Thickness Measurement

Thickness of the iron aluminide coatings on different substrates are measured on the polished cross-sections of the samples, using an optical microscope. Five readings are taken on each specimen and the average value is reported as the mean coating thickness.

3.4.3 X-Ray Diffraction Studies

X-ray diffraction technique was used to identify the different (crystalline) phases present in the coatings [**113**]. XRD analysis was done using Ni-filtered Cu-Kα radiation in a Philips X-ray diffractometer. The characteristic d-spacing of all possible values were taken from JCPDS cards and were compared with d-values obtained from XRD patterns to identify the various X-ray peaks obtained.

3.4.4 Scanning Electron Microscopic Studies

Plasma sprayed coated specimens and plasma processed powders were studied by JEOL JSM-6480 LV scanning electron microscope mostly using the secondary electron imaging. The surfaces as well as the interface morphology of all coatings were seen in the microscope. Small Specimens are sliced from the coated samples and were mounted using thermosetting molding powders. Coating cross-sections are polished in three stages using SiC abrasive papers of reducing grit sizes and then with diamond pastes on a wheel for coating interface analysis under SEM. These specimens are also utilized for the microhardness measurement.

3.4.5 Porosity Measurement

Measurement of porosity is done using the image analysis technique. The porosity of the coatings was measured by putting polished cross sections of the coating sample under a microscope (Neomate) equipped with a CCD camera (JVC, TK 870E). This system is used to

obtain a digitized image of the object [**114**]. The digitized image is transmitted to a computer equipped with VOIS image analysis software. The total area captured by the objective of the microscope or a fraction thereof can be accurately measured by the software. Hence the total area and the area covered by the pores are separately measured and the porosity of the surface under examination is determined.

3.4.6 Microhardness Measurement

Small specimens are sliced from the coated samples. Samples containing Coating cross sections are mounted and polished for the microhardness measurement. Microscopic observation under optical microscope of the polished section of the coatings exhibits three distinctly different regions/ phases namely grey, dark and spotted/mixed. Vickers

Microhardness measurement is made on these optically distinguishable phases using Leitz Microhardness Tester fig.3.4 equipped with a monitor and a microprocessor based controller, with a load of 0.245N and a loading time of 20 seconds. About twelve or more readings are taken on each sample and the average value is reported as the data point.

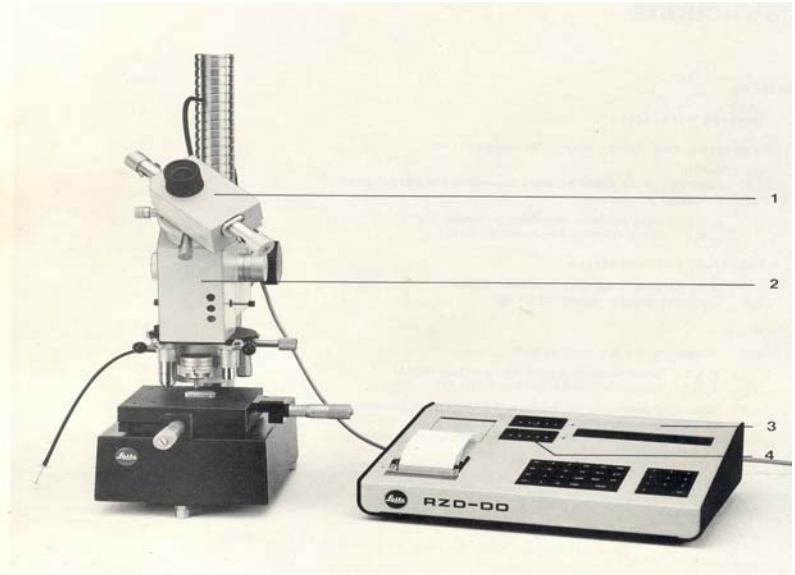

Fig.3.4 Leitz Micro hardness Test

3.4.7 Evaluation of Coating Deposition Efficiency

Deposition efficiency is defined as the ratio of the weight of coating deposited on the substrate to the weight of the expended feedstock. Weighing method is accepted widely to measure this. Each specimen is weighed before and after coating deposition. The difference is the weight (Gc) of coating deposited on the substrate. From the powder feed rate and time of deposition the weight of expended feed stock (Gp) is determined. The deposition efficiency (η) is then calculated using the following equation [**115**].$\eta = (GC / G_p \text{ X } 100)$ %

Weighing of samples is done using a precision electronic balance with $\pm$ 0.1 mg accuracy.

3.4.8 Evaluation of Coating Interface Bond Strength

To evaluate the coating adhesion strength, a special type jig (fig. 3.6a) is fabricated. Cylindrical mild steel dummy samples (length 25 mm, top and bottom diameter 12 mm) are prepared. The surfaces of the dummies are roughened by punching. These dummies are then fixed on top of the coating with the help of a polymeric adhesive (epoxy 900-C) as shown in (fig 3.6b) and pulled with tension after being mounted on the jig (fig. 3.6c). The coating pullout test is carried out using the set up Instron 1195 at a crosshead speed of 1mm/minute.

Fig. 3.5 Adhesion test set up Instron 1195

(a)

(b)

(c)

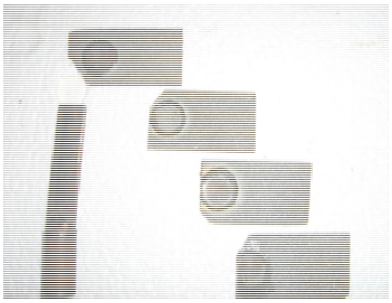

(d)

Fig. 3.6 (a) Jig used for the test, (b) Dummy fixed with the coating material, (c) Specimen under tension and (d) The coating sample after pullout.

The moment coating gets torn off from the specimen, (fig 3.6 d) the reading (of the load), which corresponds to the adhesive strength of the coating, is recorded. A typical test set up (During testing) is shown in (fig 3.5). The test is performed as per ASTM C-633.

3.5 EROSION WEAR BEHAVIOUR OF COATINGS

Solid particle erosion (SPE) is usually simulated in laboratory by one of two methods. The 'sand blast' method, where particles are carried in an air flow and impacted onto a stationary target and the 'whirling arm' method , where the target is spun through a chamber of falling particles.

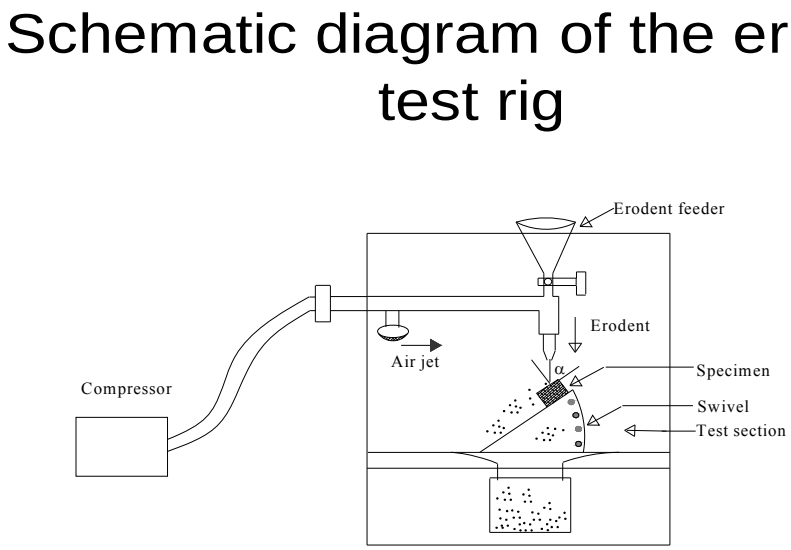

Fig 3.7 Schematic diagram of the erosion test rig.

(a) (b)

Fig. 3.8(a) Erosion test Set Up, (b) During the Test

In the present investigation, an erosion apparatus (self-made) of the 'sand blast' type is used (fig 3.7) It is capable of creating highly reproducible erosive situations over a wide range of particle sizes, velocities, particles fluxes and incidence angles, in order to generate quantitative data on materials and to study the mechanisms of damage. The test is conducted as per ASTM G76 standards as shown in fig 3.8 (a), (b).

The jet erosion test rig used in this work employs a 300 mm long nozzle of 3 mm bore and 300 mm long. This nozzle size permits a wider range of particle types to be used in the course of testing, allowing better simulations of real erosion conditions. The mass flow rate is measured by conventional method. Particles are fed from a simple hopper under gravity into the groove. Velocity of impact is measured using double disc method [**116**]. Some of the features of this test set up are:

- Vertical traverse for the nozzle: provides variable nozzle to target standoff distance, which influences the size of the eroded area
- Different nozzles may be accommodated: provides ability to change the particle plume dimensions and the velocity range
- Large test chamber with sample mount (typical sample size 25 mm x 25 mm) that can be angled to the flow direction: by tilting the sample stage, the angle of impact of the particles can be changed in the range of 0^0 – 90^0 and this will influence the erosion process.

In this work, room temperature solid particle (sand) erosion test on mild steel substrate coated with iron aluminide as feed materials (at 11 kW, 18kW) is carried out. The coating made at 11kW power level is eroded at three different impact angles 30°, 60° and 90°. The nozzle is kept at 100mm, 125mm, 150mm, 175mm & 200mm stand-off distance from the target. Dry silica sand particles of 400µm average particle size are used as erodent with an average velocity of 32m/sec,feed rate 50gm/min and pressure 4kgf/cm^2.The coating deposited at18 kW power level is eroded at 30°,45^0,60^0,75^0 and 90°angle at SOD of 200mm. Same size dry silica sand particles are used as erodent with different velocities i.e. of 32m/sec,38m/sec, 45m/sec ,52m/sec and 58m/sec and at pressures of 4kgf/cm^2,4.7kgf/cm^2,5.5kgf/cm^2,6.1kgf/cm^2,6.5kgf/cm^2 with feed rate 50gm/min,54gm/min, 58gm/min,60gm/min, 62gm/min. Amount of wear is determined on 'mass loss' basis as found for other coatings[**117**]. It is done by measuring the weight change of

the sample at regular intervals in the test duration. A precision electronic balance with + 0.01 mg accuracy is used for weighing. Erosion rate, defined as the coating mass loss per unit erodent mass (gm/gm) is calculated. The erosion rates are calculated at different velocities and impingement angles, erodent dose and stand off distances.

CHAPTER 4

COATING CHARACTERIZATION

RESULTS AND DISCUSSION

4.1 INTRODUCTION

Plasma sprayed iron aluminide coatings were deposited on different metal substrates, using a 40 kW atmospheric plasma spray system supplied by M/S Ion Arc Machines (India) Pvt. Ltd. plasma spraying was done at different input power levels i.e. between 11 kW to 21 kW. Characterization of the coatings is carried out with respect to their quality and tribological performance. The results are presented and discussed in this chapter.

4.2 PARTICLE SIZE ANALYSIS

The particle sizes of the Iron aluminide powder (the feed stock) are analyzed with Laser particle size analyzer (Malvern make). Figure.4.1 shows the particle size distribution of the fed stock before plasma spraying. It can be seen that, majority of particles are in the range of ~40 to 100 micron. The mean particle diameter is found to be ~ 61.78 micron, and maximum particles are in the range of ~75 micron.

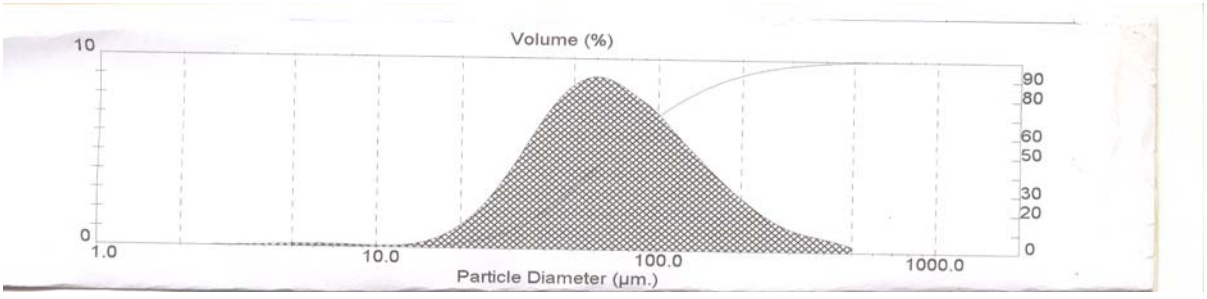

Fig.4.1 Particle size distribution of Fe-Al feed stock.

4.3 MEASUREMENT OF COATING THICKNESS

To ensure the coatability, coating thickness was measured on the polished cross-sections. The thickness values obtained for coatings deposited at different power levels are presented in table 4.1 and shown in fig.4.2. Each data point is the average of at least five readings/measurements.

Sl No.	Specimen	Substrate	Power level (kW)	Coating Thickness (~Micron)
1	Fe-Al Coating	Mild steel	11	135
2	do	Mild steel	15	170
3	do	Mild steel	18	210
4	do	Mild steel	21	200
5	do	Copper	11	142
6	do	Copper	15	193
7	do	Copper	18	223
8	do	Copper	21	205

Table 4.1. Variation of Iron aluminide coating thickness values with torch input power.

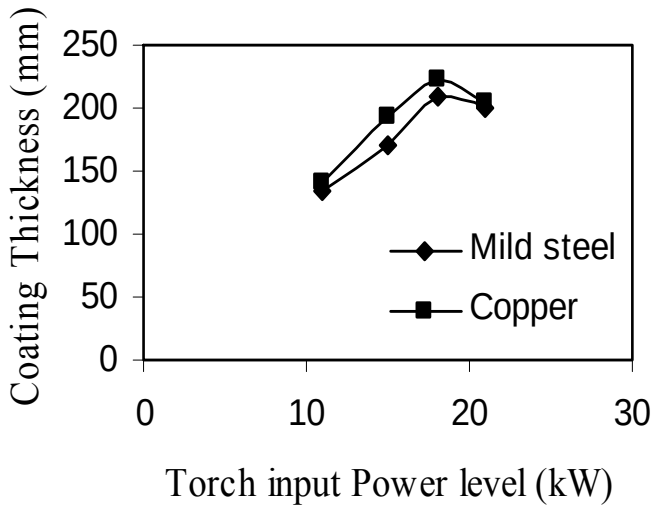

Fig. 4.2 Thickness of Iron aluminide coatings made at different power level.

Maximum coating thickness of ~ 223 micron on copper and ~ 210 micron on mild steel substrates are obtained with the coatings deposited at 18 kW power level. From the figure, it is evident that there is an increase in coating thickness with increase in input power up to about 18 kW and then with further higher input power, no improvement in coating thickness is recorded. It is also seen from the figure that, there is a difference in thickness obtained for different substrates. Coating thickness is higher in case of copper than that of mild steel at all power levels. This difference may be attributed to the thermal conductivity of the substrate material, i.e. for materials with higher thermal conductivity (i.e. copper, the heat transfer from the sprayed particles arriving the substrate) collapses the liquid formats at a faster rate than of the case of materials with lower thermal conductivity (i.e. Mild steel). This might be enhancing the deposition rate and hence the coating thickness.

4.4 COATING ADHESION STRENGTH

From the microscopic point of view, adhesion is due to physico-chemical surface forces (Vander-walls, Covalent, ionic etc.), which can be established at the coating-substrate interface [**118**] and corresponds to the work of adhesion. From the mechanical point of view, adherence can be estimated by the force corresponding interfacial fracture and is macroscopic in nature. Coating adherence tests have been carried out by many investigators with various coatings. It has been stated that, the fracture mode is adhesive if it takes place at the coating-substrate interface

and is the measure of adhesion value, the value of practical adhesion, which later is strictly an interface property, depending exclusively on the surface characteristics of the adhering phase and the substrate surface condition. [**119, 120**].

In this work, coating interface bond strength is evaluated based on coating pullout method, conforming to ASTM C-633 standard. It is found that, in all the samples fracture occurred at the coating-substrate interface. The differences and variation of adhesion strengths of Iron aluminide coatings deposited at various power levels may be due to the difference in thermal expansion coefficient of substrate material and coating and/or formation of pores, cracks, voids in the coating at coating-substrate interface.

Sl.No	Specimen	Power level (kW)	Substrate	Adhesion strength (MPa)
1	Fe-Al	11	Mild steel	4.54
2	do	15	Mild steel	6.38
3	do	18	Mild steel	12.84
4	do	21	Mild steel	4.35
5	do	11	Copper	7.2
6	do	15	Copper	9.6
7	do	18	Copper	4.89
8	do	21	Copper	4.49

Table 4.2 Adhesion strength values of iron aluminide coating on mildsteel and copper substrates at different power levels.

.

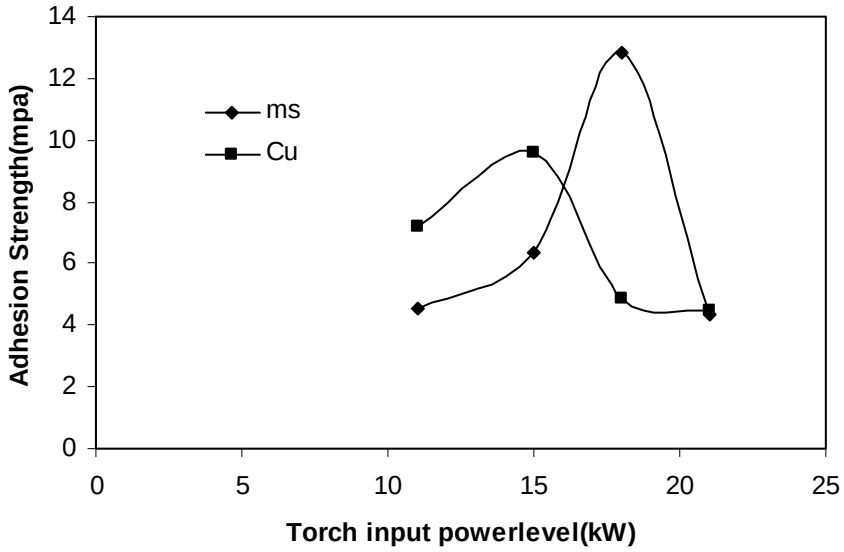

Fig. 4.3 Adhesion strength of iron aluminide coatings made at different Power level on different substrates.

The variation of adhesion strength of iron aluminide coating to the mild steel and copper substrate at different power levels is shown in fig.4.3. From the figure, it is clear that the adhesion strength varies with operating power of the plasma torch. Maximum adhesion strength of 12.84 MPa on mild steel substrate at 18 kW and of 9.6Mpa on copper substrate at 15kW is recorded. It can be visualized that, the interface bond strength increases with the input power of the torch up to a certain power level and then shows a decreasing trend in coating adhesion, irrespective of the substrate material. This might be due to the fact that, when the operating power level is increased, larger fraction of particles attain molten state as well as the velocity of the particles also increase. Therefore there is better splat formation and mechanical inter-locking of molten particles on the substrate surface leading to increase in adhesion strength [**121**]. But, at a much higher power level, the amount of fragmentation and vaporization of the particles increase. There is also a greater chance to fly off of smaller particles during in-flight traverse during plasma spraying and results in poor adhesion strength of the coatings. Coating adhesion strength is more in case of mild steel substrate than that of copper substrate may be due to the dependence of thermal conductivity for melted particle, dissipation of heat at metal interface and also may be due to thermal expansion coefficient mismatch at the interface [**122**].

4.5 MICROHARDNESS

Microscopic observation of the polished cross section of the coatings was studied under optical microscope. Three distinctly different regions/ phases namely grey, dark and spotted/mixed are visible. Micro-hardness measurement is done on these optically distinguishable phases with Leitz Micro-Hardness Tester using 25Pa (0.245N) load. The results are summarized in table 4.3, 4.4, 4.5, 4.6.

Sl.No	Coating	Power level(Kw)	Phase	Micro Hardness(HV)
1	Fe-Al	11	Mixed	67.1
2	do	11	Mixed	70.0
3	do	11	Dark	107.90
4	do	11	Dark	106.63
5	do	11	Grey	72.05
6	do	11	Grey	88.62

Table 4.3 Hardness on the coating cross section for the coating deposited at 11 kW.

Sl.No	Coating	Power level(Kw)	Phase	Micro Hardness(HV)
1	Fe-Al	15	Mixed	159.41
2	do	15	Mixed	184.54
3	do	15	Dark	113.58
4	do	15	Dark	127.70
5	do	15	Grey	116.65
6	do	15	Grey	82.9

Table .4.4 Hardness on the coating cross section for the coating deposited at 15 kW.

Sl.No	Coating	Power level(Kw)	Phase	Micro Hardness(HV)
1	Fe-Al	18	Mixed	121.29
2	do	18	Mixed	144.08
3	do	18	Dark	68.82
4	do	18	Dark	78.48
5	do	18	Grey	183.42
6	do	18	Grey	260.03

Table 4.5 Hardness on the coating cross section for the coating deposited at 18 kW.

Sl.No	Coating	Power level(Kw)	Phase	Micro Hardness(HV)
1	Fe-Al	21	Mixed	99.83
2	do	21	Mixed	177.76
3	do	21	Dark	446.97
4	do	21	Dark	461.50
5	do	21	Grey	147.12
6	do	21	Grey	220.80

Table .4.6 Hardness on the coating cross section for the coating deposited at 21 kW.

The results show that these three structurally different phases bear three different ranges of hardness that may depend on different phases present/formation in the coating, which is clear from X-ray diffraction analysis.

4.6 X-RAY PHASE COMPOSITION ANALYSIS

Micro-hardness test shows different hardness values on different optically distinct regions on the coating cross-sections. Therefore, to ascertain the phases present and phase changes / transformation taking place during plasma spraying, the X-ray diffractograms are taken on the

raw material and on some selected coatings using a Philips X Ray Diffractometer and with CuKα. The XRD results are shown in figures 4.4 to 4.8.

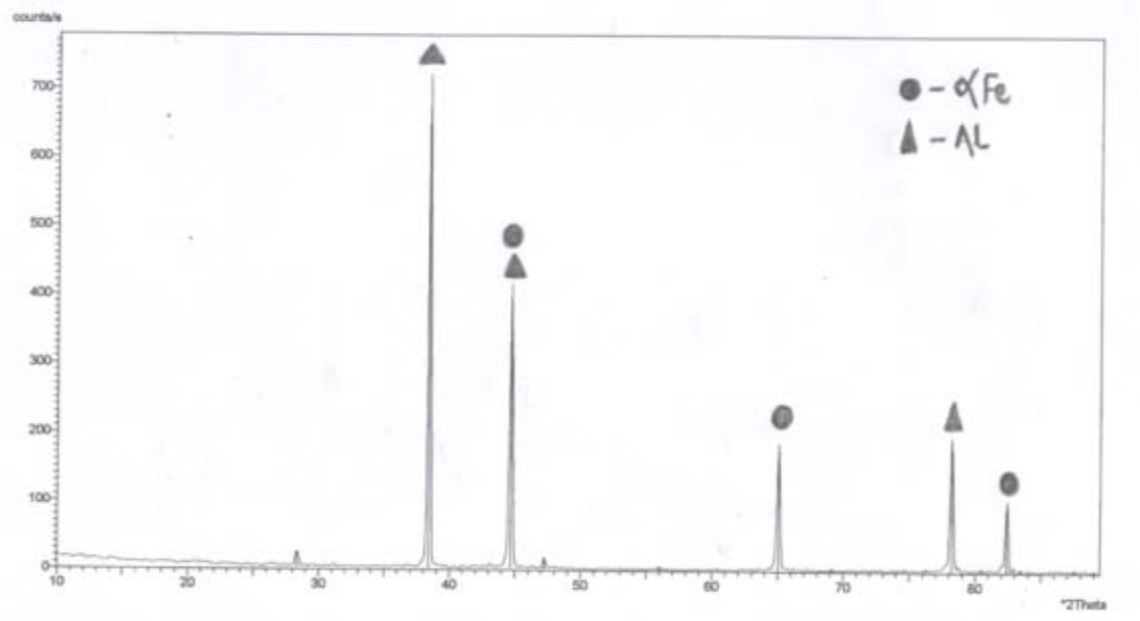

Fig.4.4 X-Ray Diffractogram of iron aluminide raw powder

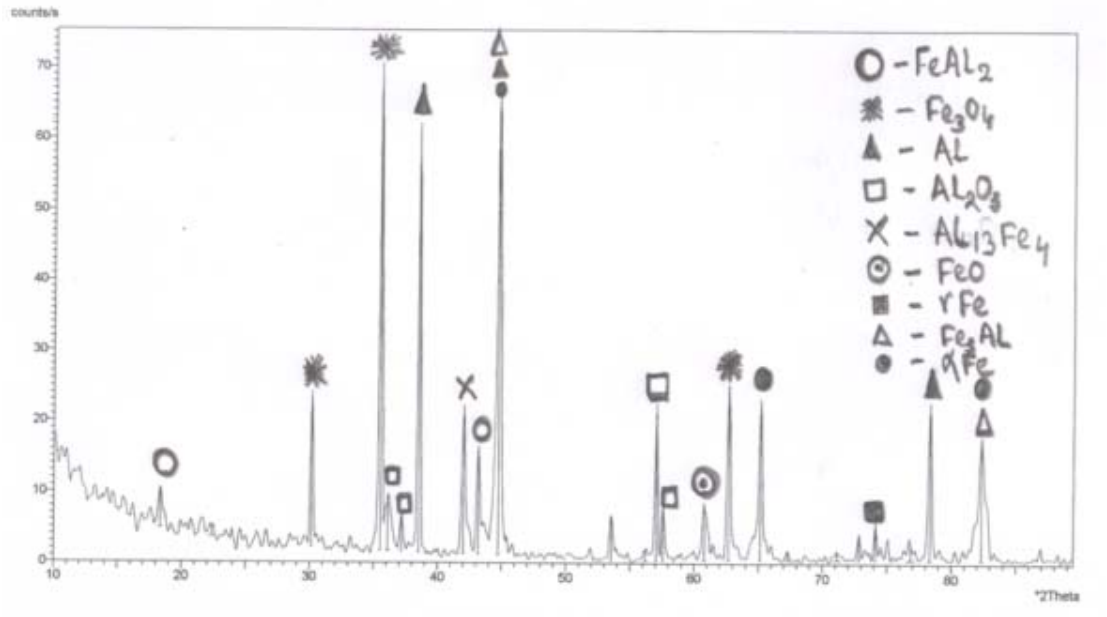

Fig. 4.5 X-Ray Diffractogram of iron aluminide coating deposited at 11kW power level

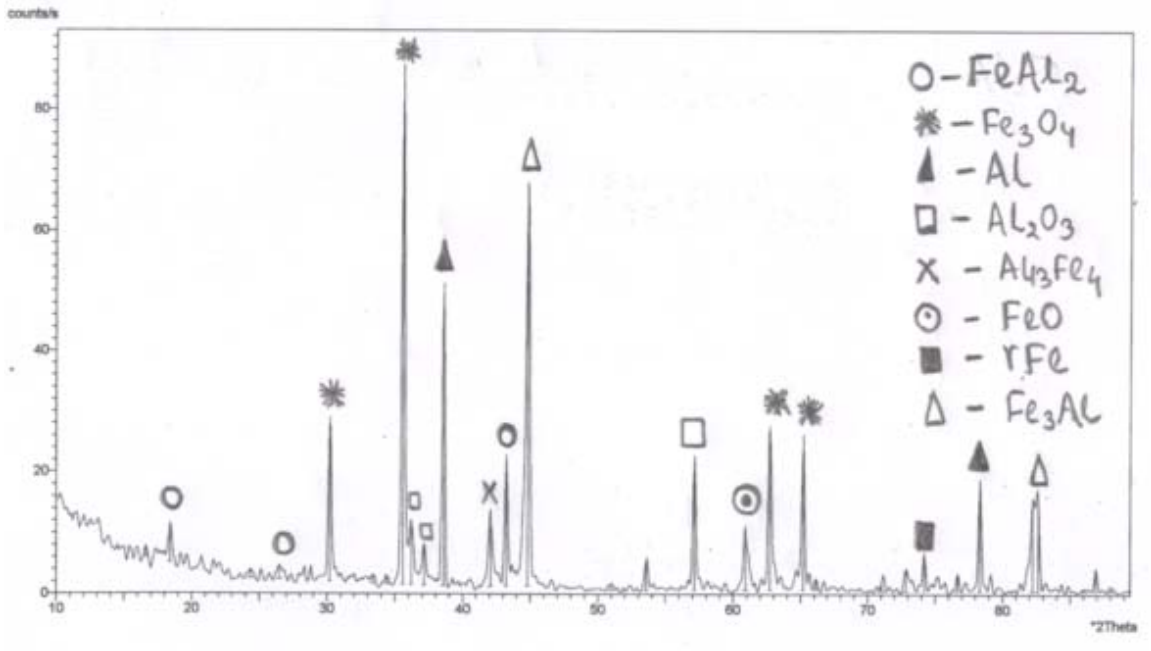

Fig.4.6 X-Ray Diffractogram of iron aluminide coating deposited at 15 kW power level

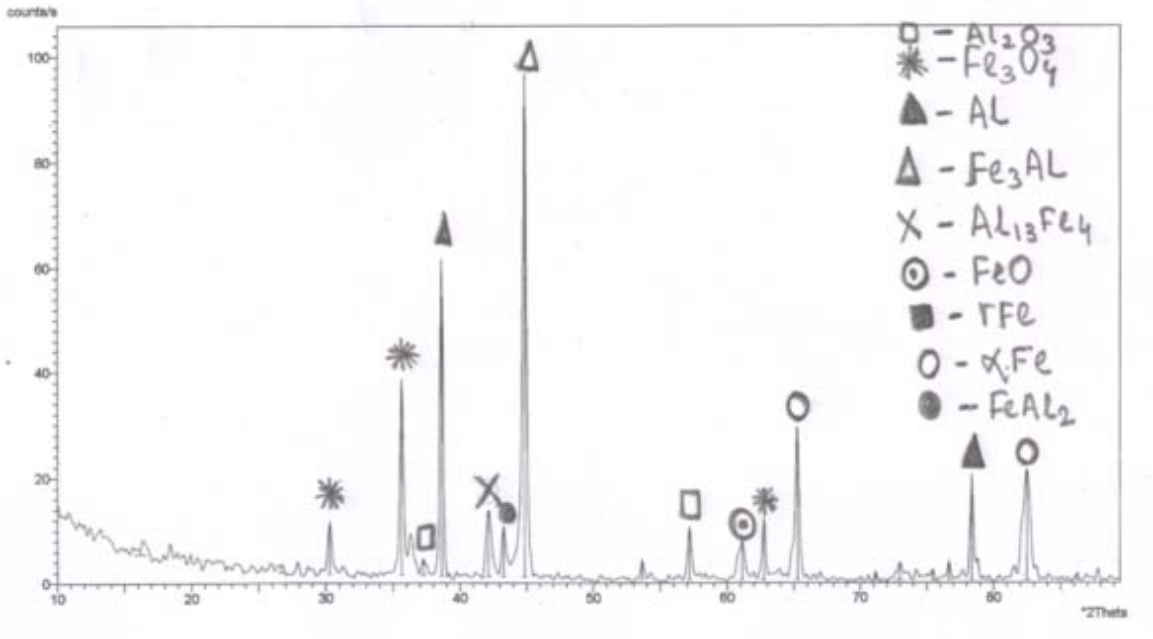

Fig.4.7 X-Ray Diffractogram of iron aluminide coating deposited at 18 kW power level

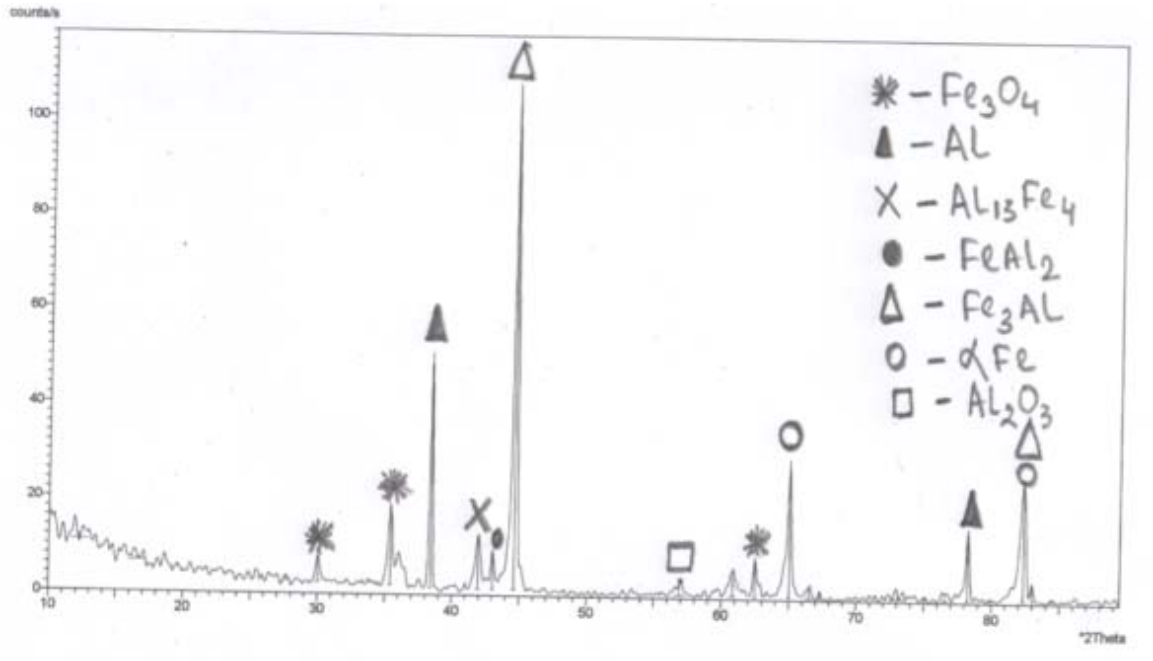

Fig. 4.8 X-Ray Diffractogram of iron aluminide coating deposited at 21kW power level

The XRD of the feed material (fig 4.4) shows the presence of Fe and Al powders; some traces of α-Fe is present. The Coating made at 11 kW power level (fig 4.5), aluminide phases viz. $Al_{13}Fe_4$, Al_2Fe, Fe_3Al and oxides of iron i.e. Fe_3O_4, FeO, etc are also seen.. Al may react with atmospheric oxygen and form Al_2O_3. The coating made at 15 kW power level (fig 4.6), contains mostly same phases i e $Al_{13}Fe_4$, Al_2Fe, Fe_3Al, Fe_3O_4, and FeO phases as that of 11Kw. From Fig (4.7), coating made at 18 kW power level, there is a variation of the iron oxide phases i.e. oxides like Al_2O_3, Fe_3O_4, and FeO goes on decreasing with increase in deposition power level. From Fig (4.8), coatings made at 21 kW power level, intensity of all oxide decreases as envisaged in literature **[123].**

4.7 COATING MORPHOLOGY

4.7.1 Powder morphology

SEM micrograph of iron 30% aluminium powders prior to coating is shown in fig.4.9. From the figure it is seen that, the particles are of varied sizes, irregular in shape. Some particles are elongated type and some are of multifaceted.

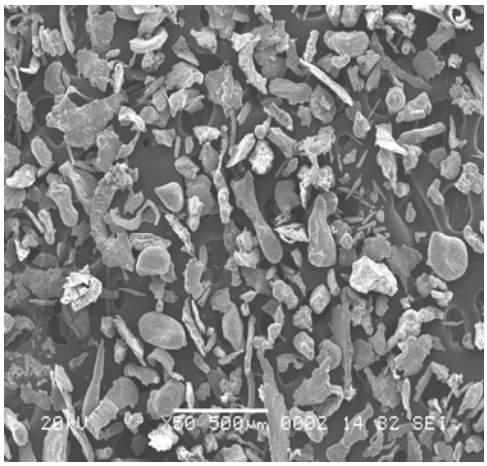

Fig 4.9 SEM micrograph of iron aluminide raw powders

4.7.2 Morphology of coating surfaces

The interface adhesion of the coatings depends on the coating morphology and inter-particle bonding of the sprayed powders. SEM micrograph of the coatings deposited at 11kW, 15kW, 18kW and 21kW are shown in fig.4.10. From the figure it is found that, coatings deposited at 11kW power level (fig.4.10 a), show uniform distribution of molten/semi molten particles. More amount of cavitations is observed, other than some large pores found on the inter particle boundaries and triple particle junctions; which may have originated during solidification of particles from un/semi-molten state. The coatings made at 15 kW (fig.4.10 b), bears a different morphology. A large number of globular particles and some flattened regions indicative of solidification of molten species during spray deposition. The grains/particles are mostly equi-axed type and with a little boundary mismatch between them. Amount of cavitations is less than that of the previous case. However, some cavity regions are seen along inter-particle / inter-grain boundaries. Coating deposited at further higher power level i.e. at 18 kW (fig.4.10 c) bears a different morphology. Larger portions of the coatings exhibit flattened regions, which might have been formed during solidification of molten species that have fused together in lumps. Less cavitations is observed at inter grain boundaries. This may be the reason for increase in adhesion strength (maximum for the coating deposited at 18kW power level). For the coatings deposited at further higher power i.e. at 21 kW, the surface morphology (fig.4.10d) is completely different. A large number of granulated/spheroidal particles of different diameters are seen, which might have been formed due to breaking/fragmentation of bigger particles which/and have

melted during in flight traverse through the plasma jet. Amount of cavitation is more than that of the coatings deposited at lower power levels.

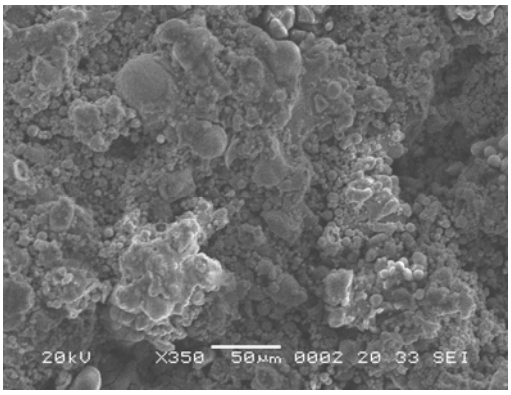

(a)

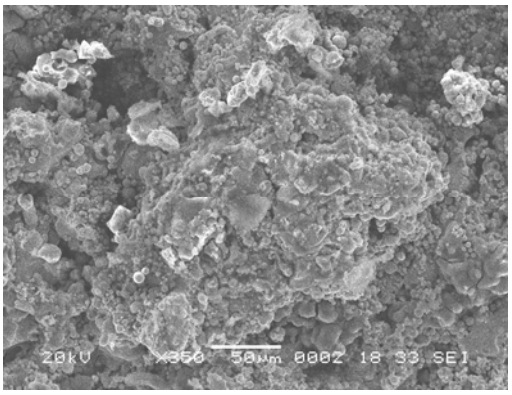

(b)

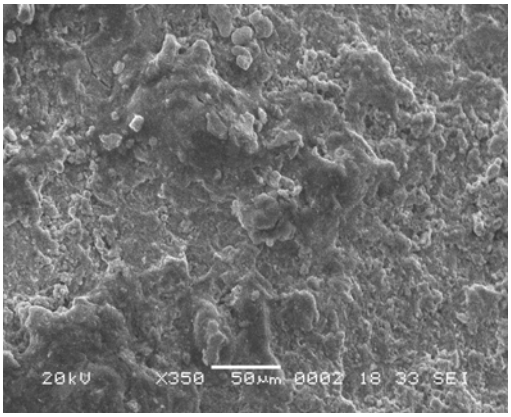

(c)

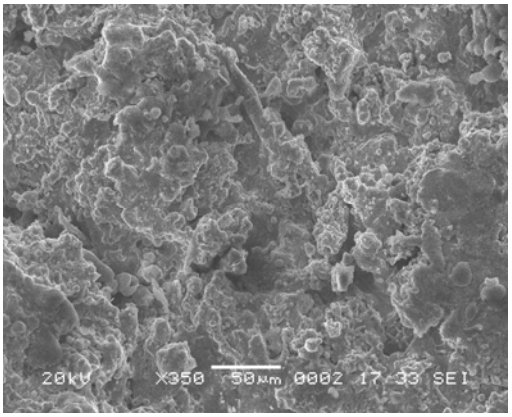

(d)

Fig 4.10.SEM photograph of FeAl coating surface at different power level, i.e. (a) 11kW, (b) 15kW, (c) 18kW, (d) 21kW.

Coatings deposited at 18kW power level are smooth, more homogenous, having least amount of porosity. This might be the reason to reduce the erosion rate for the coating deposited at 18 kW, as compared to the coating deposited at 11kW.

4.7.3 Analysis of coating interface

The coating substrate interface plays an important role on the adhesion of the coating. The surface morphology of the coating cannot predict the interior (layer deposition) structures and their importance/acceptability. The cross-sections of the samples are examined under SEM

and a typical (which has shown maximum adhesion strength) is shown in fig 4.11. From the micrograph, lamellar structure confirms the solidification of molten particles to form splats during coating deposition; the coating is homogenous through out and hence has produced higher adhesion strength.

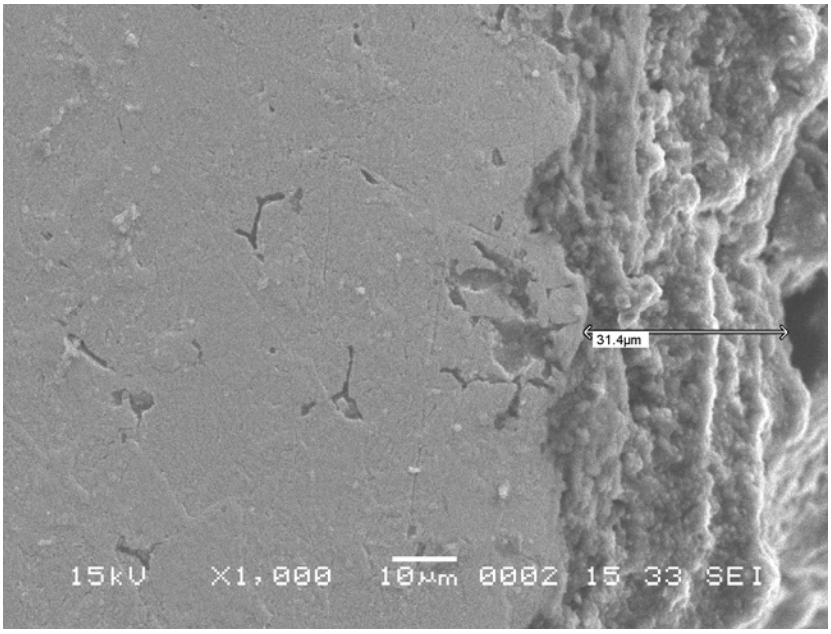

Fig 4.11 SEM photograph of FeAl coating interface.

4.7.4 Worn surfaces

Microstructural features do not reveal significant differences in topographic features between the eroded surfaces of the tested samples. Iron aluminide coatings made at 11kW and 18 kW power levels, eroded with 400µm particles (erodent) at normal impact are shown in Fig.4.12 and 4.13.

In case of the coating made at 11kW, fig.4.12 (a), it appears that, the material is removed in lumps from inter-splat boundaries. Whereas, in fig.4.12 (b) deeper groves are observed. Crack propagation is clearly visible at 18kW at some regions (fig.4.13) with high magnification. The material removal is due to formation, propagation of cracks by repeated impact of solid particles.

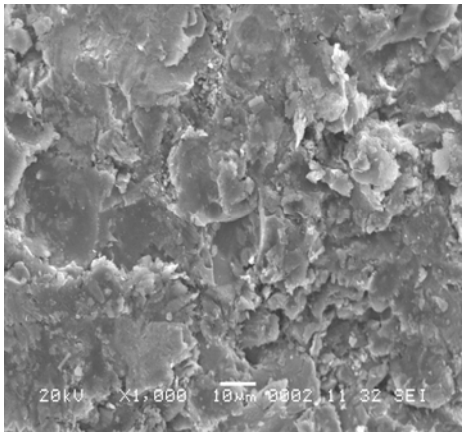

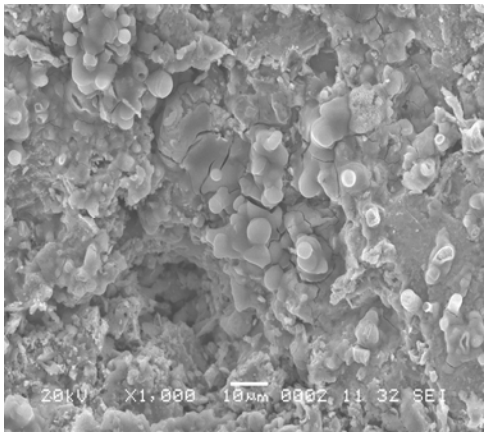

(a) (b)

Fig.4.12. Micrographs of eroded sample (a) coated at11kW power level and (b) at18kW power level.

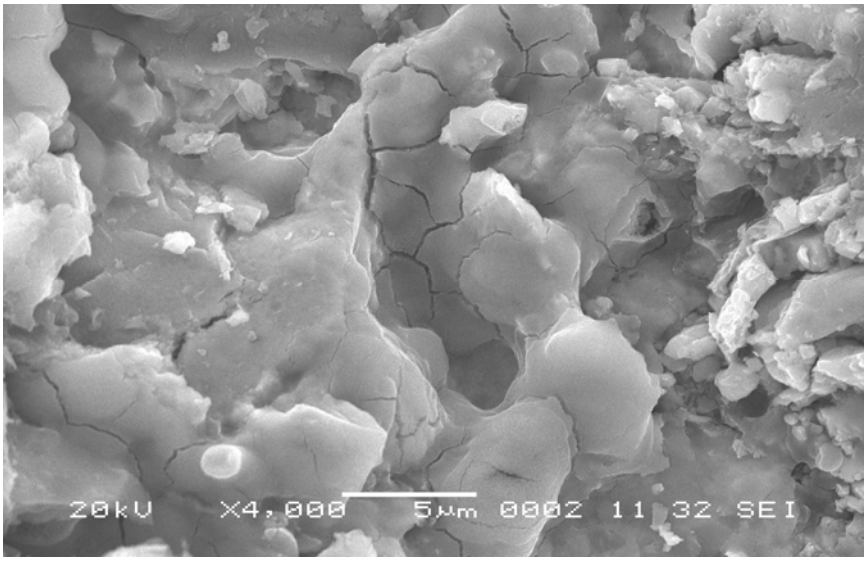

Fig.4.13. Iron aluminide coating (18 kW) showing micro cracks on and along the splats.

eroded with 400µm particles at normal impact.

All coatings show the induced cracks normal cracks formed/appeared on and within the splats (Fig.4.13). At low strains, crack initiation and propagation or propagation of pre-existing cracks in the coating occurs from relaxation of strained grains and splats. When the coated beamis subjected to higher pressure/time, the most favorably oriented cracks are activated and start linking to nearby cracks.

This linking process accelerates very rapidly and the cracks propagate through out the coating. When the crack reaches the coating/substrate interface, extensive coating delamination starts and the stresses caused by bending are relaxed. The appearances of the eroded surfaces also indicate that cracks tend to follow a variety of weak sites. The thermal cracks normal to the surface, the interfaces between adjacent layers of splats and also the columnar boundaries within the individual splats can be identified as structural weaknesses for deposited coatings, as been described in literature [**124, 125**].

Erosion has been suggested as a suitable method to evaluate the cohesion of (overlay)sprayed coatings [**126**]. A striking result in this work is that, although the wear rate spanned four orders of magnitude between erosion conditions, the ranking of the coatings stayed essentially the same. This suggests that the dominant wear mechanism, i.e. the basic mechanisms behind the formation and removal of wear fragments, is similar for all coatings irrespective of deposited power levels.

4.8 COATING POROSITY

Porosity measurement was done using the image analysis technique. The polished interfaces of various coatings were examined under optical microscope equipped with a CCD camera (JVC, TK 870E). From the digitized image coating porosity is determined using VOIS image analysis software, tabulated in table 4.7.

Sl.No	Specimen	Power level (kW)	Porosity (%)
1	Fe-Al	11	3.5
2	do	15	3.4
3	do	18	3.3
4	do	21	4.1

Table 4.7. Porosity of coating for different power levels

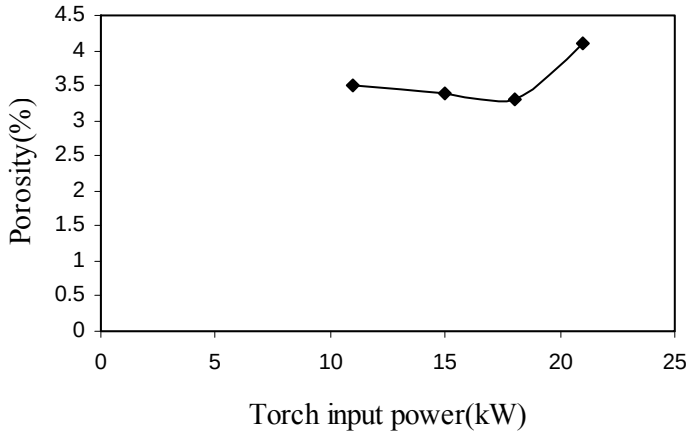

Fig. 4.14. Variation of coating porosity of iron aluminide with torch input power.

From the above figure it is observed that, porosity volume fraction of these coatings lie in the range of ~ 4 to ~ 6 %. The amount of porosity is more in the case of coatings made at lower (11kW) and at higher (21kW) power levels. However, porosity is minimum for the coating deposited at 18kW. It may be mentioned that, in conventional plasma sprayed aluminide coatings, porosity of about 3 – 6 % is generally observed [**127**]. Thus the values obtained in the coatings under this study are suffixing the acceptable range for a good quality coating. The increased value of porosity may be the reason of low adhesion strength of the coatings deposited at at high power level i.e. at 21kW.

4.9 DISCUSSION

The adherence of the plasma spray deposited coating to the substrate is of major concern. The bonding mechanism operative between the coating and substrate can be classified into three categories: mechanical, physical and physico-chemical. The molten particles striking a roughened surface, conform to the surface topography can stick to the substrate. The mechanical interlocking between the coating and the protrusions on the substrate surface is termed as

mechanical adherence. Substrate-coating adherence by Vander-walls force is classified as physical bonding. In majority of the situations encountered, adhesion is physical bonding of the coating to the substrate. The formation of an inter-diffusion zone or an intermediate compound between the coating and substrate is generally termed as chemical or metallurgical bonding. The specific mechanism operative between a coating and the substrate depends primarily on the materials used and the physical condition of these material particles reaching the substrate (may be on impact).

The analysis of coating - substrate bond strength of all the coatings, presented in table 4.2 envisages that; (i) there is an increase in adhesion strength with increase in plasma (torch) operating power (up to 18 kW) for mild steel and then with further increase in torch input power does no improvement in adhesion strength, and (ii) there is a variation in adhesion strength for different substrates.

Variation of adhesion strength with input power can be explained in terms of the thermal state of the particles striking the substrate surface. At lower power level, the plasma gas temperature is not high enough to effect complete melting of all the particles entering the plasma jet. It is also possible that, un-melted particles get embedded within the molten ones during spray deposition. Such a situation naturally leads to poor coating adhesion. When the input power to the plasma torch is increased, plasma jet temperature and heat transfer coefficient of the plasma increases leading to complete melting of a large fraction of the injected feed stocks which on hitting the substrate get fused and flattened at a relatively faster rate. Therefore, there is better splat formation (of the molten species) and mechanical inter-locking on the substrate surface leading to increase in adhesion strength. However, at much higher power level, the amount of fragmentation and vaporization of the particles increase leads to lowering the deposition efficiency and coating adhesion as well. The vapors and gaseous species of dissociated products can get entrapped in the coating and affect the porosity of the coatings. This can also lead to a decrease in the adhesion strength of the coating made at higher power level.

It has been shown in previous investigations [**121**] that, for a given material the final coating properties depend on the velocity, temperature and type of particles just before impact on the substrate (or on the coating layers). The plasma power effectively changes the temperature and particle velocity profile and therefore affects the coating properties. The composition of the

coating materials also affects the coating adhesion strength due to transformation/formation of phases and inter-oxides that favor the inter particle bonding and adhesion to the substrate. In this investigation, higher adhesion strength in substrates of lower thermal conductivity (i.e. in mild steel) is observed. It is known that the oxides adhere weakly to a substrate of high thermal conductivity owing to a low contact temperature [**127**]. Hence the relatively lower adhesion strength on copper substrates as compared to mild steel substrate may be due to this effect.

Micro-hardness measurement is made on optically distinguishable phases present in the coatings. The existence of at least three different phases (which are optically distinguishable) might have been formed during plasma spraying. The hardness values are different for different phases. On referring to the x ray diffractograms taken on raw material and coated samples, it becomes evident that, during coating deposition formation, oxidation and transformation of phases have taken place. So during spraying, the phase transformation and/or formation of inter oxides (transformation of α -Fe to γ-Fe and formation of new phases) corroborate to different micro-hardness values obtained.

The XRD study and micro-hardness results obtained in this investigation show that the different phase composition of the coatings exhibit different hardness. It is known that, with increase in the material hardness the erosion wear rate decreases. So our findings on the wear behaviour of various coatings are at par with the observations made by previous investigators (**128**).

From the microscopic studies it is seen that, the particle size and their appearance have changed with change in operating conditions of the plasma torch. Micro-cracks and cavities/pores are also found in the deposited layers. This reflects in the type of reactions (indicative of whether the particles are molten, semi-molten, un- melted, fragmented and of possible phase transformation mechanisms) which might have taken place during in-flight traverse of the powders through plasma. The molten or semi-molten species bear equi-axed structure. The fragmented particles get melted completely exhibiting spheroidal shape and partially melted/un-melted powders get stacked in the coating layers during deposition. The formation of micro-cracks are possible in the coatings near to the substrate and open pores/cracks do originate along the direction of heat flow i.e. towards the substrate due to shrinkage of particles parallel to the surface of the substrate as been also found earlier[**194**]. Hence such

microstructures affect the coating homogeneity and adhesion to the substrate. Measured values of coating porosity, presented in table 4.7. Maximum porosity of about 4.1% is recorded for the coating deposited at 21kW and is very much within the limit as observed with plasma sprayed aluminide coatings [**129-136**].

Branco et al. (**137**) reported that, the coating porosity influences the erosion in three ways. Firstly, it reduces the material strength against plastic deformation or chipping since the material at the edge of a void lacks mechanical support. Secondly, the concave surface inside a void that is not under the shadow of some void edge will see an impinging particle at an angle higher than the average target surface to impact angle (which is detrimental for brittle materials). And finally, pores can impair strength by acting as stress concentrators and/or decreasing the load-bearing surface. The coatings under this investigation are though brittle in nature, the effect of pore volume fraction on erosion wear needs a more detailed investigation.

CHAPTER 5
COATING PERFORMANCE EVALUATION RESULTS AND ANALYSIS

5.1 INTRODUCTION

Intermetallic compounds find extensive use in high temperature structural applications. The Fe_3Al based intermetallic alloys offer unique benefits of excellent oxidation and sulfidation resistance at a potential cost lower than many stainless steels. Plasma spraying is considered as a non-linear problem with respect to its variables: either materials or operating conditions. To obtain functional coating exhibiting selected in-service properties, combinations of processing parameters have to be planned. These combinations differ by their influence on the coating properties and characteristics. To control the spraying process, one must recognize the parameter interdependencies, correlations and individual effects on coating characteristics. This chapter reports the efficiency of coating deposition under various plasma spraying conditions. The calculated deposition efficiency values form a database which is used for further prediction by neural computation. This chapter also deals with the analysis of tribological performance of the coatings. It presents the results of the solid particle erosion test conducted on the coated samples. The results give an insight to the performance of the coating in an erosive environment. Artificial neural network analysis is employed and a prediction model is proposed for erosion wear rate as well. Correlation between important control factors and the wear rate has been established. This technique helps in saving time and resources for experimental trials.

5.2 COATING DEPOSITION EFFICIENCY

Coating deposition efficiency is defined as the ratio of the weight of coating deposited on the substrate to the weight of the expended feedstock. Weighing method is accepted widely to measure this. It can be described by the following equation [**115**].

$$\eta = (G_c/G_p) \text{ X } 100 \%$$

Where η is the deposition efficiency, Gc is the weight of coating deposited on the substrate and Gp is the weight expended feed stock. . Deposition efficiency values of iron aluminide

coating on different substrates at different operating power level are shown in table 5.1. For example, deposition efficiency for iron aluminide coatings ranges from 21.6% to 51.1% in case of mild steel substrate and from 29% to 53.7% in the case of copper substrate. It is interesting to note that the deposition efficiency, in all cases, has increased in a step up fashion with the increase in torch input power.

Sl. No.	Specimen	Substrate	Power level (kW)	Deposition efficiency (%)
1	Fe-Al Coating	Mild steel	11	21.6
2	do	Mild steel	15	30.9
3	do	Mild steel	18	42.2
4	do	Mild steel	21	51.1
5	do	Copper	11	29
6	do	Copper	15	39.8
7	do	Copper	18	49.7
8	do	Copper	21	53.7

Table 5.1 Coating deposition efficiency values of Iron aluminide coating on different substrates at different operating power level.

Deposition efficiency of any coating is a characteristic, which not only rates the effectiveness of the spraying method but also is a measure of the coatability of the material under study. Variation of iron–aluminide coatings, deposition efficiency on mild steel and copper substrates with operating power level is presented in fig.5.1. It is noted that the efficiency of iron-aluminum coating deposition, in case of both the substrates, increases in a sigmoidal fashion with the torch input power., maximum deposition efficiency of 53.7 % is obtained for coatings made at 21 kW operating power level of the plasma torch (on copper substrate). The maximum deposition efficiencies in case of mild steel substrates is found out to be 51.1%.

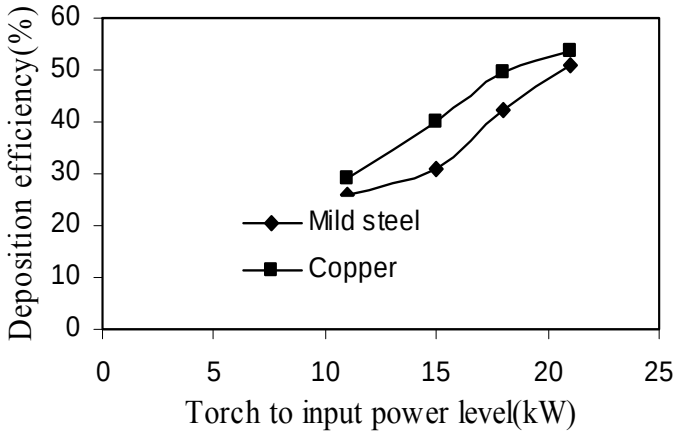

Fig. 5.1 Deposition Efficiency of Fe-Al on MS and Cu substrates

(As obtained from experimental findings)

Particle deposition i.e. the coating thickness is influenced mainly by the input power to the plasma torch. With increase in power level, the plasma density increases leading to a rise in enthalpy and thereby, the particle temperature. Hence more number of particles get melted during in-flight traverse through plasma jet. When these molten species hit the substrate, they get flattened and adhere to the surface. The deposition of layers is favoured with availability of more number of molten / semi molten particles which is enhanced by increasing the torch input power. This increases the coating thickness. But, beyond certain limit of operating power level; fragmentation and vaporization of sprayed particles do occur simultaneously and for these two mechanisms, some (powder) particles fly off during spraying restricting further increase in coating thickness. Thermal spraying is a highly complex deposition process with a large number of interrelated variables. Due to the high velocity and temperature gradients in the plasma plume, even small changes in the controllable or uncontrollable parameters can result in significant changes in the particle properties and thus in the microstructure of the coatings .In the present investigation, coatings are deposited on metal substrates of different thermal conductivity and thermal expansion coefficient. It is observed that the coating thickness varies with different substrate materials. This may be mainly due to thermal conductivity of the substrate material. When the sprayed particles impinge on the substrate surface, heat transfer and dissipation takes place. The particles dissipate heat at a faster rate through the metal substrate. Subsequent particles accumulated / deposited on the top of the first layer restrict the heat transfer towards outside environment than through the metal surface. The dissipation of heat from the

particles/coating layers is favored with increased heat dissipation rate through the substrate. So for the metals having higher thermal conductivity the layer deposition is faster. In this work, the observation of higher coating thickness and higher deposition rate on copper substrate than that on mild steel substrates may be attributed to this effect.

5.3 NEURAL COMPUTATION

Coating deposition by plasma spraying is considered as a non-linear process with respect to its variables: either materials or operating conditions. To obtain functional coatings exhibiting selected in-service properties, combinations of processing parameters have to be planned. These combinations differ by their influence on the coating properties and characteristics. In order to control the spraying process, one of the challenges nowadays is to recognize parameter interdependencies, correlations and individual effects on coating characteristics. Neural computation can be used to study these interrelated effects. In the present work, influence of plasma torch input power on coating deposition efficiency has been studied. A methodology based on artificial neural networks (ANN) is used that involves database training to predict property-parameter evolutions. This section presents the database construction, implementation protocol and a set of predicted results related to the coating deposition efficiency. The details of this methodology are described by Rajasekaran and Pai [138].

5.3.1 ANN Model: Development and Implementation (For deposition efficiency)

An ANN is a computational system that simulates the microstructure (neurons) of biological nervous system. The most basic components of ANN are modeled after the structure of brain. Inspired by these biological neurons, ANN is composed of simple elements operating in parallel. It is simple clustering of the primitive artificial neurons. This clustering occurs by creating layers, which are then connected to another. The multi layer neural network has been utilized in the most of the research works for material science. The database is built considering experiments at the limit ranges of each parameter. Experimental result sets are used to train the ANN in order to understand the input-output correlations. The database is then divided into three categories, namely: (i) a validation category, which is required to define the ANN architecture and adjust the number of neurons for each layer. (ii) a training category, which is exclusively used to adjust the network weights and (iii) a test category , which corresponds to the set that validates the results of the training protocol. The input variables are normalized so as to lie in the same range group of 0-1.

Input Parameters for Training	Values
Error tolerance	0.01
Learning parameter(ß)	0.001
Momentum parameter(α)	0.02
Noise factor (NF)	0.01
Maximum cycles for simulations	2000,000
Slope parameter (£)	0.6
Number of hidden layer neuron	6
Number of input layer neuron (I)	2
Number of output layer neuron (O)	1

Table 5.2 Input parameters selected for training (for deposition efficiency)

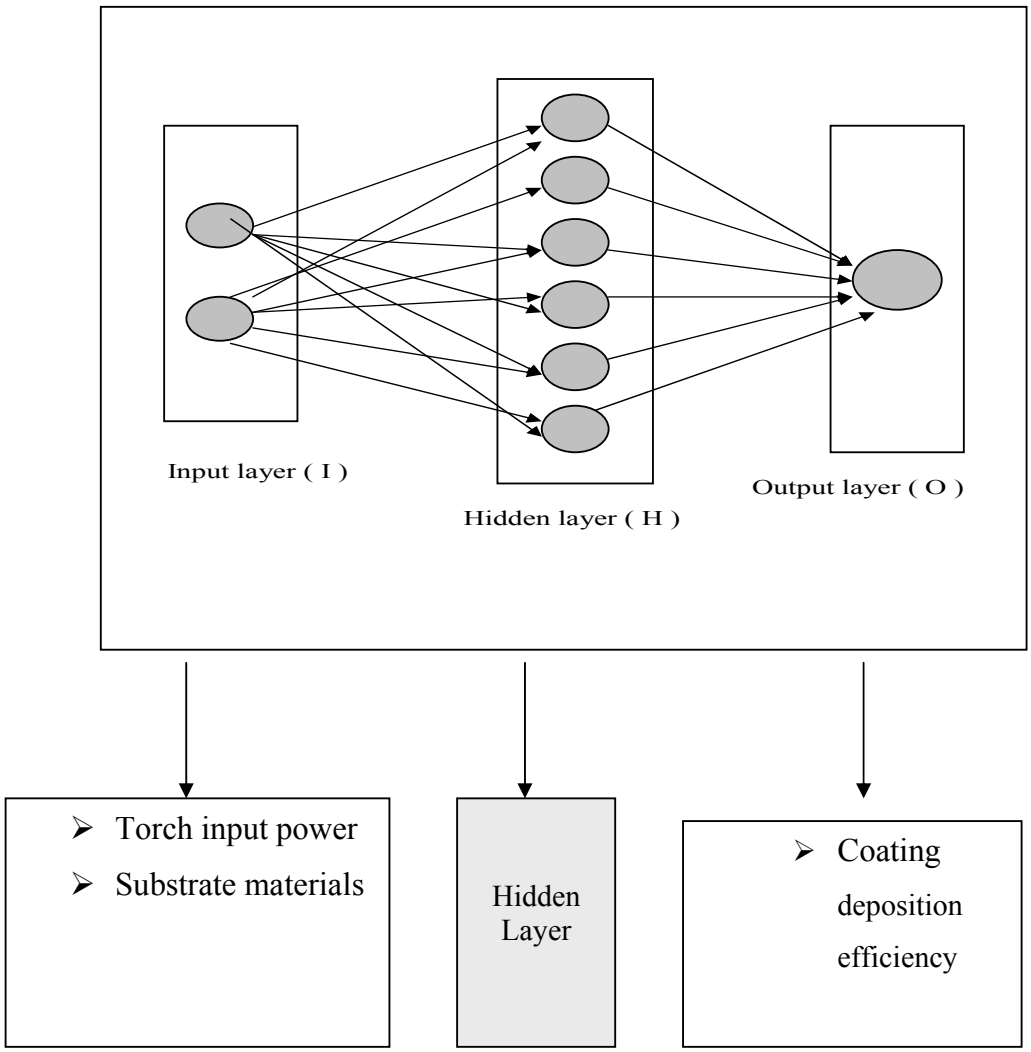

Fig. 5.2 The three layer neural network

To train the neural network used for this work, about 8 data sets of different coatings applied on selected substrates are taken. It is ensured that these extensive data sets represent all possible input variations within the experimental domain. So a network that is trained with this data is expected to be capable of simulating the plasma spray process. Different ANN structures (I-H-O) with varying number of neurons in the hidden layer are tested at constant cycles, learning rate, error tolerance, momentum parameter and noise factor and slope parameter. Based on least error criterion, one structure, shown in table 5.2, is selected for training of the input-output data. The learning rate is varied in the range of 0.001-0.100 during the training of the input-output data. The network optimization process (training and testing) is conducted for 2000,000 cycles for which stabilization of the error is obtained. Neuron numbers in the hidden layer is varied and in the optimized structure of the network, this number is 6. The number of cycles selected during training is high enough so that the ANN models could be rigorously trained. A software package NEURALNET for neural computing developed by Rao and Rao [**139**] using back propagation algorithm is used as the prediction tool for coating deposition efficiency at different operating power levels. The three-layer neural network having an input layer (I) with two input nodes, a hidden layer(H) with six neurons and an output layer (O) with one output node employed for this work is shown in fig. 5.2.

5.3.2 Prediction of Deposition Efficiency (ANN Way)

The prediction neural network was tested with four data sets from the original process data. Each data set contained inputs such as torch input power, substrate material and an output value i.e. deposition efficiency was returned by the network. As further evidence of the effectiveness of the model, an arbitrary set of inputs is used in the prediction network. Results were compared to experimental sets that may or may not be considered in the training or in the test procedures. Fig. 5.3 presents the comparison of predicted output values for deposition efficiency for coatings obtained at various operating power levels with the actual deposition efficiency found experimentally.

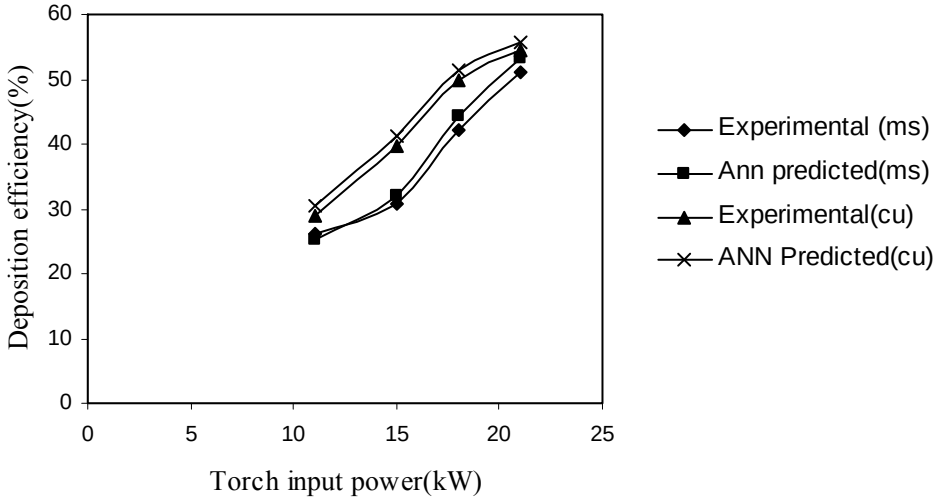

Fig 5.3 Comparison plot for predicted and experimental values of deposition efficiency of Fe-Al coatings on mild steel and copper substrates

It is interesting to note that the predictive results show good agreement with experimental sets realized. The optimized ANN structure further permits to study quantitatively the effect of torch input power on the coating deposition in range larger than the experimental limits, thus offering the possibility to use the ANN in a large parameter space. In the present investigation, this possibility was explored by selecting the torch input power in a range from 6 kW to 30 kW, and sets of predictions for deposition efficiency on all the two substrates are evolved. Fig. 5.4 illustrates the predicted evolution of deposition efficiencies with respect to torch input power for mild steel and copper substrates.

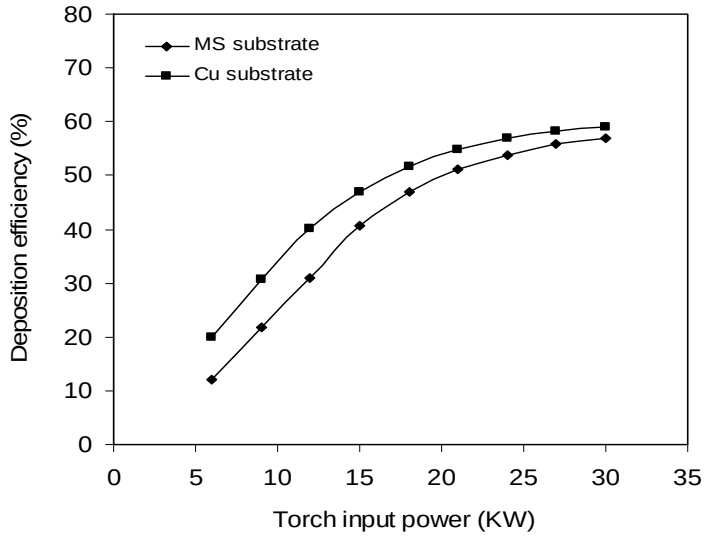

Fig.5.4 Predicted coating deposition efficiency on mild steel and copper substrates

Distinguishing features

The deposition efficiency presents a sigmoid-type evolution with the torch input power (fig. 5.3 and fig. 5.4). As the power level increases, the total and the net available energies increase (the arc current intensity increases from 250A to 480A for operating power increasing from 11 kW to 21 kW). This leads to a better in-flight particle molten state and hence to higher probability for particles to flatten. The deposition efficiency reaches a plateau for the highest current levels due to the plasma jet temperature increasing which in turn increases both the particle vaporization ratio and the plasma jet viscosity.

Functional coatings have to fulfill various requirements. The deposition efficiency is one the main requirements of the coatings developed by plasma spraying. It represents the effectiveness of the deposition process as well as the coatability of the powders under study. Neural computation can be used as a tool to process very large data related to a spraying process and to predict coating characteristic such as deposition efficiency, the simulation can be extended to a parameter space larger than the domain of experimentation.

5.4 SOLID PARTICLE EROSION WEAR BEHAVIOUR

Solid particle erosion is a wear process where particles strike against a surface and promote material loss. During flight, a particle carries momentum and kinetic energy, which can be dissipated during impact due to its interaction with a target surface. In case of plasma spray coatings encountering such situations, no specific model has been developed and thus the study of their erosion behavior has been mostly experimental data [**137**] .The jet erosion test rig used in this work employs a 300 mm long nozzle of 3 mm bore and 300 mm long. This nozzle size permits a wider range of particle types to be used in the course of testing, allowing better simulations of real erosion conditions. The mass flow rate is measured by conventional method. Particles are fed from a simple hopper under gravity into the groove. Velocity of impact is measured using double disc method [**116**]. Some of the features of this test set up are: (I) Vertical traverse for the nozzle; provides variable nozzle to target standoff distance, which influences the size of the eroded area.(II) Different nozzles may be accommodated which provides ability to change the particle plume dimensions and the velocity range. (III) Large test chamber with sample mount that can be angled to the flow direction by tilting the sample stage, the angle of impact of the particles can be changed in the range of $0^0 – 90^0$ and this will influence the erosion process.

In this work, room temperature solid particle (sand) erosion test on mild steel substrate coated with iron aluminide as feed materials (at 11 kW, 18kW) is carried out. The coating made at 11kW power level is eroded at three different impact angles 30°, 60° and 90°. The nozzle is kept at 100mm, 125mm, 150mm, 175mm & 200mm stand-off distance from the target. Dry silica sand particles of 400µm average particle size are used as erodent with an average velocity of 32m/sec,feed rate50gm/min and pressure 4kgf/cm^2.The coating deposited at18 kW power level is eroded at 30°,45^0,60^0,75^0 and 90°angle at SOD of 200mm. Same size dry silica sand particles are used as erodent with different velocities i.e. of 32m/sec,38m/sec, 45m/sec, 52m/sec and 58m/sec and at pressures of 4kgf/cm^2,4.7kgf/cm^2,5.5kgf/cm^2,6.1kgf/cm^2,6.5kgf/cm^2 with feed rate 50gm/min,54gm/min, 58gm/min,60gm/min, 62gm/min. Amount of wear is determined on 'mass loss' basis as found for other coatings[**117**]. It is done by measuring the weight change of the sample at regular intervals in the test duration. A precision electronic balance with + 0.01 mg accuracy is used for weighing. Erosion rate, defined as the coating mass loss per unit erodent mass (gm/gm) is calculated. The erosion rates are calculated at different velocities and impingement angles, erodent dose and stand off distances.

The typical incremental erosion plot for coatings deposited at 11kw is presented in fig5.5. The erodent particles strike the coated samples at 30^0, 60^0 ,90^0 angle of impact at stand of distance of 100mm, at a pressure of 4kgf/cm^2. The variations of cumulative coating mass loss with time are calculated. It is seen that, in all these cases, a transient regime in the erosion process seems to exist, during which the mass loss increases monotonically and tends to attain a constant steady state value. This constant value is referred to as the steady state erosion rate.

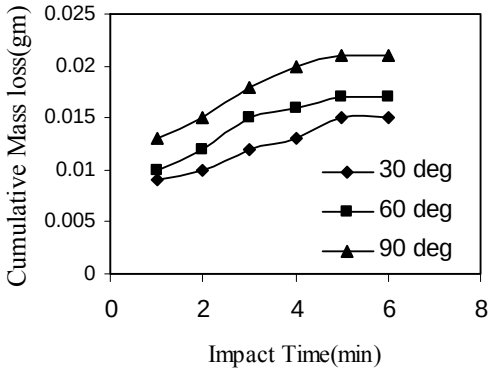

Fig5.5 Variation of Cumulative Coating mass loss with time at 30^0,60^0, 90^0 angle of impact at 11kW with stand of distance100mm at a pressure of4kgf/cm^2

The cumulative increment in material loss due to erosion wear of plasma sprayed coatings with exposure time (or erodent dose) has been reported earlier by Levy [**140**]. It has been observed that, the incremental erosion curves of brittle materials start with a high rate at the first a measurable amount of erosion, and then decreases to a much lower steady state value. In the present work, this trend is found in case of all coatings subjected to erosion test at various impact angles. This can be attributed to the fact that, the fine protrusions on the top surface of the coating may be relatively loose and removed with less energy than what would be necessary to remove a surface layer from the bottom portion of the coating. Consequently, the initial wear rate is high. With increasing exposure time the rate of wear starts decreasing and in the transient erosion regime, a sharp drop in the wear rate is obtained. As the coating surface gradually gets smoothened, the rate of erosion tends to become steady as shown in fig 5.6.

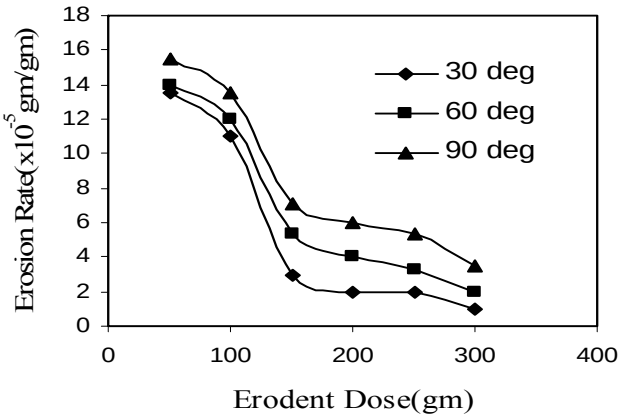

Fig 5.6.Variation of Erosion rate with Erodent dose at 30^0,60^0, 90^0 angle of impact at 11kW with stand of distance100mm at a pressure of 4kgf/cm^2

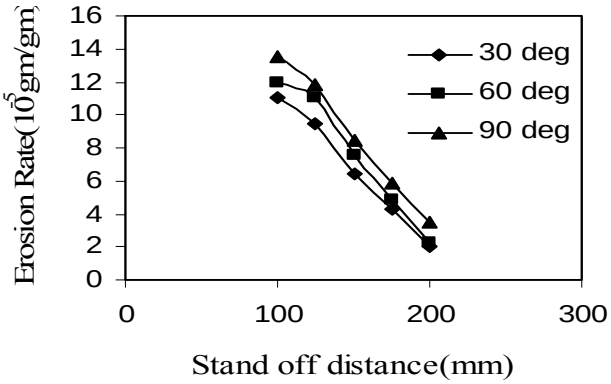

Fig 5.7 .Variation of Erosion rate with stand off distance after 4 minute at 30^0,60^0, 90^0 angle of impact at 11kW at a pressure of 4kgf/cm^2

Variation of Erosion rate with stand off distance (after 4 min.) at 30^0,60^0, 90^0 angle of impact at a pressure of 4kgf/cm^2 is shown in fig 5.7. Erosion rate decreases with increasing stand off distance as the impact will be less with increasing stand off distance. Similar observations are also reported by Chang-Jiu Li et al [**141**].

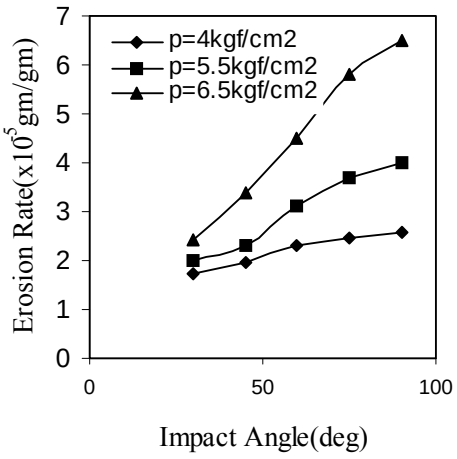

Fig 5.8 Variation of Erosion rate with impact angle of impact after 4 minute at 18kW with stand of distance100mm at pressure of 4,5.5,6.5kgf/cm^2

Figure 5.8 illustrates the effect of impact angle (α) on the erosion rate of coatings subjected to solid particle erosion. The erosion results for coatings of materials deposited at 18 kW operating power of the plasma torch at impact angles of 30, 60 and 90 degrees are shown. It is seen from the graph that irrespective of the pressure of the erodent, the erosion mass loss is higher at larger angle of impact and the maximum erosion takes place at $\alpha = 90^0$. Alahelisten [**142**], has studied erosion wear rate for diamond coating and found maximum erosion at for 90^0 impact angle. Also reported that erosion rate also increases with increase of erodent pressure. This is typical of brittle coatings. The relationship between erosion rate E and impact angle (α) is suggested by Bayer [**143**] as

$$E = (Kd\ v^n\ Cos^n\ \alpha + K_b\ v^m\ Sin^m\ \alpha)\ M$$

For a particular test condition, velocity of impact v, erodent supply rate M is constant. The constants K_d, K_b m, n are determined by fitting the equation to experimental data. For typical brittle materials $K_d = 0$ and the erosion rate is maximum at 90^0 impact angle. For typical ductile material, $K_b=0$ and erosion rate is largest at $20^0 – 30^0$ impact angles. Here the trend of the erosion coatings seems to follow the mechanism predicted for brittle materials. The results obtained in the present work show that for 90^0 impact angle, Iron aluminide

coating loses 21 mg in 6 minutes at 4kgf/cm^2 at SOD of 100 mm for the Iron aluminide coating deposited at 11kW power level while the mass loss is only 17 mg in case of $\alpha = 60^0$ and 15mg for $\alpha = 30^0$. This variation of erosion wear loss confirms that the angle at which the stream of solid particles impinges the coating surface influences the rate at which the material is removed. It further suggests that, this dependency is also influenced by the nature of the coating material. The angle of impact determines the relative magnitude of the two components of the impact velocity namely, the component normal to the surface and parallel to the surface. The normal component will determine how long the impact will last (i.e. contact time) and the load. The product of this contact time and the tangential (parallel) velocity component determines the amount of sliding that takes place. The tangential velocity component also provides a shear loading to the surface, which is in addition to the normal load that the normal velocity component causes. Hence as this angle changes the amount of sliding that takes place also changes as does the nature and magnitude of the stress system. Both of these aspects influence the way a coating wears. These changes imply that different types of material would exhibit different angular dependency.

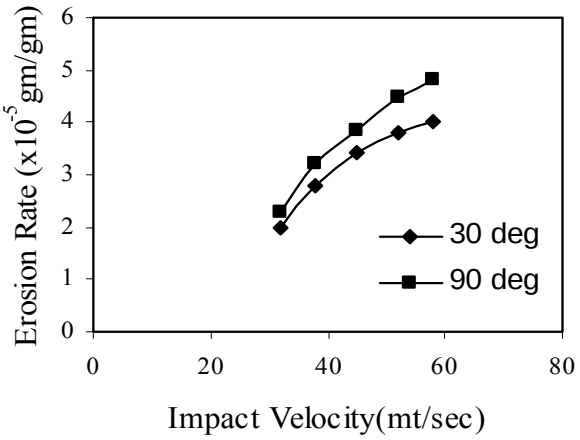

Fig 5.9 Variation of Erosion rate with impact velocity after 4 minute at 18kW with Stand of distance 200mm at 30^0, 90^0 angle of impact

Variation of Erosion rate with impact velocity after 4 minute at 18kW with stand of distance 200mm at 30^0,60^0, 90^0 angle of impact is shown in fig 5.9. Erosion rate increases with increasing velocity. It is obvious that, with increasing velocity the particles will have high kinetic energy which transformed at impact and hence remove more particles from the impacted surface [**144**] and it is maximum for 90^0 angles. Such findings are also reported by Lathabai et al for different coatings [**145**]. To assess the suitability of these coatings for tribological applications, solid particle erosion wear behaviour is studied. From the observed

results, it can be said that, the erosion wear rate varies with (i) erodent dose, (ii) impact angle of the solid particles on the coating surface, (iii) the velocity of erodent, (iv) stand off distance, (v) input power of the plasma torch and also time dependant. With increase in impact angle, the erosion wear increases and is maximum at 90^0 of impact.

The erosion wear for different coatings can also be attributed to the phase constituents of the coatings type, volume and distribution of pores/cavities/cracks, protruding present in the coatings. The erosion of aluminide coatings is shown to be controlled by the formation and removal of surface scales. This implies that the use of aluminide coatings will increase the erosion resistance of typical turbine blade materials because of the superior oxidation and corrosion resistance of this coating. This increase in erosion resistance will be particularly significant at higher operating temperatures, above 900 ^{0}C [**146**].

5.4.1 ANN Model: Development and Implementation (For erosion wear)

To train the neural network used for this work, about 25 data sets of different velocity and different angles are taken. Impact velocity, impact angle are taken as input and erosion wear behaviour is taken as output. The three layer neural network is shown in fig5.2

Input Parameters for Training	**Values**
Error tolerance	0.001
Learning parameter(ß)	0.002
Momentum parameter(α)	0.002
Noise factor (NF)	0.001
Maximum cycles for simulations	2000000
Slope parameter (£)	0.6
Number of hidden layer neuron	6
Number of input layer neuron (I)	2
Number of output layer neuron (O)	1

Table5.3 Input parameters selected for training (for erosion rate)

5.4.2 ANN Implementation in Prediction of Erosion Wear Rate

Neural computation is used to predict erosion rate of iron-aluminide coating. The network is trained with the database generated from experimental results by taking suitable input

parameters for training. Prediction results are compared to experimental sets. Figures 5.10, present the comparison of predicted output values for erosion rate obtained at various impact angles with the actual values found experimentally at different impact speeds.

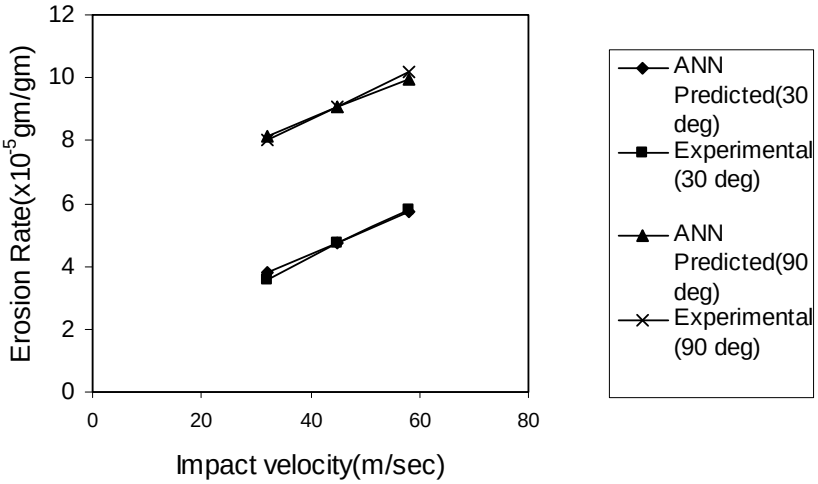

Fig.5.10 Comparison plot for predicted and experimental values of Erosion rate
[Impact velocity =58.5m/s SOD = 100 mm]

It is interesting to note that the predictive results show good agreement with experimental sets realized after having generalizing the ANN structures. The optimized ANN structure further permits to study quantitatively the effect of the considered impact velocity. The range of the chosen parameter can be larger than the actual experimental limits, thus offering the possibility to use the generalization property of ANN in a large parameter space. In the present investigation, this possibility was explored by selecting the impact velocity in a range from 20 to 70 m/sec for 30^0,90^0 and a set of prediction for erosion wear rate is evolved. Fig.5.11illustrates the predicted evolution of erosion wear rate of iron aluminide coatings on mild steel substrates with the impact velocity.

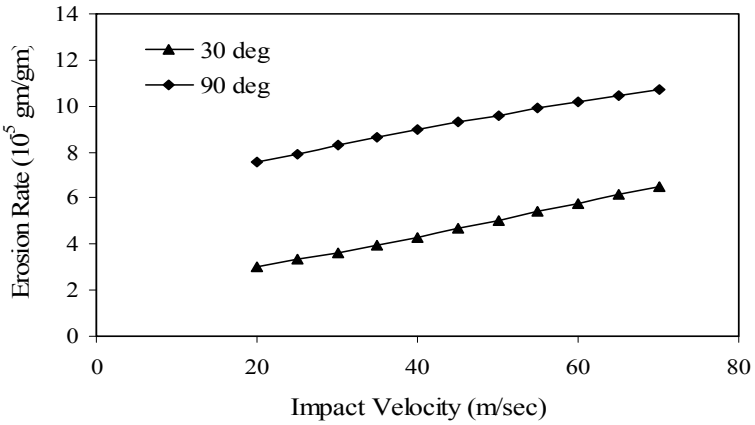

Fig.5.11 Predicted Erosion rate for different impact angles with impact velocity
SOD = 100mm

From the predicted graph in fig.5.11 with increasing velocity erosion rate increases for different angles. It is obvious that, with increasing velocity the particles will have high kinetic energy which transformed at impact and hence remove more particles from the impacted surface and it is maximum at 90^0 angle.

In the present investigation, this possibility was explored by selecting the impact angle in a range from 10^0 to 90^0 angle for velocities 32m/sec, 45m/sec, 58m/sec and a set of prediction for erosion wear rate is evolved. Fig.5.12 illustrates the predicted evolution of erosion wear rate of iron aluminide coatings on mild steel substrates with the impact angle.

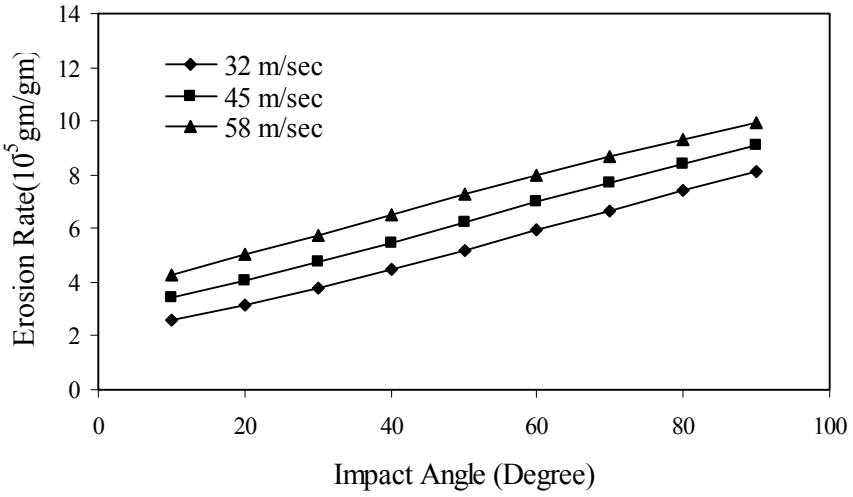

Fig.5.12 Predicted Erosion rate for different impact velocities with impact angle
SOD = 100mm

From the predicted graph in fig.5.12 with increasing impact angle erosion rate increases for different impact velocity, and it is maximum at 58m/sec.The optimized ANN structure further permits to study the effect of impact angle and velocity on the coating erosion in a domain larger than the experimental limits.

5.5 Correlation between Erosion Wear Rate, Impact Velocity and Impact Angle

In this study, an attempt is made to derive a correlation of the control factors for quantifying the erosion rate. The single-objective quantitative determination of the relationship between coating erosion rate and two important control factors i.e. impact velocity and the angle of impingement has been found out using non-linear regression analysis with the help of SYSTAT 7 software. For erosion rate **E** in terms of impact velocity (V) and angle of impact (α), the following mathematical model is suggested.

$$E = KV^{n}(\sin^{m}\alpha)$$

Here, E is the performance output terms and **K, m and n** are the model constants. From regression analysis, the constant are found out to be

$$K = 3.12 \times 10^{-6}$$

$$m = 0.880$$

$$n = 0.996$$

This makes the equation as follows:

$$E = 3.12 \times 10^{-6} V^{0.996} (\sin \alpha)^{0.880}$$

The correctness of the calculated constants is confirmed as high correlation coefficients (r^2) in the tune of 0.96 are obtained for the equation and therefore, the model is quite suitable to be used for further analysis.

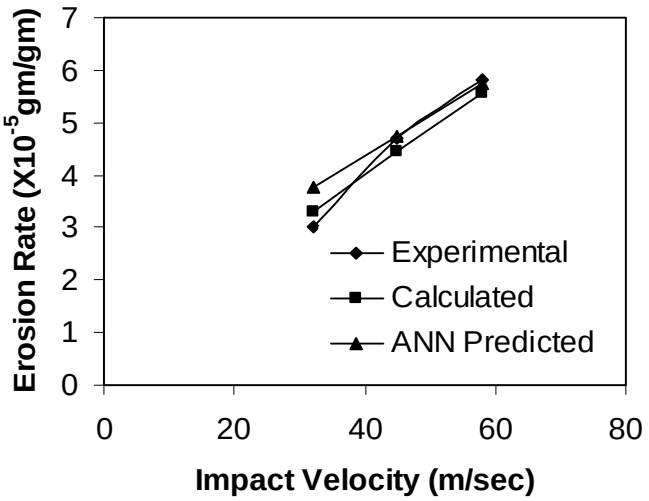

Fig.5.13 Comparison plot for predicted, formula and experimental values of Erosion rate [Impact angle =30^0 SOD = 100 mm]

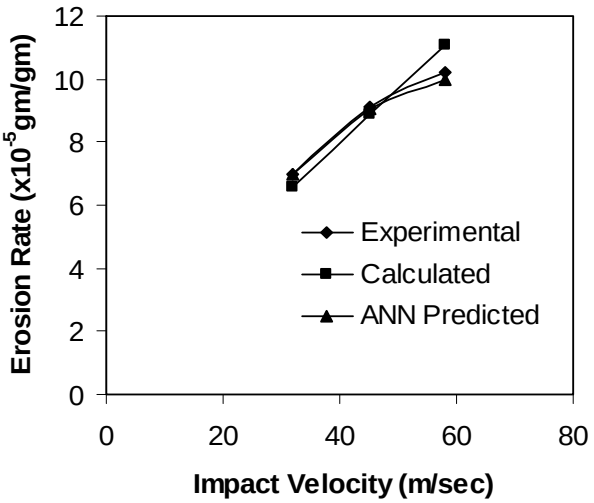

Fig.5.14 Comparison plot for predicted, formula and experimental values of Erosion rate [Impact angle =90^0, SOD = 100 mm]

Impact angle (degree)	Impact velocity (m/s)	Erosion rate (x10^{-5}g/g)			% Error
		Expt.Value	Calculated Value	Ann predicted	
30	32	3.0	3.30	3.78	10
30	45	4.72	4.45	4.74	5.7
30	58	5.8	5.57	5.76	3.9
90	32	7	6.58	8.14	6
90	45	9.1	8.89	9.08	2.3
90	58	10.2	11.1	9.96	8.8

Table 5.4 Comparison of experimental predicted and calculated values of erosion rates with the associated percentage error

Figures 5.13, 5.14 show comparisons of the coating erosion rate values predicted by ANN and the values calculated using the suggested correlation with those obtained experimentally at different operational conditions. Table 5.4 presents these values along with the associated percentage error in a tabular form.

It is seen from the comparison plots that the prediction model and the correlation model proposed for the erosion rate are in reasonably good agreement with the experimental

data. Thus the models are quite suitable to be used for any further analysis of erosion in plasma sprayed iron-aluminide coatings.

Distinguishing features

The results presented in fig. 5.11 and 5.12 confirm that the angle at which the stream of solid particles impinges the coating surface influences the rate at which the material is removed. It further suggests that, this dependency is also influenced by the nature of the coating material. Normally, for brittle materials subjected to erosion, the maximum wear rate occurs at 90^0 impact and for ductile material this is 15^0-30^0. In the present investigation, the peak erosion rate is recorded at 30^0 for the coatings regardless the impact velocity and the stand-off distance. This implies the brittle behavior of the coating under study. The angle of impact determines the relative magnitude of the two components of the impact velocity namely, the component normal to the surface and parallel to the surface. The normal component will determine how long the impact will last (i.e. contact time) and the load. The product of this contact time and the tangential (parallel) velocity component determines the amount of sliding that takes place. The tangential velocity component also provides a shear loading to the surface, which is in addition to the normal load that the normal velocity component causes. Hence as this angle changes the amount of sliding that takes place also changes as does the nature and magnitude of the stress system. Both of these aspects influence the way a coating wears. These changes imply that different types of material would exhibit different angular dependency.

CHAPTER 6
CONCLUSIONS

The conclusions drawn from the present work are as follows:

- Fe-Al when coated on metal substrates employing thermal plasma spray technique possess desirable coating characteristics such as good adhesion strength, hardness etc. comparable to those of other conventional plasma sprayed aluminide coatings.

- Maximum adhesion strength of ~12.84 MPa is recorded for iron aluminide coatings on mild steel and ~9.6 MPa for Cu substrate

- Operating power level of the plasma torch influences the coating adhesion strength, deposition efficiency and coating hardness to a great extent. The coating morphology is also largely affected by the torch input power.

  Due to phase transformations and inter-oxide formation during plasma spraying, changes in the coating characteristics such as hardness etc. are observed.

- From surface morphological study it is concluded that Coatings deposited at 18kW power level are smooth, more homogenous, having least amount of porosity. This might be the reason to reduce the erosion rate for the coating deposited at 18 kW, as compared to the coating deposited at 11kW.

- The entire series of coatings developed in this work are much harder than the parent metals on which they are deposited. Hence, these coatings may be recommended for tribological applications.

- Artificial neural networks can be gainfully employed to simulate property-parameter correlations in a space larger than the experimental domain. It is evident that with an appropriate choice of processing conditions a sound and adherent iron aluminide coating are achievable using iron aluminium powders.

- Deposition efficiency deposition efficiency for iron aluminide coatings ranges from 21.6% to 51.1% in case of mild steel substrate and from 29% to 53.7% in case of copper substrate. It is interesting to note that the deposition efficiency, in all cases, has increased in a step up fashion with the increase in torch input power.

- The deposition efficiency is one the main requirements of the coatings developed by plasma spraying. It represents the effectiveness of the deposition process as well as the coatability of the powders under study. Neural computation can be used as a tool to process very large data related to a spraying process and to predict coating characteristic such as deposition efficiency, the simulation can be extended to a parameter space larger than the domain of experimentation.

- Erosion wear behaviour is one of the main requirements of the coatings developed by plasma spraying for recommending specific application. In order to achieve tailored erosion wear rate accurately and repeatedly, the influence of the process parameters are to be controlled accordingly. The solid particle erosion wear resistance of the Iron aluminide coatings is fairly good and is comparable to that of conventional wear resistant overlay coatings. The maximum wear rate occurs at 90^0 impact for brittle material and for ductile material the angle is 15^0-30^0. In the present investigation, the peak erosion rate is recorded at 30^0 for the coatings regardless the impact velocity and the stand-off distance. This implies the brittle behavior of the coating under study.

SCOPE FOR FUTURE WORK

The variation of amount of aluminide phases with plasma operating parameters viz. power level, feed rate etc. are to be studied to find out the suitability of the particular aluminide phases responsible for increase in interface bonding and the wear resistance etc.

******

REFERENCES

1. Matejka D. and Benko B., Plasma Spraying of Metallic and Ceramic materials. Chichester, UK: John Wiley & Sons Ltd, 1989.

2. Pauloski L., The Science and Engineering of Thermal Spray Coatings. Chichester, UK: John Wiley & Sons Ltd, 1989.

3. Taylor P.R., Das A.K., "Thermal plasma processing of Materials" Power Beams and Materials Processing PBAMP, Allied Publishers Pvt. Ltd., Mumbai, India, (2002): p. 13-20.

4. Bandopadhyaya P.P., Processing and Characterization of Plasma Sprayed Ceramic Coatings on Steel Substrate". -- PhD. Thesis, IIT, Kharagpur, India, (2000).

5. Soliman H.M., El-Azim M.E.A., Journal of Material Science and Technololy. Volume 13, (1997**)**: p. 462.

6. Soliman H.M., Mohamed K.E., El-Azim M.E.A., Hammd F.H., Journal of Material Science and Technology. Volume 13, (1997**)**: p.383.

7. Kircher T.A., McMordie B.G., McCarter A.,"Performance of a silicon-modified aluminide coating in high temperature hot corrosion test conditions" Surface Coating and Technology. Volume 68, No. 69, (1994): p. 32-37.

8. El-Azim M.E.A, Mohamed K.E., Soliman H.M., Ham-mad F.H., Metall. Sci. Technol. Volume 12, No.1, (1994**)**: p.

9. Soliman H.M., El-Azim M.E.A, J. Mater. Sci. Technol., Volume 13, (1997): p. 462-466.

10. Morley J., Park A., Proceedings of the International Symposium on Materials for Resource Recovery and Transport, in: L Collins_Eds.., Calgary, Alberta, Canada, Volume 16-18, (August 1998): p.553.

11. Restall J. E., Proc. 3rd Conf. on Gas Turbine Materials in a Marine Environment, Bath, (1976): Ministry of Defence, London: Session V, Paper 10.

12. Galsworthy J. C., Restall J. E. and Booth G. C., Brunetaud R., Coutsouradis D., Gibbons T. B., Lindblom Y., Meadow croft D. B. and Stickler R. (eds.), "Proc. Conf. on High Temperature Alloys for Gas Turbines", Liege, Volume 4 - 6, (October 1982): p. 207.

13. Nagarajan V. and Wright I. G., in R. A. Rapp (ed.), Nate 6, Proc.Conf. On highTemperature Corrosion, San Diego, CA, 1981, National Association of Corrosion Engineers, Houston, TX, 1981, p. 398 - 405.

14. Stephenson D. J., Nicholls J. R. and Hancock P., in J. E. Field and N. S. Corney (eds.), "Erosion by Liquid and Solid Impact", Proc. 6th Znt. Conf on Cambridge, Cambs. September 5 - 8, 1983, Cavendish Laboratory, Cambridge, Cambs. 1983, p. 48.1 - 48.8.

15. Stephenson D. J., Nicholls J. R. and Hancock P., "Particle-surface interactions during the erosion of a gas turbine material" (MarMOO2) by pyrolytic carbon Particles, Wear. Volume 111, (1986): p. 15.

16. Bell T, "Surface engineering, past, presentandfuture."Surface engineering. Volume 6, No.1, (1990): p. 31-40.

17. Burakowski T, Rolinski E. and Wierzchon T., "Metal surface engineering" (In polish).Warsaw University of Technology Publications, Warsaw, 1992.

18. Burakowski T; Rolinski E, and Wierzchon T; A word about surface engineering (In polish).Metaloznawstwo, Obrobka Cieplna, Inzynieria Powierzchni (Metallurgy, Heat Treatment, Surface engineering), No. 121-123, (1993): pp 16-31.

19. Hieman R.B., Plasma Spray Coating-Principles and Applications, VCH Publishers Inc., New York, USA, 1996.

20. Rickerby D.S. and A Matthews. Advanced Surface Coatings: A Handbook of Surface engineering, Chapman and Hall, New York, pp.1-13, 1991**.**

21. Budinski K.G, Surface Engg.For Wear Resistance, N.J., USA, 1988.

22. Stratford K.N., "Coatings and Surface treatments for Corrosion and Wear Resistance", Inst. Of Corrosion Sc.and Tech., Birmingham, UK, 1984.

23. Pauloski L, The Science and Engineering of Thermal Spray Coatings, John Wiley & Sons Ltd, Chichester,UK,1989**.**

24. Edwards R., Cutting Tools. The Institute of materials, UK, 1993**.**

25. Budinski K. G., Surface Engg. For Wear Resistance, N.J., USA, 1988.

26. Durney L. J., Electroplating Engineering Handbook, Van Norstand, NY, USA. 1984.

27. Biestek T. and Weber J., "Electrolytic and Chemical Conversion Coating", Portcullis Press Ltd, Warsaw, Poland. 1976.

28. Tape N. A, Baker E. A. and Jackson B. C., "Plating and Surface Finishing", 1976, October, p 30.

29. Fieldstein N, Materials Engg. 1981July, p. 38.

30. Spencer C. F., Metal Finishing, 1975 January, p 38.

31. Mcdermott J., Electroless Plating and Coating of Metals, Noyes Data Corp, NJ., USA: 1972.

32. Ashby M. F. and Jones D. R. H., Engineering Materials, Pergamon press, NY, USA: 1980.

33. Brooks C. R., Heat Treatment of Ferrous Metals, Hemisphere Publishing Co., Washington, USA:1979.

34. Dawes C. and Tranter D. F., Metal Progress, 1983, December, p 17.

35. Linial A. V. and. Hunterman H. E, Wear of Materials, ASME, NY, US: 1979.

36. Bhattacharya S. and Seaman F. D., "Laser Heat Treatment for Gear Application in "Laser Processing of Materials." The Metallurgical. Soc. Of AIME. (1985): p. 211.

37. Smidt F. A., Ion Implantation for Material Processing, Noyes Data Corp, NJ, USA: 1983.

38. Bunshah R. F., Deposition Technologies for Films and Coatings, Noyes Publications, NJ, USA: 1982.

39. Vossen J. and Kern W., "Thin Film Processes", Academic Press, NY, USA: 1978.

40. Legg H. S. and. Legg K. O, "Ion Beam Based Techniques for Surface Modification in "Surface Modification Technologies", by T.S. Sudarsan (ed), Marcell Dekker Inc, USA: 1989, p 219.

41. Blocher J. M., Vapour Deposited Materials in "Vapour Deposition", by C. F. Powell, J. H. Oxley and J. M. Blocher (eds), Willwy, NY, US: 1966.

42. Bhatt D. G., Chemical Vapour Deposition, in "Surface Modification Technologies", by T. S. Sudarsan (ed), Marcell Dekker Inc, USA: 1989, p 141.

43. Little R. L., Welding and Welding Technology, TMH Publications, New Delhi, India: 1979.

44. The Welding Handbook, American Welding Soc., USA: 1980.

45. Houldcroft P. T., Welding Process Tech., Welding Process Tech., Cambridge Univ Press, UK: 1967.

46. Longo L. F, Thermal Spray Coatings, ASM, USA: 1985.

47. Meringolo V., Thermal Spray Coating, Tappi Press, Atlanta, USA: 1983.

48. Morris J. L., Welding Principle for Engineers, Prentice Hall, USA: 1951.

49. Powloski L., The Sc. And Engg. Of Thermal Spraying, Willey, USA: 1995.

50. Lugscheider, E. Technica. Volume 19, 1992, p 19.

51. McCartney D. G., Surf. Engg. Volume 14, No. 2, (1998): p 204.

52. Sobolev V. V., Guilemany J.M., Nutting J. and Miquel J.R., Int. Mat. Rev. Volume 42, No.3, (1997): p117.

53. Xu B, Shinning M. and Wang J., Surf. Engg.Volume11, No. 1, (1995): p 38.

54. Metco, Plasma Spraying Manual, Metco, USA: 1993.

55. Wrigren J., Surf. Coat. Tech., Volume 45, (1991): p 263.

56. Nicholas M. G. and Scott K. T., Surfacing Journal. Volume 12, (1981): p 5.

57. Funk W. and Goebe F., Thin Solid Film. Volume 128, (1985): p 45.

58. Wielage B., Hofmann V., Steinhauser A. and Zimmerman G., Wear, Volume 14, No. 2, (1998): p136.

59. Lee N. Y., Stinton D. P., Brandt C.C., Erdogan F., Lee Y. D. and Mutasim Z. ,J. Am. Cer. Soc. Volume 79, No. 12, (1996): p 3003.

60. Pajares A., Wei L., Lawn B.R. and Berndt C.C., J. Am. Cer. Soc. Volume79, No. 7, (1996): p 1907.

61. Novak R. C., J. Gas Turbines and Power. Volume 110, (1988): p 110.

62. Nash A.R., Weare N. E. and Walker D. L., J. Metals, July, 1961, p 473.

63. Gruner H., "Vacuum plasma spray quality control" Thin Solid Film. Volume 118, (1984): p 409.

64. Eaton H. and Novak R. C. "Coating bond strength of plasma-sprayed stainless steel" Surf. and Coating Technology. Volume 27, (1986): p 257.

65. Eaton H. and Novak R. C., "A study of the effects of variations in parameters on the strength and modulus of plasma sprayed zirconia" Proc. Int. Conf on metallurgical Coatings. San Diego, USA.

66. K Ramchandran. and Selvarajan P. A., "The influence of copper upon the atmospheric corrosion of iron" Thin Solid Film. Volume 315, (1998), p 149.

67. Ingham H. S. and Fabel A. J., Welding Journal. February, (1975), p 101.

68. Oki S., Gonda S. and Yanokawa M., Proc. 15th International Thermal Spray Conference, 1998, 25 – 29th May, France, p 593.

69. A.F.Puzryakov, S.A.Levitin and V.A Garanov., Poroshkovaya Metallurgya. Volume 8, No. 272, (1985): p 55.

70. Hennaut J., Othzemouri J. and Charlier J., "The solid reaction products of the catalytic decomposition of carbon monoxide on iron at 550°C" Mat. Sc and Tech. Volume11, (1995): p 174.

71. Sampath S., Neiser R. A., Herman H., Kirkland J. P. and Elan W. T.., J. Mat. Res., Volume 8, No. 1, **(**1993): p 78.

72. Hennaut J., Othmezouri J. and Charlier J**.**, Mat. Sc and Tech. Volume 11, (1995): p 174.

73. Ulhmann's Encyclopedia of Industrial Chemistry, 1990, v 1/16 Elvers B., Hawkins S. and Schultz G. (eds), VCH, p 433.

74. KubelC.J. Adv. Mat. Proc. Volume 12, (1990): p 24.

75. Matejka D. and Benko B, "Plasma Spraying of Metallic and Ceramic Materials.", John Wiley & Sons Ltd, Chichester, UK: 1989.

76. Pauloski. The Science and Engineering of Thermal Spray Coating. Chichester, UK: John Wiley & Sons Ltd, 1989**.**

77. Metals Handbook, ASM, Metals Park, Ohio, USA.

78. Atamert S. and Stekly J. "Microstructure", Surf. Engg. Volume 9, No. 3, (1993): p 231.

79. Price M. O., Wolfla T. A. and Tucker R. C., Thin Solid Films. Volume 45, (1977): p 309.

80. Moore M. A., Wear. Volume 28, (1994): p 59.

81. Hurricks P. L., Wear. Volume 22, (1972): p 291.

82. Habsur M. G. and Miner R. V., Mat. Sc. Engg. Volume 83, **(**1986): p 239.

83. Daroliaetal R., "Structural Intermetallics" The minerals metals and materials society, 1993.

84. R. Holm, "The frictional force over the real area of Contact." Wiss. Vereoff. Siemens Werken. Volume 17, No. 4, (1938): p. 38-42.

85. M.F.Ashby and S.C.Lim, "Wear-mechanism maps.", Scripta Metallurgical et Materialia. Volume 24, (1990): p. 805-810.

86. Y. Wang, T.C. lei and C.Q. Gao, "Influence of isothermal hardening on the sliding wear behaviour of 52100 bearing steel." Tribology International, Volume 23, No. 1, (1990): p. 47-53.

87. Soda N., "Wear of some F.F.C metals during unlubricated sliding part-1. Effects of load, velocity and atmospheric pressure on wear." Wear. Volume 33, (1975): p. 1-16.

88. J.T. Burwell and C.D Strang, "Metallic wear." Proc.Soc (London). 212A May 1953, pp 470-477.

89. J.T Burwell., "Survey of possible wear mechanisms." Wear. Volume 58, (1957): p. 119-141.

90. Zumgahr K.H., "Microstructure and wear of materials" Elsevier, Amsterdam, 1987.

91. Guo D.Z., Li F.L., Wang J.Y, Sun J.S., "Effects of post-coating processing on structure and erosive wear characteristics of flame and plasma spray coatings" Surf. Coat. Technol. Volume 73, (1995): p73.

92. Kosel T.H., Friction, Lubrication and Wear Technology, ASM Handbook, Volume 18, 1992, p. 199.

93. Tabakoff W., Surf. Coat. Technol. Volume 120– 121, (1999): p. 542.

94. Levy A.V., "The erosion of carbide-metal composites." Surf. Coat. Technol. Volume 36, (1988): p. 387.

95. Shipway P.H., Hutchings I.M., "Measurement of coating durability by solid particle erosion." Surf. Coat. Technol. Volume 71, (1995): p. 1.

96. Angle P. A. Impact Wear of Materials, Elsevier; New York: 1976.

97. Tilly, G.P. "Erosion Caused by Impact of Solid Particles", in H. Herman (ed), Treatise on Materials Science and Technology. Volume 13:D. Scott(ed), Wear. (Academic Press: New York, 1979) p. 287 – 320.

98. Erosion by Liquid and Solid Impact. Cavendish Laboratory, University of Cambridge: Cambridge, England: 1979.

99. Erosion by Liquid and Solid Impact. Cavendish Laboratory, University of Cambridge: Cambridge, England, 1987.

100. Evans, A. G. "Impact Damage Mechanism – Solid Projectile", in H. Herman (ed.), Treatise on Materials Science and Technology, Vol. 16: C. M. Preece (ed.), Materials Erosion, Academic Press: New York, 1979, p. 1 – 67.

101. Hogmark S, Westergard R, Erickson L. C., Axen N., and Hawthorne H. M. "The erosion and abrasion characteristics of alumina coatings plasma sprayed under different spraying conditions." Tribology International Volume 1, (May 1998): p. 271 – 279.

102. R. C. Jr. Tucker, "On the relationship between the microstructure and the wear characteristics of selected thermal spray coatings." Proceeding of ITSC, Kobe, Japan, 1995, pp. 477 – 482.

103. Hawthorne H. M., Erickson L. C., Ross D., Tai H.and Troczynski T., "The microstructurral dependence of wear and indentation behaviour of some plasma sprayed alumina coatings." Wear. Volume 203 – 204, (1997): pp. 709 – 714.

104. Erickson L. C., Troczynski T., Ross D., Tai H. and Hawthorne H. M., "Processing – dependent microstructure and wear – related surface properties of plasma sprayed alumina coatings", presented to World Tribology Congress, London, U. K., September (1997).

105. Erickson, L. C., Troczynski, T., Hawthorne, H. M., Tai, H. and Ross, D., Alumina coatings by plasma spraying of monosize sapphire powders, published in the proceedings of ITSC'98, Nice, France.

106. A.Ohmori, C. – J. Li and Y. Arata, Influence of Plasma spray conditions on the structure of Al_2O_3 coatings. Trans. Of JWRI 19 2 (1990), pp. 99 – 110.

107. Grosdidier Thierry, J Gang, Bernard Fre´de´ric , Gaffet Eric, A Zuhair. Munir, "Synthesis of bulk FeAl nanostructured materials by HVOF spray forming and Spark Plasma Sintering"Intermetallics V4 2006 1208 P213.

108. Binshi Xua , Zixin Zhua, Shining Maa, Wei Zhang and Weimin Liu, "Sliding Wear behaviur of FeAland Fe–Al/WC coatings prepared by high velocity arc Spraying." Wear. Volume 257, (2004): p. 1089–1095.

109. Guilemany J.M., Lima C.R.C., Cinca N., Miguela J.R., "Studies of Fe–40Al coatings obtained by high velocity oxy-fuel Surface & Coatings" Technology (2006).

110. Jia G., Grosdidiera T., Liaoa H.L., Mornirolib J.-P, , Coddeta C., "Spray forming thick nanostructured and microstructured FeAl deposits." Intermetallics. Volume 13, (2005): p. 596–607.

111. Houngninou, Chevalier S., Larpin J.P., "Synthesis and characterization of pack cemented aluminide coatings on metals." Applied Surface Science. Volume 236, (2004): p. 256–269.

112. Martinez M., Viguier B., Maugis P., Lacaze J., Relation between composition, Microstructure and oxidation in iron aluminides." Intermetallics CIRIMAT, UMR 5085, ENSIACET, 31077 Toulouse Cedex 4, France: (2006) 14.

113. Cullity B.D., Elements of X-Ray Diffraction, Addition-Wasley, Reading, MA, 1972, p.102.

114. Wojnar L., Image Analysis Applications in Materials Engineering, CRC Press, Boca Raton, 1999.

115. Chen H., Lee S.W., Hao Du, Chuan X Ding and Chul Ho Cho, "Influence of feed stock and spraying parameters on the deposition efficiency. and micro hardness of plasma sprayed zirconia coatings." Materials Letter. Volume 58, No. 7 – 8, (March 2004): p. 1241 – 1245.

116. Venkataraman B. "Evaluation of Tribological Coatings" – Proc. of DAE-BRNS Workshop on Plasma Surface Engineering, BARC, Mumbai, September 2004, pp. 217 – 235.

117. Nicholls R., Deakin M.J, Rickerby D.S., "A comparison between the erosion behaviour of thermal spray and electron beam physical vapour deposition thermal barrier coatings." Wear. Volume 233–235, (1999): p. 352–361.

118. G .Lalleman – Tallaron, Study of Microstructure and adhesion of spinelles coatings Formed by plasma spraying, Ph. D. Thesis E. C. Lyon, France: No. 96 – 58 (1996).

119. Mishra. S. C., Rout K. C., Ananthapadmanabhan P. V. and Mills B. "Plasma Spray Coating of Fly Ash Pre-Mixed with Aluminium Powder Deposited on Metal Substrates". J. Material Processing Technology. Volume 102, No. 1 – 3, (2000): pp. 9 – 13.

120. Lima C.R.C. Trevisan. R.E., J.Thermal Spray Tech. Volume 62, (1997): p. 199.

121. Vardelle A., Vardellet M., Person. Mc. P. Fanchais – Proc. of 9th National Themal Spray Conference (1980) pp.155.

122. Lech Pawlowski – The Science and Engineering of Thermal Spray Coatings, John Wiley & Sons, New York (1995). pp. 235.

123. Sisco F.T.,Aluminium in iron & Steel, John Willy & Sons,Inc.N.Y.,19853.

124. S.F. Wayne, S. Sampath, Structure/property relationships in sintered and thermally sprayed WC-Co, J. Thermal Spray Technol. 1 (1992) 307–315.

125. Hawthorne H.M., Erickson L.C, Ross D., Tai H., Troczynski T., "The Microstructural dependence of wear and indentation behaviour of some plasma Sprayed alumina coatings." Wear. Volume 203/204, (1997): p. 709–714.

126. Erickson L.C., Westergård. R., Wiklund U., Hawthorne H.M., Axén N., Hog mark S., "Cohesion in plasma sprayed coatings — a comparison between Evaluation methods." Wear. Volume 214, (1998): p. 30–37.

127. Pawlowski Lech – The Science and Engineering of Thermal Spray Coatings, John Wiley & Sons, New York (1995) pp.218.

128. Padmanabhan P.V. A., Thiyagarajan T.K., Sreekumar K.P., Venkatramani N., "In-flight particle behaviour and its effect on co-spraying of alumina–titania." Scripta Materialia. Volume 50, (2004): p. 143-147.

129. Choi H.M., Kang B.S., Choi W.K., Choi D.G., Mater J.. Sci. Volume 33, (1998): p. 5895.

130. Mater. Celik E , Demirkan. A.S, Avci E., Surf. Coat. Technol. Volume 116 – 119, (1999): p. 1061.

131. Steeper T.J., Rotolico A.J., Nerz J.E., "Optimizing plasma sprayed alumina-titania coatings using statistical methods", Proceedings of the 1993 National Thermal Spray Conference, Anaheim, CA, 7– 11, June 1993.

132. Li Khor K.A., Surf. Coat. Technol. Volume 150, (2002): p. 125.

133. Sampath S., Jiang X., Kulkarni A., Matejicek J., Gilmore D.L., Neiser R.A., "Development of process maps for plasma spray: case study for molybdenum." Mater. Sci. Eng. A, Volume A 348, (2003): p. 54.

134. Sampath S, Jiang J., Matejicek, Leger A.C., Vardelle A., "Substrate temperature effects on splat formation, microstructure development and properties of plasma spraye coatings Part I: Case study for partially stabilized zirconia." Mater.Sci. Eng. A Volume A 272, (1999): p. 181.

135. Staia M.H., Valente T., Bartuli C., Lewis D.B, "Part II: tribological performance of Cr_3C_2-25% NiCr reactive plasma sprayed coatings deposited at different pressures." Surf. Coat. Techno. Volume 146–147, (2001): p. 563.

136. Kucuk, Berndt C.C., Senturk U., Lima R.S., Influence of plasma spray parameters on mechanical properties of yttria stabilized zirconia coatings. II: Acoustic emission response Mater. Sci. Eng. A. Volume 284, (2000): p. 41.

137. Branco J. R. T., Gansert R., Sampath S., Berndt C. C, Herman H.—"Solid Particle Erosion of Plasma Sprayed Ceramic Coatings." Materials Research. Volume 7, No.1, (2004): p. 147-153.

138. S Rajasekaran. G. A Vijayalakshmi Pai. –Neural Networks, Fuzzy Logic And Genetic Algorithms—Synthesis and Appl Vij Vijayalakshmi Pai ayalakshmi Pai publication – Prentice Hall of India Pvt. Ltd. , New Delhi: (2003).

139. Rao V. and. Rao H 'C++ Neural Networks and Fuzzy Systems' BPB Publications, 2000.

140. Stephenson D. J., Nicholls J. R and Hancock P., "Particle-surface interactions during the erosion of aluminide-coated." Wear. Volume 111, (1986): p. 31 – 39.

141. Levy A. V., "The erosion corrosion behavior of protective coatings." Surf. and Coat. Techn. Volume 36, (1988): p. 387 – 406.

142. Chang-Jiu L., Yang Guan-Jun, Ohmori Akira, "Relationship between particle erosion and lamellar microstructure for plasma-sprayed alumina coatings." Wear. Volume 260, (2006): p. 1166–1172.

143. Alahelisten A., Hollman P., S. Hogmark, "Solid particle erosion of hot flame-deposited diamond coatings on cemented carbide." Wear. Volume 177, (1994): p. 159-165.

144. Bayer G. – Mechanical Wear Prediction and Prevention – Marcel Dekkar, Inc., New York: (1994) pp. 396.

145. Nicholls J.R., Deakin M.J, D.S. Rickerby, "A comparison between the erosion behaviour of thermal spray and electron beam physical vapour deposition thermal barrier coatings." Wear. Volume 233–235, (1999): p. 352–361.

146. Lathabai S., M. Ottmu¨ller 1, Fernandez I., "Solid particle erosion behaviour of thermal sprayed ceramic, metallic and polymer coatings." Wear. Volume 221, (1998): p. 93-108.